

Climate change amplifies extinction risk of a subshrub in anthropogenic landscapes

A manuscript for consideration as a Research Article for publication in Journal of Ecology

Eva Conquet^{1*}, Arpat Ogzul¹, Susana Gómez-González^{2,3}, Fernando Ojeda², Maria Paniw^{1,4}

1. Department of Evolutionary Biology and Environmental Studies, University of Zurich, Zurich 8057, Switzerland

2. Departamento de Biología-IVAGRO, Universidad de Cádiz, Campus Río San Pedro, 11510 Puerto Real, Spain

3. Center for Climate and Resilience Research, (CR)2, Santiago, Chile

4. Department of Conservation and Global Change, Doñana Biological Station (EBD-CSIC), Seville 41092, Spain

Author's ORCID IDs:

Eva Conquet: 0000-0002-8047-2635

Arpat Ozgul: 0000-0001-7477-2642

Susana Gómez-González: 0000-0002-3779-8701

Fernando Ojeda: 0000-0001-5480-0925

Maria Paniw: 0000-0002-1949-4448

* Corresponding author's email address: eva.conquet@gmail.com

Word count (abstract through references): 10891

Number of citations: 96

Number of tables in main document: 0

Number of figures in main document: 5

Acknowledgments

We are grateful to all the helpers who have contributed to the data collection and to the Spanish military Campo de Adiestramiento de la Armada in Sierra del Retín (Cádiz), who granted access to some study populations. We acknowledge the E-OBS dataset from the EU-FP6 project UERRA (<https://www.uerra.eu>) and the Copernicus Climate Change Service, as well as the data providers in the ECA&D project (<https://www.ecad.eu>). EC was supported by a Swiss National Science Foundation Grant (31003A_182286) to AO. MP was funded by the grant RYC2021-033192-I by MCIN/AEI/10.13039/501100011033 and “European Union NextGenerationEU/PRTR”. SG-G was funded by the Agencia Estatal de Investigación (Spain; PID2019-106908RA-I00/AEI/10.13039/501100011033) and ANID/FONDAP (Chile; 1522A0001).

Author Contributions

Eva Conquet: Conceptualization, Methodology, Software, Validation, Formal analysis, Investigation, Data curation, Writing - Original Draft, Writing - Review and Editing, Visualization. **Arpat Ozgul:** Conceptualization, Methodology, Resources, Writing - Review and Editing, Supervision, Project administration, Funding acquisition. **Susana Gómez-González:** Validation, Investigation, Resources, Writing - Review and Editing. **Fernando Ojeda:** Investigation, Resources, Writing - Review and Editing, Supervision, Project administration, Funding acquisition. **Maria Paniw:** Conceptualization, Methodology, Software, Validation, Formal analysis,

Investigation, Data curation, Writing - Original Draft, Writing - Review and Editing, Supervision, Project administration, Funding acquisition.

Data and Code Availability Statement

The data necessary for reproducing results and graphs presented in this study are available on Zenodo [link] (+ ref). Original data can be requested from Maria Paniw (maria.paniw@ebd.csic.es). Code for formatting data, implementing and running models and analyses, and plotting results is available on GitHub:

<https://github.com/EvaCnqt/DewyPinesLandUseClimateChange>. The version of code used for this study is archived on Zenodo [link] (+ref).

Conflict of Interest Statement

The authors declare no conflict of interest.

Statement on Inclusion

Our work was performed in collaboration with scientists based in the country where the study was initiated and carried out. The perspective of locally based authors who have strong experience with the focal system was paramount to ensure our conclusions took into account the local context. Additionally, we relied on literature previously published by scientists from the region.

1 **Climate change amplifies extinction risk of a subshrub in**

2 **anthropogenic landscapes**

3

4 **Abstract**

- 5 1. In most ecosystems, the increasingly strong effects of climate change on
6 biodiversity co-occur with other anthropogenic pressures, most importantly
7 land-use change. However, many long-term studies of population dynamics
8 focus on populations monitored in protected areas, and our understanding of
9 how climate change will affect population persistence under anthropogenic
10 land use is still limited.
- 11 2. To fill this knowledge gap, we assessed the consequences of co-occurring
12 land-use and climate change on population dynamics of a fire-adapted
13 Mediterranean carnivorous subshrub, the dewy pine (*Drosophyllum*
14 *lusitanicum*). We used seven years of individual data on 4,753 plants
15 monitored in three natural heathland sites that experience primarily fire as a
16 main disturbance, and five anthropogenic sites, where fires have been
17 replaced by persistent disturbances from browsing or mechanical vegetation
18 removal as a consequence of land-use change. All sites are projected to
19 experience increasingly hotter summers and drier falls and winters. We used
20 generalised additive models to model non-linear responses of survival,
21 growth, and reproduction to rainfall, temperature, size, density, and time since
22 fire in anthropogenic and natural dewy-pine populations. We then projected
23 population dynamics under climate-change scenarios using an individual-
24 based model.

25 3. Our findings reveal that vital rates respond differently to climate change in
26 anthropogenic compared to natural habitats. While extinction risks do not
27 change under climate change in natural habitats, future higher summer
28 temperatures decrease survival and lead to population declines and higher
29 extinction probabilities in anthropogenic habitats.

30 4. *Synthesis*: Our results highlight the possible dramatic effects of climate
31 change on populations largely confined to chronically disturbed,
32 anthropogenic habitats and provide a foundation for devising relevant
33 management strategies aiming towards the protection of species in human-
34 disturbed habitats of the Mediterranean habitat. Overall, our findings
35 emphasise the need for more long-term studies in managed landscapes.

36

37 **Keywords**

38 plant population and community dynamics, anthropogenic landscape, climate
39 change, land-use change, disturbance regime, fire adaptation, Mediterranean
40 habitat, population persistence

41

42 **Introduction**

43

44 Land-use change has been identified as the most important driver of
45 biodiversity declines in most ecosystems (Sala et al., 2000; Díaz et al., 2019; IPBES,
46 2019). Across the globe, human expansion has caused habitat loss and
47 fragmentation through the modification of lands for urbanisation or agricultural
48 purposes (Foley et al., 2005), with dire consequences on local and regional species

49 persistence (Selwood et al., 2015) and cascading effects at the community and
50 ecosystem levels (Garnier et al., 2007; Kampichler et al., 2012; Alberti, 2015).
51 Meanwhile, the effects of land-use change on species are increasingly compounded
52 by more severe impacts of climate change on natural systems (Brook et al., 2008;
53 Mantyka-Pringle et al., 2012; Oliver & Morecroft, 2014).

54

55 The complex interplay of land-use and climate change is reshaping ecosystems at
56 an unprecedented rate, with profound implications for the persistence of many
57 species. Nonetheless, many studies assess the persistence of populations under
58 climate change in protected areas (Murali et al., 2022)—which are generally
59 sheltered from anthropogenic land use and habitat loss (Geldmann et al., 2013;
60 Watson et al., 2014; but see Clark et al., 2013), and where populations are thus
61 overall doing better than those outside protected regions (Geldmann et al., 2013;
62 Gray et al., 2016). This means that, in many studies, the key role of land-use change
63 in shaping the response of populations to changes in climate is omitted (Titeux et al.,
64 2016). Land-use and climate change can have reciprocal effects on each other,
65 leading to non-additive effects of these pressures on populations and communities
66 (Brook et al., 2008; Mantyka-Pringle et al., 2012; Oliver & Morecroft, 2014; Montràs-
67 Janer et al., 2024). Thus, the effects of climate change might differ among land use
68 types, and the consequences of land-use change could depend on the strength of
69 climate change (Mantyka-Pringle et al., 2012). Understanding these dynamics
70 beyond the confines of protected areas is crucial for devising effective conservation
71 strategies.

72

73 Land-use, climate change, and their interaction (Brook et al., 2008) can affect
74 populations via changes in key vital rates through multiple mechanisms such as
75 inbreeding depression (Leimu et al., 2010; Bijlsma & Loeschcke, 2012), physiological
76 stress (Selwood et al., 2015), or phenotypic selection (Alberti, 2015). Negative
77 effects of climate change on survival could be exacerbated by anthropogenic land
78 use, as habitat fragmentation could hamper individual dispersal, thereby preventing
79 populations to shift their habitat range to respond to the new conditions arising under
80 climate change (Lawson et al., 2010; Oliver & Morecroft, 2014). Additionally,
81 negative correlations between adaptations to land use and to climate change could
82 cause the selection for the tolerance of one pressure to reduce the capacity to adapt
83 to the other (Chevin et al., 2010; Oliver & Morecroft, 2014). As population sizes
84 decrease, these detrimental effects could be amplified through demographic
85 stochasticity and inbreeding depression (Fagan & Holmes, 2006), as a decrease in
86 genetic variability and its subsequent fitness reduction would lower the capacity of
87 individuals to cope with challenging environmental conditions (Leimu et al., 2010;
88 Bijlsma & Loeschcke, 2012). Nonetheless, in face of the prevalence of negative
89 effects of both anthropogenic land use and climate change, and given their
90 interacting effects on demographic parameters (Brook et al., 2008; Titeux et al.,
91 2016) and biodiversity (Montràs-Janer et al., 2024), exhaustively assessing
92 population persistence under changing climatic conditions requires studying
93 populations in anthropogenic landscapes.

94

95 Mediterranean biomes are among the most sensitive to interacting pressures derived
96 from land-use and climate change (Newbold et al., 2020). In these ecosystems, fire
97 is a recurrent disturbance that has shaped plant traits over evolutionary time (Keeley

98 et al., 2012). However, many fire-adapted plant species in the Mediterranean Basin
99 are now largely found in anthropized habitats where fire regimes have been
100 substantially altered or suppressed altogether by changes in land use (Pausas &
101 Keeley, 2014), which can have strong impacts on plant population dynamics (Paniw,
102 Quintana-Ascencio et al., 2017). Mediterranean plant populations are also
103 increasingly exposed to shorter and drier winters and hotter summers, jeopardising
104 the persistence of shrubland communities (Paniw et al., 2021). While the effects of
105 human activities in fire-disturbed habitats on plant population persistence have
106 previously been studied (e.g. Paniw, Quintana-Ascencio et al., 2017), we still lack a
107 full understanding on population dynamics under the interacting pressures of land-
108 use and climate change.

109

110 Here, we use a Mediterranean, fire-adapted subshrub, the dewy pine (*Drosophyllum*
111 *lusitanicum*), as a case study to investigate the effects of changing climatic
112 conditions on population dynamics in natural and anthropogenic habitats. We used
113 seven years of individual-based data, collected as part of long-term demographic
114 monitoring (since 2011) in natural and anthropogenic (i.e., highly human-dominated
115 permanently disturbed sites) habitats, to parameterize vital-rate responses to
116 interacting climate (temperature and rainfall) and biotic (plant size and intraspecific
117 density) drivers and project resulting population dynamics under climate-change
118 scenarios. We expected higher extinction probabilities in anthropogenic habitats
119 under current climatic conditions, as previous research has shown human
120 disturbances to have a negative effect on population dynamics (Paniw, Quintana-
121 Ascencio et al., 2017; Conquet et al., 2023). Additionally, given the negative effects
122 of compound anthropogenic pressures on natural systems (Zscheischler et al.,

123 2018), we expected sharper declines in anthropogenic populations than in natural
124 ones under climate change.

125

126 **Methods**

127

128 Study species

129

130 *Life history*

131

132 The dewy pine, *Drosophyllum lusitanicum* (Drosophyllaceae), is a rare
133 carnivorous subshrub endemic to the western end of the Mediterranean basin and
134 tightly associated to fire-prone Mediterranean heathlands of southern Spain,
135 Portugal, and northern Morocco (Correia & Freitas, 2002; Garrido et al., 2003; Paniw
136 et al., 2015). As many species in fire-prone habitats, dewy pines have adapted their
137 life history to persist under recurring fire regimes that remove all aboveground
138 vegetation. Populations rely on a persistent soil seedbank (Fig. 1), whose dynamics
139 strongly vary with time since fire (TSF_t , where t is the number of years after a fire;
140 Paniw, Quintana-Ascencio et al., 2017; Conquet et al., 2023). When a fire occurs
141 (TSF_0), the combined effect of heat and vegetation and litter removal trigger the
142 germination of the major part of seeds stored in the seedbank (Fig. 1; Appendix S1:
143 Table S1; Cross et al., 2017; Paniw, Quintana-Ascencio et al., 2017; Gómez-
144 González et al., 2018). Germination from the seedbank continues in later post-fire
145 years but greatly decreases from TSF_2 . New seedlings mostly grow during the first
146 year after a fire (TSF_1) and become reproductive plants from the second year after
147 the population burned (TSF_2 ; Fig. 1). The majority of seeds produced by these

148 individuals do not germinate directly but go to the soil seedbank to replenish the
149 population at the next fire (Fig. 1). This occurs because dewy pines are increasingly
150 overgrown by dominant shrub vegetation, which hinders seed germination (Gómez-
151 González et al., 2018) and insect prey capture (Paniw et al., 2018), drastically
152 decreasing the survival of aboveground plants after TSF₄ (Paniw et al., 2015).
153
154 Despite being fire-adapted, active fire suppression and general degradation of
155 heathland habitats under land-use change (for instance through vegetation removal
156 for wide firebreaks or pine afforestations) mean that most populations of dewy pines
157 as well as numerous other heathland species persist in highly and permanently
158 human-disturbed (hereafter anthropogenic) habitats (Paniw et al., 2015). In such
159 habitats, periodic mechanical clearing of vegetation or browsing—of surrounding
160 vegetation but not on dewy pines—and trampling by domestic ungulates act as a
161 constant disturbance resembling the effect of fire by the removal of aboveground
162 vegetation, but lasting much longer. This has led to important changes in the
163 demographic processes of dewy pines (Paniw, Quintana-Ascencio et al., 2017;
164 Conquet et al., 2023). Seedbanks in chronically disturbed, anthropogenic
165 populations are likely depleted because the long-term clearance of vegetation means
166 that relatively more seeds germinate immediately instead of going into the seedbank
167 (Appendix S1: Table S1; Gómez-González et al., 2018). Vital rates of aboveground
168 individuals are affected as well; while juvenile survival rapidly decreases after a fire
169 in natural populations, it remains stable across time under human disturbances.
170 However, smaller mature individuals in anthropogenic populations have a lower
171 survival than in natural populations, and reproduction is decreased as well.

172 Moreover, negative density feedbacks are stronger in anthropogenic populations
173 (Conquet et al., 2023).

174

175 Anthropogenic pressures in dewy pine habitats are also increasingly interacting with
176 climate change. Temperatures have been increasing in the last four decades (on
177 average by 0.033 °C per year) and will continue to do so in the future (Appendix S2:
178 Fig. S1 and S2). Contrastingly, while the recent increase in rainfall variability is
179 predicted to reverse, rainfall is forecasted to be less abundant in the future (-0.16
180 mm per year on average). Such variations in environmental patterns have already
181 shown to lead to population declines in natural shrublands (Paniw et al., 2023).
182 Dewy pines will therefore likely be increasingly affected by interactions of climate
183 change and human disturbance. Therefore, understanding their response to climate
184 effects will help us discern the joint role of different pressures on plants persisting in
185 anthropogenic habitats.

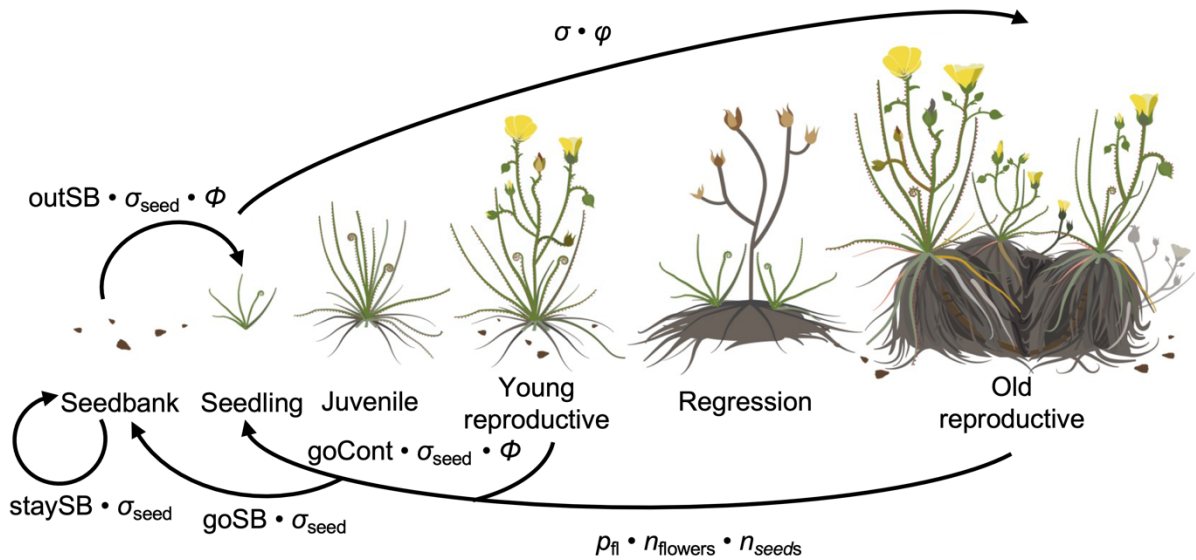
186

187 *Demographic data*

188

189 We used individual demographic data collected on 4753 dewy pines from eight
190 populations of southern Spain, located in two types of habitats: Mediterranean
191 heathlands experiencing recurrent fire regimes and low levels of anthropogenic
192 pressures such as cattle browsing and trampling (natural populations); and
193 mediterranean heathlands that have not burned in the past 40 years but where high
194 anthropogenic pressures constantly remove aboveground vegetation (anthropogenic
195 populations) (see Appendix S1 for details).

196



197 **Figure 1 – Dewy-pine life cycle.** After a fire, conditional on seed survival
 198 (σ_{seed}), seeds in the seedbank germinate to become seedlings of a given size (Φ)
 199 conditional on germination probability ($outSB$), or remain dormant underground
 200 ($staySB$). Individuals then grow conditional on survival and size at the next timestep
 201 (σ and φ) and become reproductive from two years after a fire occurred. Reproductive
 202 individuals produce seeds conditional on flowering probability (ρ_{fi}), the number of
 203 flowers ($n_{flowers}$), and the number of seeds per flower (n_{seeds}). These seeds, conditional
 204 on their survival (σ_{seed}), either germinate directly ($goCont$) and become seedlings of a
 205 given size (Φ) or contribute to the underground seedbank ($goSB$).

206

207 Estimation of seedbank parameters

208

209 To quantify the probabilities of seed germination ($goCont$ for seeds germinating
 210 without going to the seedbank and $outSB$ for seeds germinating from the seedbank),
 211 dormancy ($staySB$) and transition to the seedbank ($goSB$) (Fig. 1), we used data

212 from seed-burial and greenhouse germination experiments (Paniw, Quintana-
213 Ascencio et al., 2017; Gómez-González et al., 2018). In natural populations, most
214 produced seeds (97.4%; 95% CI [96.3%–98.4%]) go to the underground seedbank
215 (Appendix S1: Table S1). While 81% [77.4%–85.2%] of the seeds germinate from the
216 seedbank right after a fire (TSF₀), that proportion greatly decreases in later post-fire
217 habitat stages (6.09% [4.44%–7.75%] in TSF₁ and 3.47% [2.31%–4.63%] in later
218 TSFs). In contrast, in chronically disturbed, anthropogenic populations, a much lower
219 proportion of the produced seeds goes to the seedbank (82.2% [65.3%–97.5%]). In
220 these populations, although 59.8% [56.6%–63.0%] of the underground seeds remain
221 underground, seedbanks are depleted due to the decreased proportion of seeds
222 produced by aboveground plants entering dormancy.

223

224 Estimation of aboveground vital rates

225

226 We investigated how rainfall, temperature, and density affect the survival, growth,
227 and reproduction of individuals in natural and anthropogenic dewy-pine populations.
228 We used Generalised Additive Models—fitted with the *gam* function of the *mgcv*
229 package (Wood, 2011; Wood et al., 2016; Wood, 2017)—to estimate (1) survival (σ)
230 and flowering probability (p_{fi}) (using a binomial distribution), (2) the number of flowers
231 per individual ($n_{flowers}$; using a negative binomial distribution), and (3) growth (φ) and
232 seedling size (Φ), with size = log(number of leaves × length of the longest leaf) (Fig.
233 1; Paniw, Quintana-Ascencio et al., 2017). We modelled the latter two vital rates
234 using a scaled *t* distribution (“scat” in the family parameter of the *gam* function)
235 instead of a Gaussian distribution to accommodate the heavy-tailed nature of the
236 response variables. We tested for the nonlinear responses of all vital rates to lag

237 cumulative rainfall and average daily maximum temperature, and aboveground
238 density of large (i.e., size > 4.5) intraspecific neighbours. In addition, to account for
239 effects of post-fire habitat stages, we tested for nonlinear effects of time since fire
240 (TSF) on vital rates of natural populations. We used a cubic spline basis with three
241 dimensions ($k = 3$) for all these covariates (except for the size effect on the number
242 of flowers, where we used $k = 4$ to model a decline in the number of flowers of large
243 individuals as has been observed in all populations), and a gamma value of 1.4, as is
244 commonly used to reduce the risk of overfitting (Wood, 2017). We also included
245 random year and population effects in all models using a random-effect spline. We
246 performed all analyses in R 4.2.2 via RStudio (R Core Team, 2022; Posit team,
247 2023).

248

249 *Vital-rate responses to climatic variables (cumulative rainfall and*
250 *average maximum daily temperature)*

251

252 We extracted daily rainfall and maximum temperature data with a resolution of 0.1
253 degree for all dewy-pine population locations from the E-OBS dataset from the EU-
254 FP6 project UERRA and the Copernicus Climate Change Service (Cornes et al.,
255 2018; see Appendix S2 for details). We obtained the monthly cumulative rainfall and
256 average maximum temperature in each population by averaging the values recorded
257 within a buffer of 0.1×1.5 degrees (i.e. 1.5 times the grid resolution) around the
258 population coordinates. We assessed the presence of rainfall and temperature lag
259 effects on dewy-pine vital rates using GAMs including cumulative rainfall and
260 average maximum daily temperature across several biologically relevant periods. For
261 survival and growth, we assessed the effect of climate following the annual

262 population census (set to the 1st of May), while for reproductive parameters (i.e.,
263 flowering probability, number of flowers, and seedling size), we assessed the effect
264 of climate in periods prior to the census. More specifically, we considered the effect
265 of post-census average maximum temperature in summer (May–September) and of
266 cumulative rainfall in fall (September–November), winter (January–April), or both
267 (September–April), on survival and growth. We tested for the effect of pre-census
268 average maximum daily temperature in winter (January–April), and of cumulative
269 rainfall in fall (September–November) and winter (January–April) on reproductive
270 rates. We considered that the effects of longer lag periods are effectively absorbed
271 by changes in plant size.

272

273 *Vital-rate responses to large aboveground individual density*

274

275 To understand how intraspecific interactions affect dewy-pine vital rates, we included
276 in our models the density of aboveground individuals, specific to a 1-m² quadrat in a
277 given population. This spatial resolution matches the study design—where plants are
278 censused in four transects of ten 1-m² quadrats (Paniw, Quintana-Ascencio et al.,
279 2017)—and corresponds to the observed scale at which the plant-plant interactions
280 affecting the demography of dewy pines occur. We only considered individuals of
281 size > 4.5, which corresponds to the minimum observed size of reproductive plants.
282 Smaller plants are largely seedlings which have relatively weak effects on plant vital
283 rates, as large individuals are unlikely to be affected by small plants and small plants
284 are primarily affected by large shrubs (Brewer et al., 2021). We did not use a
285 spatially explicit formulation of density dependence (e.g. using the crowding
286 approach described in Adler et al., 2010), as such an approach requires knowledge

287 of the spatial distribution of individuals and seeds, which we lacked for some sites
288 and years.

289

290 *Vital-rate model selection*

291

292 We selected the best vital-rate models using the Akaike Information Criterion (AIC,
293 using a threshold of $\Delta AIC > 2$ to identify a model as performing better than another;
294 Burnham et al., 2011; Wood, 2017) and the number of degrees of freedom. Prior to
295 model selection, we standardised and checked for correlations between all
296 covariates (see Appendix S1 for more details). We first selected the best lag period
297 for the effect of rainfall and temperature and then added—in a forward selection
298 framework—density and size to the model selection and, for natural populations,
299 time since last fire (Appendix S1: Table S3 for more details). We considered
300 interactions among the climatic variables, density, size, and TSF as well as site-
301 specific random slopes (e.g., site-specific effects of density or size) in our model
302 selection, using random-effect splines.

303

304 Population projections under climate change scenarios

305

306 *Individual-Based Model definition*

307

308 We used the estimated vital rates to parameterize an Individual-Based Model (IBM)
309 and project each natural and anthropogenic dewy-pine population under current and
310 predicted climate conditions. The following is a summary of the IBM specificities; a
311 more detailed description of the different modules of the projection model following

312 the ODD (Overview, Design concepts, Details) protocol (Grimm et al., 2006; 2020)
313 can be found in Appendix S3. We performed 500 30-year projections of each dewy-
314 pine population under two scenarios: (1) a control scenario corresponding to current
315 climatic conditions where 30 years—and the corresponding rainfall and temperature
316 values—were sampled at random among the past observed ones (2016–2021); and
317 (2) a climate-change scenario where the rainfall and temperature values
318 corresponded to projected climatic conditions from 2021 to 2050 according to the
319 RCP8.5 climate-change scenario (Riahi et al., 2011). The climate-change scenario
320 comprised 11 sets of 500 population projections, each set corresponding to future
321 rainfall and temperature conditions extracted from 11 global circulation models
322 (GCM; Appendix S2: Table S2) from the Coupled Model Intercomparison Project 6
323 (CMIP6; Eyring et al., 2016; Pascoe et al., 2020; Waliser et al., 2020) available from
324 the Earth System Grid Federation’s (ESFG; Petrie et al., 2021) web application
325 accessible at <https://aims2.llnl.gov/search>. These models have been used in several
326 studies on ecological systems (Tredennick et al., 2016; Paniw et al., 2022) and differ
327 in their parameterisation, enabling us to project the dewy-pine populations under a
328 wide range of possible future climatic conditions and thereby reduce bias in our
329 population projections (Sanderson et al., 2015).

330

331 Because most GCMs comprised projected rainfall and temperature values beyond
332 the values observed in our populations, we capped these values to the maximum
333 and minimum observed. This approach, as well as using RCP8.5, which is the most
334 extreme climate-change scenario, allowed us to investigate the response of dewy-
335 pine populations to substantial increases in the frequency of extreme climatic
336 conditions, rather than changes in absolute rainfall and temperature values.

337

338 Each population projection started with a population vector of z -sized individuals
339 from 2021—the last year used to estimate vital rates—, and the initial population
340 thus comprised individuals observed in the population in that year. This also applies
341 to the initial rainfall and temperature values, and the aboveground density of large
342 individuals. While we assumed no fire occurred in anthropogenic populations, we
343 simulated a sequence of 30 post-fire habitat stages for each projection of natural
344 populations. The first post-fire state corresponded to the one observed in 2021, and
345 the subsequent ones were determined based on a Markov matrix containing the
346 among-TSF transition probabilities based on a fire frequency of $1/30$ representing
347 the stochastic fire regime occurring in natural dewy-pine populations (see Appendix
348 S3 for details; see also Conquet et al., 2023).

349

350 We projected each initial population in discrete yearly steps determining which
351 aboveground individuals reproduced, survived, and grew, and how many seeds
352 germinated—from the seedbank or directly after reproduction—or entered or
353 remained in the seedbank. As annual censuses took place during the flowering
354 period (pre-reproductive census), each projected year started with the reproduction
355 sub-model. This sub-model sampled reproductive individuals (0 or 1) based on a
356 binomial distribution parameterised with the estimated mean flowering probability
357 (p_{fl}). If any individual reproduced, its number of flowers was sampled from a negative
358 binomial distribution based on the estimated mean number of flowers per plant
359 ($n_{flowers}$); and the number of seeds per flower (n_{seeds}) was sampled from a Poisson
360 distribution with a mean of 9.8—the average number of seeds per flower used in
361 Paniw et al. (2017). To avoid excessive reproductive values in natural populations,

362 we capped the number of flowers per individual to the maximum observed number of
363 flowers in each population. In natural populations, where fires could occur, the
364 reproduction sub-model was skipped in the first year after fire, as dewy pine adults
365 are killed by fire and postfire recruits do not reproduce until two years after
366 germination.

367

368 The reproduction sub-model was followed by the survival and growth sub-model,
369 which sampled the surviving individuals from a binomial distribution based on the
370 mean estimated survival rate, and assigned them a size to which they would grow at
371 the next time step by sampling from a scaled t distribution (to accommodate for
372 heavy-tailed size values when fitting the growth model) based on the mean, standard
373 deviation, and degrees of freedom of the fitted growth model. Sporadically sampled
374 positive infinite sizes were set to the maximum observed size in the population in the
375 currently projected year, while negative infinite sizes were set to zero.

376

377 Finally, at the end of each projected year, the seedbank sub-model sampled seeds
378 from the seedbank that remained dormant or germinated from binomial distributions
379 based on the respective probabilities (staySB and outSB). The seeds that did not
380 survive—i.e., neither germinated or stayed dormant—were removed from the
381 seedbank. The seeds germinating without going through the seedbank were
382 sampled from a binomial distribution based on the probability of continuous
383 germination (goCont). Some seedbank processes are hidden processes that cannot
384 be easily determined in the field without perturbing the populations. To reduce the
385 resulting bias, we applied a correction factor representing seed survival (σ_{seed}) to the
386 seedbank parameters in anthropogenic populations (see Appendix S1 and Paniw,

387 Quintana-Ascencio et al., 2017 for more details), and further corrected outSB and
388 goCont in Sierra Carbonera Disturbed by reducing them to 40 % of their values. We
389 also capped the number of recruits to the maximum number of seedlings observed in
390 all natural populations as well as in two anthropogenic populations: Bujeo and Sierra
391 Carbonera Disturbed. Ultimately, all recruits were assigned a size by sampling from
392 a scaled t distribution based on the estimated mean seedling size as well as its
393 standard deviation and degrees of freedom.

394

395 At the end of a projected year, we updated the size of individuals that grew during
396 the previous year as well as the aboveground density for each 1-m² quadrat in the
397 population. We also calculated and recorded the annual population growth rate
398 (annual $\log \lambda$), which we used to calculate the stochastic growth rate $\log \lambda_s$ for each
399 projection (see Appendix S3 for more details; see also Conquet et al., 2023). In each
400 projection, the population was considered extinct if it went below the quasi-extinction
401 threshold set at 5 aboveground individuals and 50 seeds in the seedbank.

402

403 *Model validation*

404

405 We calibrated our vital-rate and individual-based models by projecting each dewy-
406 pine population from the year it was first censused to 2022. We then compared
407 observed and projected aboveground population sizes and population growth rates,
408 as well as individual size distributions across time. For natural populations, we used
409 the observed post-fire habitat stages and did not simulate fire frequencies. This
410 process enabled us to validate our IBM by assessing its ability to well represent the

411 dynamics of the dewy-pine populations in years that were not used in the model-
412 fitting part of our analysis (i.e., years before 2016 when available, and 2022).

413

414 **Results**

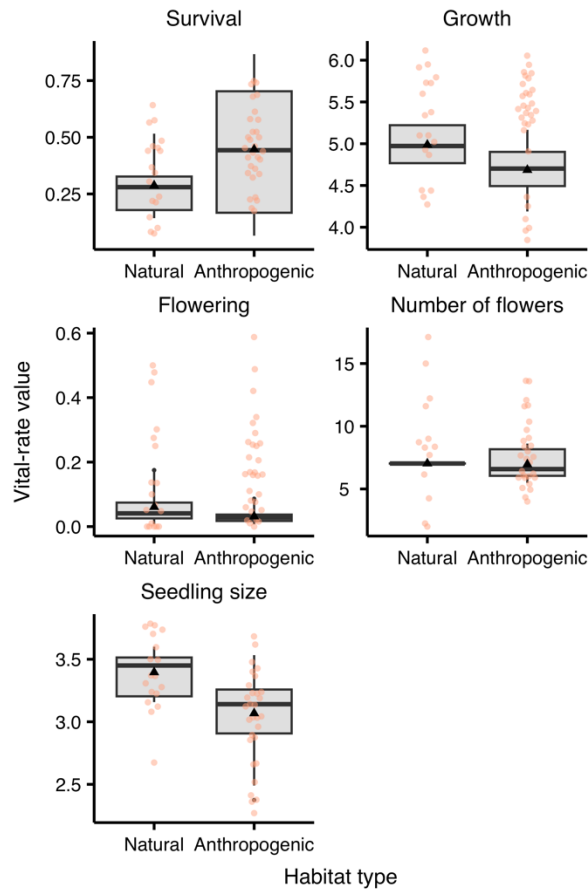
415

416 Vital-rate responses to habitat disturbance

417

418 Dewy-pine vital rates varied between natural and anthropogenic habitats (Fig.
419 2). Survival was on average higher in anthropogenic (mean = 0.42 and 95%
420 confidence interval = [0.18, 0.70]) than in natural habitats (0.27 [0.17, 0.40]; Fig. 2).
421 In contrast, we found the opposite pattern for growth, which was higher in natural
422 (size 5.0 [4.7, 5.2] at the next time step, calculated as $\log(\text{number of leaves} \times \text{length}$
423 $\text{of the longest leaf})$) than in anthropogenic sites (4.7 [4.4, 4.9]), as well as flowering
424 probability (0.039 [0.013, 0.11] in natural and 0.025 [0.013, 0.045] in anthropogenic
425 populations), and seedling size (3.4 [3.2, 3.5] and 3.0 [2.8, 3.3], respectively; Fig. 2).
426 However, there was no difference between habitat types in the number of flowers per
427 individual (6.9 [6.2, 7.7] on average in natural populations and 6.7 [5.8, 7.8] in
428 anthropogenic populations; Fig. 2). Notably, we found more among-site variation in
429 anthropogenic than in natural conditions, possibly because the level of
430 anthropogenic disturbance differed between sites (Appendix S1: Fig. S3).

431
432
433
434
435
436
437
438
439
440
441



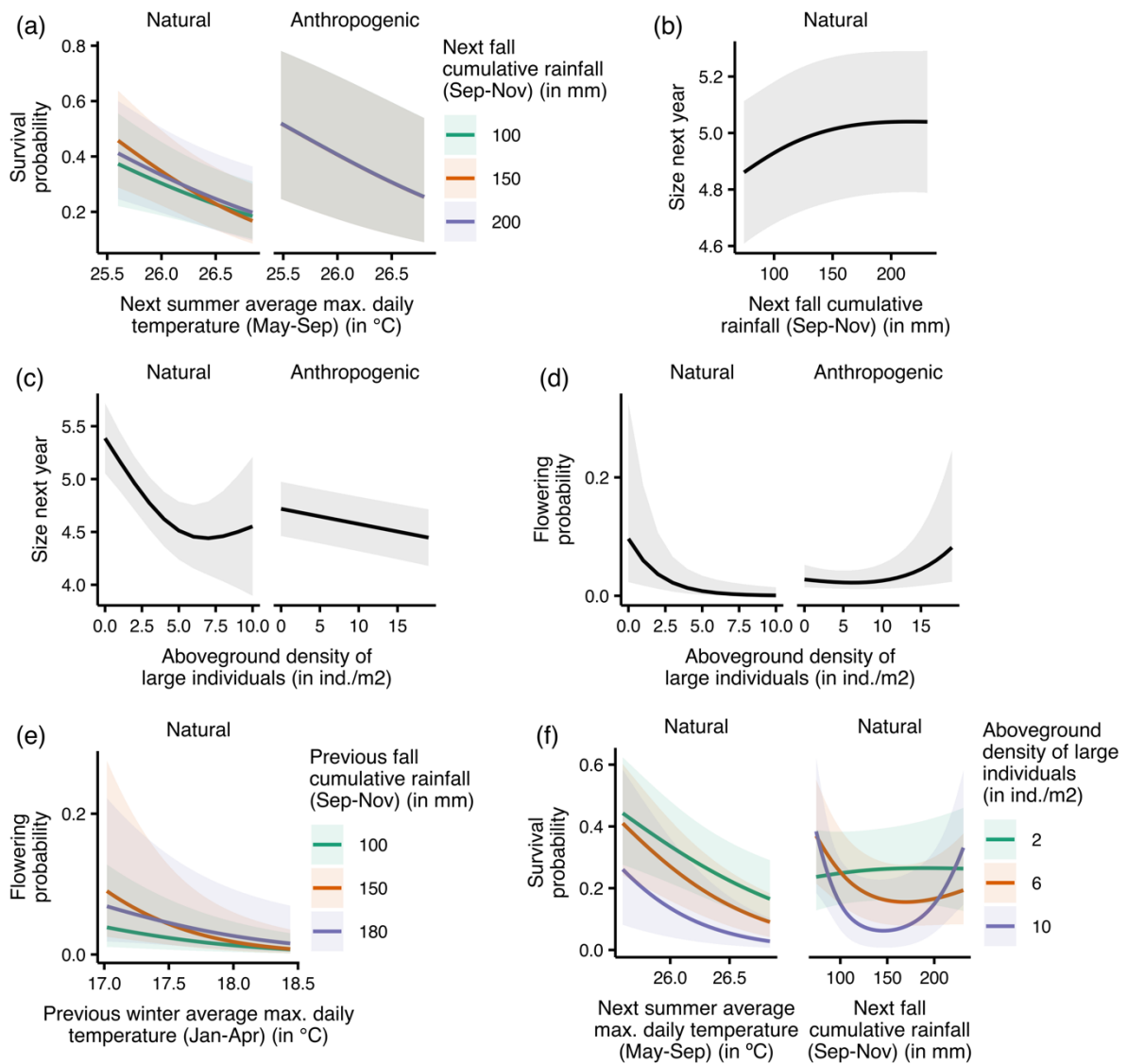
442
443
444
445
446
447
448
449
450

Figure 2 – Predicted and observed average vital-rate values in natural and anthropogenic populations. The boxplots represent the distribution of the predicted average values of habitat-specific survival, growth, and flowering rates, as well as the number of flowers and seedling size estimated for each population and year from GAMs. The whiskers represent the 2.5th and 97.5th percentiles and the black triangle the mean estimate. We kept covariates at their mean values (scaled value = 0) except for the number of flowers, where we used the mean size of reproducing individuals. The coloured dots represent the observed average vital rates in each population and year.

451 Vital-rate responses to climatic variables

452

453 In both anthropogenic and natural habitats, the variation of most vital rates was
454 associated with changes in at least one of the two climatic variables considered in
455 our analysis: monthly cumulative rainfall (hereafter rainfall) or monthly average daily
456 maximum temperature (hereafter temperature) (Fig. 3; Appendix S1: Table S4). Most
457 vital rates were more strongly associated with the same climatic variable in the same
458 period of the year in both habitats (e.g. variation in survival was associated with
459 changes in summer temperatures and fall rainfall in both natural and anthropogenic
460 populations). Overall, larger variations in vital rates were associated with changes in
461 temperature than with rainfall (Fig. 3; Appendix S1: Table S4).



462 **Figure 3 – Relationships between dewy-pine vital rates and climatic**
 463 **variables and aboveground density of large individuals.** Predictions from the
 464 GAM models show variation in (a) survival and (b) flowering probability with changes
 465 in temperature (next summer and previous winter, respectively) and rainfall (next and
 466 previous fall), (c) flowering probability with changes in previous fall rainfall and
 467 density, and growth with (d) changes in next fall rainfall, and (e) aboveground density
 468 of large individuals (size > 4.5). Lines show the mean vital-rate values and shaded
 469 areas the associated 95% confidence interval.
 470

471 In both natural and anthropogenic populations, survival was the only vital rate for
472 which variation was associated with changes in both rainfall and temperature (i.e.,
473 the fixed effects of both climatic variables were retained in the model selection). With
474 all other covariates held constant at their average value in the respective habitat
475 types, survival was negatively associated with an increase in summer temperatures
476 (i.e., average maximum daily temperature from May to September) (Fig. 3a). For
477 example, when temperature increased from 25.5 to 26.5 °C, the average survival
478 rate decreased from 0.47 [0.29, 0.66] to 0.23 [0.14, 0.35] in natural populations, and
479 from 0.51 [0.24, 0.78] to 0.31 [0.12, 0.60] under anthropogenic conditions. In both
480 habitats, variation in survival was also associated with changes in the amount of
481 rainfall in fall (i.e., September–November; Fig. 3a, Appendix S1: Table S4 and Fig.
482 6e). In natural populations, this association was on average positive (from 0.25 [0.14,
483 0.39] under 80 mm of rain to 0.28 [0.16, 0.45] under 200 mm). In contrast, in
484 anthropogenic populations, average survival across sites did not change with rainfall,
485 but investigating this relationship at the site level revealed important among-
486 population variability, with positive associations in some sites (e.g. from 0.39 [0.16,
487 0.67] under 80 mm of rain to 0.46 [0.21, 0.74] under 200 mm in Sierra del Retín
488 Disturbed) and negative associations in others (e.g. from 0.46 [0.21, 0.74] to 0.36
489 [0.15, 0.65] in Prisioneros; Appendix S1: Fig. S3). Such among-site differences were
490 almost ubiquitous across vital rates in anthropogenic populations (Appendix S1: Fig.
491 S4), but not in natural habitats. For example, on average across all natural sites,
492 individuals grew more with higher amounts of rainfall. More specifically, the longest
493 leaf of an average-sized individual grew from 4.3 to 4.9 [4.6, 5.1] in a year under 80
494 mm of rain but to 5.0 [4.8, 5.3] under 200 mm (Fig. 3b).

495

496 Vital-rate responses to aboveground density of large plants

497

498 In both anthropogenic and natural habitats, plants grew less when densities of
499 large individuals increased (Fig. 3c). Under human disturbance, an average-sized
500 individual grew from 4.1 to 4.7 [4.4, 4.9] in a year with 2 large individuals/m² but to
501 4.6 [4.3, 4.8] with 10 ind./m² (Fig. 3c). In natural conditions, an individual grew from
502 4.3 to 5.0 [4.7, 5.2] with a density of 2 ind./m² but only to 4.6 [3.9, 5.2] with 10 ind./m²
503 (Fig. 3c). Seedling size also decreased with higher numbers of large individuals
504 aboveground (Appendix S1: Fig. S5a). Interestingly, the direction of the association
505 between density and flowering probability differed between habitat types, as the
506 flowering rate was positively associated with density in anthropogenic populations
507 (from 0.50 [0.28, 0.72] with 2 ind./m² to 0.65 [0.35, 0.86] with 15 ind./m²), but strongly
508 negatively in natural ones (from 0.68 [0.41, 0.87] with 2 ind./m² to 0.10 [0.013, 0.50]
509 with 7 ind./m²) (Fig. 3d).

510

511 Vital-rate responses to interactions between climate, density, size,
512 and post-fire habitat conditions

513

514 In natural—but not in anthropogenic—populations, high amounts of rainfall
515 mitigated the strength of the negative association between temperature and survival,
516 which decreased from 0.48 [0.30, 0.67] at 25.5 °C to 0.23 [0.14, 0.36] at 26.5 °C
517 under 150 mm of rainfall but only from 0.43 [0.26, 0.63] at 25.5 °C to 0.25 [0.13,
518 0.41] at 26.5 °C under 200 mm (Fig. 3a). We found a similar pattern for the
519 association between previous winter temperatures and flowering probability, which

520 decreased from 0.72 [0.45, 0.89] at 17.5 °C to 0.29 [0.076, 0.66] at 18.5 °C with 150
521 mm of rain but only from 0.73 [0.43, 0.90] to 0.46 [0.15, 0.80] with 180 mm (Fig. 3e).

522

523 Additionally, in natural populations, survival increased with rainfall at low densities
524 (Fig. 3f; from 0.26 [0.16, 0.40] to 0.28 [0.16, 0.44] for 100 and 200 mm of rain at 2
525 ind./m²); but these variables had a u-shaped relationship at high densities, with
526 lowest survival rates reached for about 145 mm of rain (e.g. 0.076 [0.021, 0.24] at 10
527 ind./m²). The decline in survival with increasing summer temperatures was also
528 weaker at low (e.g. from 0.47 [0.29, 0.66] at 25.5 °C to 0.22 [0.14, 0.35] at 26.5 °C
529 with 2 ind./m²) than at high densities (from 0.45 [0.26, 0.65] to 0.14 [0.077, 0.25] with
530 6 ind./m²) (Fig. 3f). We also found density-dependent variation in flowering
531 probability and growth with rainfall and seedling size with temperature (Appendix S1:
532 Fig. S5). Additionally, the strength and direction of the association between survival
533 rates and both rainfall and temperature in natural populations were also size
534 dependent (Appendix S1: Fig. S6g,h).

535

536 Individual Based Model

537

538 *Population projections*

539

540 The projections of our individual-based model over the observed period
541 showed that our parameterization enabled us to correctly represent the population-
542 specific pattern of changes in mean annual change in aboveground population size
543 and of population abundance (Fig. 4; Appendix S1: Fig. S1). Additionally, observed

544 and projected time-varying size distributions were largely overlapping, with a slight
 545 bias towards small individuals in some populations (Appendix S1: Fig. S2).

546

547

548

549

550

551

552

553

554

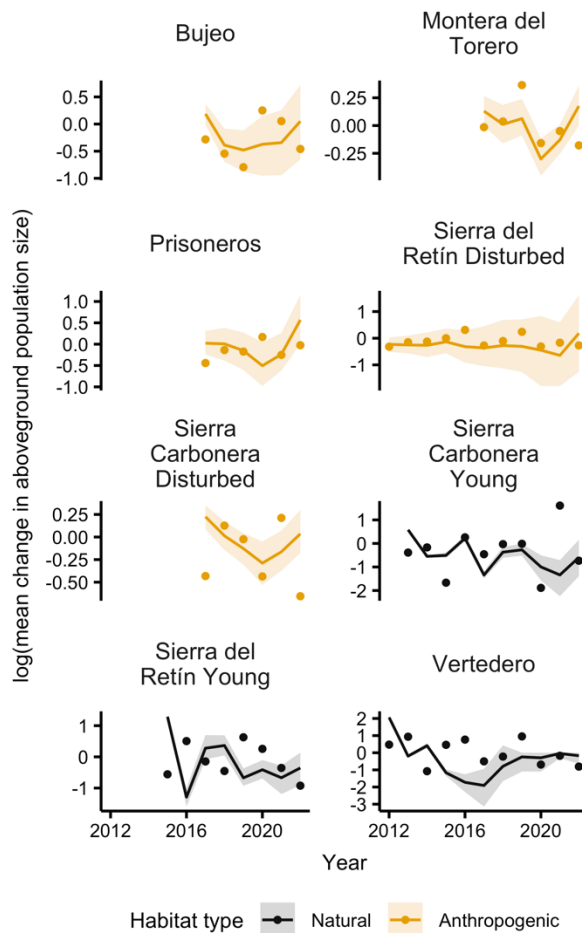
555

556

557

558

559



560

Figure 4 – Observed and projected average change in aboveground

561 **population abundance.** We projected each natural and anthropogenic population

562 for 500 times across the range of observed years available for each population

563 (maximum range from 2011 to 2022) to perform an out-of-sample validation of our

564 individual-based model parameterization. For each projection, we calculated the log

565 of the average change in aboveground population abundance between years (i.e.,

566 $\log(N_t/N_{t-1})$ with N_t the aboveground population size in year t) and obtained the

567 average (line) and 25th and 95th percentile of the population-specific distribution

568 (shaded ribbon). We compared these projected values to the observed ones (dots).

569

570 Projecting natural and anthropogenic populations under a control scenario (i.e.,
571 assuming similar environmental conditions in the future as currently observed)
572 showed that the average population growth rates ($\log \lambda_S$) did not vary much between
573 habitat types (mean = -0.15, 2.5 and 97.5% quantiles = [-0.62, 0.33] in natural and -
574 0.19 [-0.89, 0.63] in anthropogenic populations; Fig. 5). On the other hand, the
575 probability of quasi-extinction (p_{q-ext}) was on average higher in anthropogenic (0.56
576 [0.026, 1.0]) than in natural populations (0.17 [0.062, 0.26]). Extinction probabilities
577 also varied much more among anthropogenic than among natural populations in the
578 control scenario (Fig. 5). In natural populations, the stochastic fire regime in our
579 projections increased the population growth rate substantially after fires, avoiding the
580 quasi-extinction threshold (i.e., 5 aboveground individuals and 50 seeds in the
581 seedbank) in simulations where fires occurred regardless of the population (Conquet
582 et al., 2023). Anthropogenic populations, on the other hand, varied substantially in
583 size, and the high variation in p_{q-ext} reflects the consistently higher variation in
584 dynamics among populations (Appendix S1: Fig. S7).

585
586
587
588
589
590
591
592
593
594
595
596
597
598
599
600
601
602
603
604
605
606
607
608
609

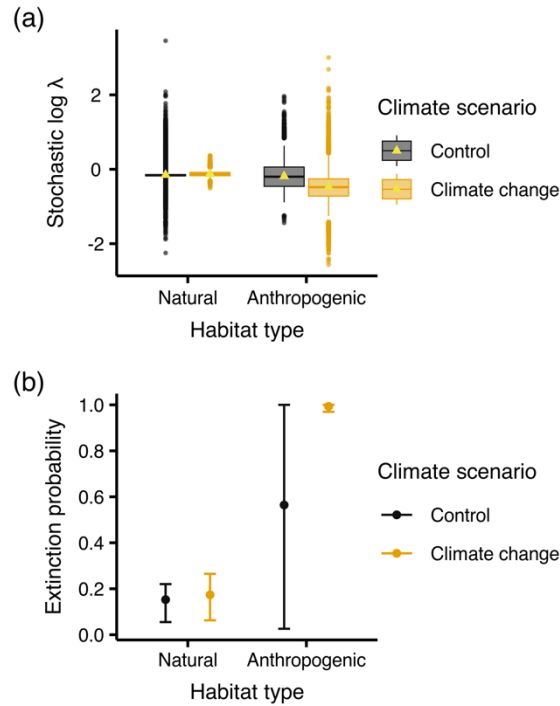


Figure 5 – Demographic consequences of climate change in natural and anthropogenic populations of dewy pines. We projected each natural and anthropogenic population 500 times for 30 years under a control (keeping temperature and rainfall conditions as currently observed) and a climate-change scenario. To assess the demographic consequences of climate change in populations experiencing different levels of human disturbance, we computed for each population: (a) the stochastic population growth rate across 30 years for each population projection ($\log \lambda_S$; including both the seedbank and aboveground individuals) and (b) the probability of quasi-extinction (p_{q-ext}). Here we summarise these metrics per habitat type, and the variability in the values therefore correspond to among-population and among-projection differences.

In contrast with the control scenario, population growth rates differed between habitats under climate change (Fig. 5). While the population growth rate (-0.12 [-

610 0.28, 0.072]) and extinction probability (0.17 [0.070, 0.26]) of natural populations did
611 not vary under climate change, our projections show a decrease in $\log \lambda_S$ in
612 anthropogenic sites (-0.47 [-1.3, 0.45]), accompanied by an increase in the extinction
613 probability (0.99 [0.97, 1.0]).

614

615 **Discussion**

616

617 Our individual-based models projecting natural and anthropogenic populations
618 of dewy pines using habitat-specific survival, growth, and reproductive rates revealed
619 that the current decline of anthropogenic populations will worsen under climate
620 change, leading to increased extinction risk. While the increasing frequency of
621 extreme high summer temperatures affected both natural and anthropogenic
622 populations negatively, occasionally high rainfall and compensatory density
623 dependence greatly reduced this effect in natural populations. Under chronic,
624 anthropogenic disturbance, however, the decline in survival was not compensated by
625 either of these factors. Consequently, with the frequency of extreme climatic
626 conditions increasing under climate change, populations in anthropogenic habitats—
627 which are currently already decreasing—were negatively affected by future climatic
628 conditions. Habitat dynamics shaped by fires also dominated the effects of
629 environmental perturbations in natural habitats, highlighting the importance of fire
630 regimes in Mediterranean heathlands (Ojeda, Pausas, and Verdú, 2010; Keeley et
631 al., 2011). Adaptations to anthropogenic disturbances meanwhile can lead to
632 changes in vital-rate responses to climate and density, with detrimental
633 consequences on population persistence. The implications of our findings extend
634 beyond ecological theory, offering tangible guidance for conservation policies. By

635 showing the consequences of climate and land-use changes in non-protected
636 habitats, our study provides a foundation for informing relevant stakeholders and
637 developing management strategies that protect biodiversity in the Mediterranean
638 biome, where interacting effects of local and global anthropogenic pressures affect
639 population viability.

640

641 Land-use change (e.g. grazing) often has stronger effects on populations than
642 climate change (Sirami et al., 2017). However, few studies assess the consequences
643 of interactions between these two environmental pressures on population dynamics,
644 despite evidence of land-use change mediating the effect of climate change on
645 species abundance and diversity (Mantyka-Pringle, Martin, and Rhodes, 2012; Oliver
646 and Morecroft, 2014). Such interactions are likely to be strong drivers of population
647 dynamics in habitats such as Mediterranean heathlands, which are among the
648 ecosystems most affected by climate and land-use change (Newbold et al., 2020),
649 the latter leading to changes in disturbance regimes in the habitats. Consequently,
650 interactions between these two pressures might have strong effects on systems such
651 as the dewy pine, where we observe differences among disturbance levels in vital-
652 rate responses to climate, density, and their interactions among natural and highly
653 disturbed habitats. Our projections of natural and anthropogenic dewy-pine
654 populations under climate change indicate that future changes in climate
655 environmental conditions will spare populations in natural habitats but will have
656 adverse effects on populations experiencing anthropogenic disturbances, which is
657 the majority of dewy pine populations (Garrido et al., 2003), as well as many other
658 Mediterranean shrublands (Newbold et al., 2020).

659

660 As previously observed in our study populations, anthropogenic disturbances not
661 only lead to increased continuous seed germination and decreased seed dormancy
662 (Appendix S1), but also allowed aboveground individuals to survive longer in the
663 absence of shrub encroachment (Paniw, Quintana-Ascencio et al., 2017).
664 Consequently, dewy pines in chronically disturbed, anthropogenic habitats reached
665 higher sizes than those in natural habitats. This is contrary to many studies
666 assessing trait-level consequences of land-use change—and more specifically
667 grazing—on plants. In these studies, plants in grazed sites adapted to this
668 disturbance by shrinking over time to avoid being consumed by herbivores (Fischer
669 et al., 2011; Kerns et al., 2011; Völler et al., 2017). However, with their mucilage-
670 covered leaves, dewy pines are not palatable to herbivores (Ojeda et al., 2021), and
671 therefore do not require such an adaptation. On the contrary, the small amount or
672 absence of damage dealt to plants by herbivores along with the removal of other
673 plants and the subsequent release of both intra- and interspecific competition, might
674 allow dewy pines in anthropogenic populations to grow without surrounding
675 vegetation hampering their nutrient acquisition (Paniw et al., 2018) and growth
676 (Grime, 1973; Hjalten et al., 1993; Kambatuku et al., 2011; Fig. 3c).

677

678 While anthropogenic disturbances allow dewy pine plants to survive and grow better
679 than in natural conditions, this comes at the cost of reproduction, with flowering
680 probability decreasing in the largest individuals. Although the consequences of land-
681 use change on plant reproduction are clearly species- and site-dependent (Kerns et
682 al., 2011; Völler et al., 2017), tradeoffs similar to those observed in our populations
683 are common across taxa (Stearns, 1989). Such negative correlations between vital
684 rates might be more striking under stressful conditions such as low resource

685 availability (Villemas & García, 2018). This might be the case in anthropogenic
686 populations of dewy pines particularly. Plants rely almost exclusively on capturing
687 prey invertebrates for nutrient uptake (Paniw, Gil-Cabeza et al., 2017; Skates et al.,
688 2019). In natural populations, invertebrates, especially insect pollinators, are
689 abundant after fires, when many post-fire ephemeral species flower, and dewy pine
690 plants are more conspicuous to insects, thus facilitating prey capture and nutrient
691 uptake (Paniw et al., 2018). In anthropogenic habitats, intense browsing or
692 mechanical vegetation removal are likely to decrease invertebrate abundances with
693 respect to natural sites (Mayer, 2004; Carpio et al., 2014). When shrub cover is
694 chronically low or sparse, dewy pine plants are more conspicuous to prey insects but
695 they may also be more exposed to wind and solar radiation, thus resulting in
696 relatively more stressful environmental conditions (Paniw et al., 2018). In turn, while
697 populations in these chronically disturbed, anthropogenic habitats appear to persist,
698 a low reproductive output may generate an extinction debt, where the population
699 structure is skewed towards old individuals that cannot be replaced in the long term
700 (Matías et al., 2019).

701

702 Adverse disturbance effects on vital rates can be exacerbated under unfavourable
703 climatic conditions (e.g. Hindle et al., 2023; see also; Nolan et al., 2021 and
704 references therein). Plants commonly suffer from extreme temperatures and drought,
705 which affect individuals through processes such as heat stress, photosynthesis
706 inhibition, or reduced soil moisture and water resources (e.g. Larcher, 2000;
707 McDowell et al., 2008; Nolan et al., 2021). While dewy pines are somewhat adapted
708 to dry and hot summer conditions (Darwin 1875; Adlassnig et al., 2006; Adamec,
709 2009), survival greatly decreased with increasing summer temperatures. In addition

710 to the aforementioned processes reducing the survival of plants experiencing high
711 temperatures, such extreme conditions could lead to a great reduction in prey
712 availability. These carnivorous subshrubs indeed rely on droplets of mucilage on
713 their leaves to capture insects, from which they obtain nutrients (Paniw, Gil-Cabeza
714 et al., 2017). However, increasing temperatures and the subsequent decrease in
715 humidity could prevent plants from forming these droplets, and thereby from
716 accessing these resources.

717

718 Rainfall also played an important role in shaping dewy-pine demography. In addition
719 to limiting water resources (McDowell et al., 2008), extremely low amounts of rain do
720 not provide enough moisture for dewy pines to produce mucilage on their leaf-traps
721 (Darwin 1875; Adlassnig et al., 2006; Adamec, 2009). As a result, plants might not
722 get enough nutrients to allocate to the different demographic processes. However, in
723 natural populations, high amounts of rainfall seemed to slightly buffer negative
724 temperature effects, likely by compensating the low humidity and water resources
725 under high temperatures. This process did not seem to occur in anthropogenic
726 populations, where the increased exposure to extreme temperatures due to sparse
727 vegetation cover might be too intense to counterbalance.

728

729 In addition to interactions between climatic variables, density-dependent effects of
730 climate are common across taxa and can play a key role in shaping population
731 dynamics, for example by enhancing or mitigating adverse environmental effects
732 (Gamelon et al., 2017; Paniw et al., 2019). In plant populations, vital-rate density
733 dependence can be attributed to two main biological processes: competition (e.g. for
734 light or pollinators; Craine & Dybzinski, 2013) and facilitation (i.e., the positive effect

735 of neighbours on a focal individual, e.g., through shading or protection from
736 herbivory; Callaway & Pugnaire, 2007; Graff et al., 2007; Le Bagousse-Pinguet et al.,
737 2012). According to the stress-gradient hypothesis, variations in environmental
738 conditions can lead to shifts between these two processes in a given population
739 (Bertness & Callaway, 1994; Maestre et al., 2005), for example under increased
740 levels of disturbance (Graff et al., 2007; Villarreal-Barajas & Martorell, 2009; Le
741 Bagousse-Pinguet et al., 2012) or extreme climatic conditions (Callaway & Pugnaire,
742 2007; Grant et al., 2014; Olsen et al., 2016). This was the case in dewy pines, where
743 intraspecific density had opposite effects on some vital rates between natural—
744 where competition prevailed—and anthropogenic populations—where facilitation
745 was at play.

746

747 As commonly observed in plant communities (Villalobos et al., 2016; Adler et al.,
748 2018), increasing intraspecific densities in natural conditions led to declining
749 survival—with the exception of early post-fire conditions, where facilitation generally
750 predominates in fire-adapted plant communities (Vilà & Sardans, 1999; Paniw et al.,
751 2018). For dewy pines, in addition to the more common resources for which plants
752 compete (e.g. light or pollinators), such negative effects of conspecifics on survival
753 could arise from competition for prey (Craine & Dybzinski, 2013). Contrastingly,
754 individuals in anthropogenic populations benefited from higher intraspecific densities.
755 In addition to the competition release stemming from the removal of surrounding
756 vegetation (Catling et al., 2024), increasing levels of disturbance such as browsing
757 might lead to a shift from competition to facilitation, as neighbours might act as a
758 barrier against browsers (Le Bagousse-Pinguet et al., 2012).

759

760 In addition to the consequences on vital rates, future increases in temperatures and
761 decreases in rainfall under climate change are expected to lead to higher frequency
762 and intensity of wildfires (Turco et al., 2019; Nolan et al., 2021). In populations where
763 land-use change led to seedbank depletions through increase in continuous
764 germination and dormancy loss, returning fire regimes will likely have strong
765 negative consequences on population persistence, as reduced soil seedbanks will
766 not be enough to replenish populations following the removal of aboveground
767 individuals by fire. Decrease in the ability of fire-adapted plants to germinate or
768 resprout after more frequent and intense fire could have dramatic consequences for
769 the persistence of plant communities in fire-prone habitats (Enright et al., 2015;
770 Nolan et al., 2021).

771

772 Overall, our findings highlight the existence of demographic responses to climate
773 and land-use change and call for conservation policies taking into account the
774 detrimental effects of climate change on populations persisting under human
775 alterations to their habitats, more specifically in fire-adapted systems. Moreover,
776 species-specific effects of interactions between climate and land-use change
777 highlight the need for studies assessing these effects at the community level—
778 accounting for the effects of both climate and intra- and inter-specific density—to
779 understand how interactions between these pressures might affect fire-prone and
780 more generally anthropogenic landscapes.

781 **References**

782

783 Adamec, L. (2009). Ecophysiological Investigation on *Drosophyllum Lusitanicum*:

784 Why Doesn't the Plant Dry Out? *Carnivorous Plant Newsletter*, **38**(3), 71–74.

785 <https://doi.org/10.55360/cpn383.la180>

786 Adlassnig, W., Peroutka, M., Eder, G., Pois, W., & Lichtscheidl, I. K. (2006).

787 Ecophysiological Observations on *Drosophyllum Lusitanicum*. *Ecological*

788 *Research*, **21**(2), 255–62. <https://doi.org/10.1007/s11284-005-0116-z>

789 Adler, P. B., Ellner, S. P., & Levine, J. M. (2010). Coexistence of Perennial Plants:

790 An Embarrassment of Niches. *Ecology Letters*, **13**(8), 1019–29.

791 <https://doi.org/10.1111/j.1461-0248.2010.01496.x>

792 Adler, P. B., Smull, D., Beard, K. H., Choi, R. T., Furniss, T., Kulmatiski, A., Meiners,

793 J. M., Tredennick, A. T., & Veblen, K. E. (2018). Competition and Coexistence

794 in Plant Communities: Intraspecific Competition Is Stronger than Interspecific

795 Competition. *Ecology Letters*, **21**(9), 1319–29.

796 <https://doi.org/10.1111/ele.13098>

797 Alberti, M. (2015). Eco-Evolutionary Dynamics in an Urbanizing Planet. *Trends in*

798 *Ecology & Evolution*, **30**(2), 114–26. <https://doi.org/10.1016/j.tree.2014.11.007>

799 Bertness, M. D., & Callaway, R. (1994). Positive Interactions in Communities. *Trends*

800 *in Ecology & Evolution*, **9**(5), 191–93. <https://doi.org/10.1016/0169->

801 [5347\(94\)90088-4](https://doi.org/10.1016/0169-5347(94)90088-4)

802 Bijlsma, R., & Loeschcke, V. (2012). Genetic Erosion Impedes Adaptive Responses

803 to Stressful Environments. *Evolutionary Applications*, **5**(2), 117–29.

804 <https://doi.org/10.1111/j.1752-4571.2011.00214.x>

805 Brewer, J. S., Paniw, M., & Ojeda, F. (2021). Plant Behavior and Coexistence: Stem

806 Elongation of the Carnivorous Subshrub *Drosophyllum Lusitanicum* within
807 Xerophytic Shrub Canopies. *Plant Ecology*, **222**(11), 1197–1208.
808 <https://doi.org/10.1007/s11258-021-01170-0>

809 Brook, B. W., Sodhi, N. S., & Bradshaw, C. J. A. (2008). Synergies among Extinction
810 Drivers under Global Change. *Trends in Ecology & Evolution*, **23**(8), 453–60.
811 <https://doi.org/10.1016/j.tree.2008.03.011>

812 Burnham, K. P., Anderson, D. R., & Huyvaert, K. P. (2011). AIC Model Selection and
813 Multimodel Inference in Behavioral Ecology: Some Background,
814 Observations, and Comparisons. *Behavioral Ecology and Sociobiology*, **65**(1),
815 23–35. <https://doi.org/10.1007/s00265-010-1029-6>

816 Callaway, R. M., & Pugnaire, F. I. (2007). Facilitation in Plant Communities. In F. I.
817 Pugnaire, & F. Valladares (Eds.), *Functional Plant Ecology* (2nd ed., pp. 435–
818 55). CRC Press.

819 Carpio, A. J., Castro–López, J., Guerrero–Casado, J., Ruiz–Aizpurua, L., Vicente, J.,
820 & Tortosa, F. S. (2014). Effect of Wild Ungulate Density on Invertebrates in a
821 Mediterranean Ecosystem. *Animal Biodiversity and Conservation*, **37**(2), 115–
822 25. <https://doi.org/10.32800/abc.2014.37.0115>

823 Catling, A. A., Mayfield, M. M., & Dwyer, J. M. (2024). Individual Vital Rates Respond
824 Differently to Local-Scale Environmental Variation and Neighbour Removal.
825 *Journal of Ecology*, **112**(6), 1369–82. [https://doi.org/10.1111/1365-](https://doi.org/10.1111/1365-2745.14308)
826 [2745.14308](https://doi.org/10.1111/1365-2745.14308)

827 Chevin, L.-M., Lande, R., & Mace, G. M. (2010). Adaptation, Plasticity, and
828 Extinction in a Changing Environment: Towards a Predictive Theory. *PLOS*
829 *Biology*, **8**(4), e1000357. <https://doi.org/10.1371/journal.pbio.1000357>

830 Clark, N. E., Boakes, E. H., McGowan, P. J. K., Mace, G. M., & Fuller, R. A. (2013).

831 Protected Areas in South Asia Have Not Prevented Habitat Loss: A Study
832 Using Historical Models of Land-Use Change. *PLOS ONE*, **8**(5), e65298.
833 <https://doi.org/10.1371/journal.pone.0065298>

834 Conquet, E., Ozgul, A., Blumstein, D. T., Armitage, K. B., Oli, M. K., Martin, J. G. A.,
835 Clutton-Brock, T. H., & Paniw, M. (2023). Demographic Consequences of
836 Changes in Environmental Periodicity. *Ecology*, **104**(3), e3894.
837 <https://doi.org/10.1002/ecy.3894>

838 Cornes, R. C., van der Schrier, G., van den Besselaar, E. J. M., & Jones, P. D.
839 (2018). An Ensemble Version of the E-OBS Temperature and Precipitation
840 Data Sets. *Journal of Geophysical Research: Atmospheres*, **123**(17), 9391–
841 409. <https://doi.org/10.1029/2017JD028200>

842 Correia, E., & Freitas, H. (2002). *Drosophyllum Lusitanicum*, an Endangered West
843 Mediterranean Endemic Carnivorous Plant: Threats and Its Ability to Control
844 Available Resources. *Botanical Journal of the Linnean Society*, **140**(4), 383–
845 90. <https://doi.org/10.1046/j.1095-8339.2002.00108.x>

846 Craine, J. M., & Dybzinski, R. (2013). Mechanisms of Plant Competition for
847 Nutrients, Water and Light. *Functional Ecology*, **27**(4), 833–40.
848 <https://doi.org/10.1111/1365-2435.12081>

849 Cross, A. T., Paniw, M., Ojeda, F., Turner, S. R., Dixon, K. W., & Merritt, D. J.
850 (2017). Defining the Role of Fire in Alleviating Seed Dormancy in a Rare
851 Mediterranean Endemic Subshrub. *AoB PLANTS*, **9**(5), plx036.
852 <https://doi.org/10.1093/aobpla/plx036>

853 Darwin, C. (1875). *Insectivorous Plants*. John Murray, London.
854 <https://doi.org/10.1017/CBO9780511694127>

855 Díaz, S., Settele, J., Brondízio, E. S., Ngo, H. T., Agard, J., Arneeth, A., Balvanera, P.,

856 Brauman, K. A., Butchart, S. H. M., Chan, K. M. A., Garibaldi, L. A., Ichii, K.,
857 Liu, J., Subramanian, S. M., Midgley, G. F., Miloslavich, P., Molnár, Z., Obura,
858 D., Pfaff, A., ... Polasky, S. (2019). Pervasive Human-Driven Decline of Life
859 on Earth Points to the Need for Transformative Change. *Science*, **366**(6471),
860 eaax3100. <https://doi.org/10.1126/science.aax3100>

861 Enright, N. J., Fontaine, J. B., Bowman, D. M. J. S., Bradstock, R. A., & Williams, R. J.
862 (2015). Interval Squeeze: Altered Fire Regimes and Demographic Responses
863 Interact to Threaten Woody Species Persistence as Climate Changes.
864 *Frontiers in Ecology and the Environment*, **13**(5), 265–72.
865 <https://doi.org/10.1890/140231>

866 Eyring, V., Bony, S., Meehl, G. A., Senior, C. A., Stevens, B., Stouffer, R. J., &
867 Taylor, K. E. (2016). Overview of the Coupled Model Intercomparison Project
868 Phase 6 (CMIP6) Experimental Design and Organization. *Geoscientific Model*
869 *Development*, **9**(5), 1937–58. <https://doi.org/10.5194/gmd-9-1937-2016>

870 Fagan, W. F., & Holmes, E. E. (2006). Quantifying the Extinction Vortex. *Ecology*
871 *Letters*, **9**(1), 51–60. <https://doi.org/10.1111/j.1461-0248.2005.00845.x>

872 Fischer, M., Weyand, A., Rudmann-Maurer, K., & Stöcklin, J. (2011). Adaptation of
873 *Poa alpina* to Altitude and Land Use in the Swiss Alps. *Alpine Botany*, **121**(2),
874 91–105. <https://doi.org/10.1007/s00035-011-0096-2>

875 Foley, J. A., DeFries, R., Asner, G. P., Barford, C., Bonan, G., Carpenter, S. R.,
876 Chapin, F. S., Coe, M. T., Daily, G. C., Gibbs, H. K., Helkowski, J. H.,
877 Holloway, T., Howard, E. A., Kucharik, C. J., Monfreda, C., Patz, J. A.,
878 Prentice, I. C., Ramankutty, N., & Snyder, P. K. (2005). Global Consequences
879 of Land Use. *Science*, **309**(5734), 570–74.
880 <https://doi.org/10.1126/science.1111772>

881 Gamelon, M., Grøtan, V., Nilsson, A. L. K., Engen, S., Hurrell, J. W., Jerstad, K.,
882 Phillips, A. S., Røstad, O. W., Slagsvold, T., Walseng, B., Stenseth, N. C.,
883 Sæther, B.-E. (2017). Interactions between Demography and Environmental
884 Effects Are Important Determinants of Population Dynamics. *Science*
885 *Advances*, **3**(2), e1602298. <https://doi.org/10.1126/sciadv.1602298>

886 Garnier, E., Lavorel, S., Ansquer, P., Castro, H., Cruz, P., Dolezal, J., Eriksson, O.,
887 Fortunel, C., Freitas, H., Golodets, C., Grigulis, K., Jouany, C., Kazakou, E.,
888 Kigel, J., Kleyer, M., Lehsten, V., Lepš, J., Meier, T., Pakeman, R., ... Zarovali,
889 M. P. (2007). Assessing the Effects of Land-Use Change on Plant Traits,
890 Communities and Ecosystem Functioning in Grasslands: A Standardized
891 Methodology and Lessons from an Application to 11 European Sites. *Annals*
892 *of Botany*, **99**(5), 967–85. <https://doi.org/10.1093/aob/mcl215>

893 Garrido, B., Hampe, A., Marañón, T., & Arroyo, J. (2003). Regional Differences in
894 Land Use Affect Population Performance of the Threatened Insectivorous
895 Plant *Drosophyllum Lusitanicum* (Droseraceae). *Diversity and Distributions*,
896 **9**(5), 335–50. <https://doi.org/10.1046/j.1472-4642.2003.00029.x>

897 Geldmann, J., Barnes, M., Coad, L., Craigie, I. D., Hockings, M., & Burgess, N. D.
898 (2013). Effectiveness of Terrestrial Protected Areas in Reducing Habitat Loss
899 and Population Declines. *Biological Conservation*, **161**(May), 230–38.
900 <https://doi.org/10.1016/j.biocon.2013.02.018>

901 Gómez-González, S., Paniw, M., Antunes, K., & Ojeda, F. (2018). Heat Shock and
902 Plant Leachates Regulate Seed Germination of the Endangered Carnivorous
903 Plant *Drosophyllum Lusitanicum*. *Web Ecology*, **18**(1), 7–13.
904 <https://doi.org/10.5194/we-18-7-2018>

905 Graff, P., Aguiar, M. R., & Chaneton, E. J. (2007). Shifts in Positive and Negative

906 Plant Interactions Along a Grazing Intensity Gradient. *Ecology*, **88**(1), 188–99.
907 [https://doi.org/10.1890/0012-9658\(2007\)88\[188:SIPANP\]2.0.CO;2](https://doi.org/10.1890/0012-9658(2007)88[188:SIPANP]2.0.CO;2)

908 Grant, K., Kreyling, J., Heilmeyer, H., Beierkuhnlein, C., & Jentsch, A. (2014).
909 Extreme Weather Events and Plant–Plant Interactions: Shifts between
910 Competition and Facilitation among Grassland Species in the Face of Drought
911 and Heavy Rainfall. *Ecological Research*, **29**(5), 991–1001.
912 <https://doi.org/10.1007/s11284-014-1187-5>

913 Gray, C. L., Hill, S. L. L., Newbold, T., Hudson, L. N., Börger, L., Contu, S., Hoskins,
914 A. J., Ferrier, S., Purvis, A., & Scharlemann, J. P. W. (2016). Local
915 Biodiversity Is Higher inside than Outside Terrestrial Protected Areas
916 Worldwide. *Nature Communications*, **7**(1), 12306.
917 <https://doi.org/10.1038/ncomms12306>

918 Grime, J. P. (1973). Competitive Exclusion in Herbaceous Vegetation. *Nature*,
919 **242**(5396), 344–47. <https://doi.org/10.1038/242344a0>

920 Grimm, V., Berger, U., Bastiansen, F., Eliassen, S., Ginot, V., Giske, J., Goss-
921 Custard, J., Grand, T., Heinz, S. K., Huse, G., Huth, A., Jepsen, J. U.,
922 Jørgensen, C., Mooij, W. M., Müller, B., Pe'er, G., Piou, C., Railsback, S. F.,
923 Robbins, A. M., ... DeAngelis, D. L. (2006). A Standard Protocol for
924 Describing Individual-Based and Agent-Based Models. *Ecological Modelling*,
925 **198**(1), 115–26. <https://doi.org/10.1016/j.ecolmodel.2006.04.023>

926 Grimm, V., Railsback, S. F., Vincenot, C. E., Berger, U., Gallagher, C., DeAngelis, D.
927 L., Edmonds, B., Ge, J., Giske, J., Groeneveld, J., Johnston, A. S. A., Milles,
928 A., Nabe-Nielsen, J., Polhill, J. G., Radchuk, V., Rohwäder, M.-S., Stillman, R.
929 A., Thiele, J. C., & Ayllón, D. (2020). The ODD Protocol for Describing Agent-
930 Based and Other Simulation Models: A Second Update to Improve Clarity,

931 Replication, and Structural Realism. *Journal of Artificial Societies and Social*
932 *Simulation*, **23**(2), 7. [https://doi.org/ 10.18564/jasss.4259](https://doi.org/10.18564/jasss.4259)

933 Hindle, B. J., Quintana-Ascencio, P. F., Menges, E. S., & Childs, D. Z. (2023). The
934 Implications of Seasonal Climatic Effects for Managing Disturbance
935 Dependent Populations under a Changing Climate. *Journal of Ecology*,
936 **111**(8), 1749–61. <https://doi.org/10.1111/1365-2745.14143>

937 Hjalten, J., Danell, K., & Ericson, L. (1993). Effects of Simulated Herbivory and
938 Intraspecific Competition on the Compensatory Ability of Birches. *Ecology*,
939 **74**(4), 1136–42. <https://doi.org/10.2307/1940483>

940 IPBES. (2019). Global Assessment Report on Biodiversity and Ecosystem Services
941 of the Intergovernmental Science-Policy Platform on Biodiversity and
942 Ecosystem Services. E. S. Brondizio, J. Settele, S. Díaz, & H. T. Ngo (Eds.).
943 IPBES secretariat, Bonn, Germany. <https://doi.org/10.5281/zenodo.6417333>

944 Kambatuku, J. R., Cramer, M. D., & Ward, D. (2011). Intraspecific Competition
945 between Shrubs in a Semi-Arid Savanna. *Plant Ecology*, **212**(4), 701–13.
946 <https://doi.org/10.1007/s11258-010-9856-0>

947 Kampichler, C., van Turnhout, C. A. M., Devictor, V., & van der Jeugd, H. P. (2012).
948 Large-Scale Changes in Community Composition: Determining Land Use and
949 Climate Change Signals. *PLOS ONE*, **7**(4), e35272.
950 <https://doi.org/10.1371/journal.pone.0035272>

951 Keeley, J. E., Bond, W. J., Bradstock, R. A., Pausas, J. G., & Rundel, P. W. (2012).
952 *Fire in Mediterranean Ecosystems: Ecology, Evolution and Management*.
953 Cambridge University Press.

954 Kerns, B. K., Buonopane, M., Thies, W. G., & Niwa, C. (2011). Reintroducing Fire
955 into a Ponderosa Pine Forest with and without Cattle Grazing: Understory

956 Vegetation Response. *Ecosphere*, **2**(5), art59. [https://doi.org/10.1890/ES10-](https://doi.org/10.1890/ES10-00183.1)
957 [00183.1](https://doi.org/10.1890/ES10-00183.1)

958 Larcher, W. (2000). Temperature Stress and Survival Ability of Mediterranean
959 Sclerophyllous Plants. *Plant Biosystems - An International Journal Dealing*
960 *with All Aspects of Plant Biology*, **134**(3), 279–95.
961 <https://doi.org/10.1080/11263500012331350455>

962 Lawson, D. M., Regan, H. M., Zedler, P. H., & Franklin, J. (2010). Cumulative Effects
963 of Land Use, Altered Fire Regime and Climate Change on Persistence of
964 *Ceanothus Verrucosus*, a Rare, Fire-Dependent Plant Species. *Global*
965 *Change Biology*, **16**(9), 2518–29. [https://doi.org/10.1111/j.1365-](https://doi.org/10.1111/j.1365-2486.2009.02143.x)
966 [2486.2009.02143.x](https://doi.org/10.1111/j.1365-2486.2009.02143.x)

967 Le Bagousse-Pinguet, Y., Gross, E. M., & Straile, D. (2012). Release from
968 Competition and Protection Determine the Outcome of Plant Interactions
969 along a Grazing Gradient. *Oikos*, **121**(1), 95–101.
970 <https://doi.org/10.1111/j.1600-0706.2011.19778.x>

971 Leimu, R., Vergeer, P., Angeloni, F., & Ouborg, N. J. (2010). Habitat Fragmentation,
972 Climate Change, and Inbreeding in Plants. *Annals of the New York Academy*
973 *of Sciences*, **1195**(1), 84–98. [https://doi.org/10.1111/j.1749-](https://doi.org/10.1111/j.1749-6632.2010.05450.x)
974 [6632.2010.05450.x](https://doi.org/10.1111/j.1749-6632.2010.05450.x)

975 Maestre, F. T., Valladares, F., & Reynolds, J. F. (2005). Is the Change of Plant–Plant
976 Interactions with Abiotic Stress Predictable? A Meta-Analysis of Field Results
977 in Arid Environments. *Journal of Ecology*, **93**(4), 748–57.
978 <https://doi.org/10.1111/j.1365-2745.2005.01017.x>

979 Mantyka-Pringle, C. S., Martin, T. G., & Rhodes, J. R. (2012). Interactions between
980 Climate and Habitat Loss Effects on Biodiversity: A Systematic Review and

981 Meta-Analysis. *Global Change Biology*, **18**(4), 1239–52.
982 <https://doi.org/10.1111/j.1365-2486.2011.02593.x>

983 Matías, L., Abdelaziz, M., Godoy, O., & Gómez-Aparicio, L. (2019). Disentangling the
984 Climatic and Biotic Factors Driving Changes in the Dynamics of Quercus
985 Suber Populations across the Species' Latitudinal Range. *Diversity and*
986 *Distributions*, **25**(4), 524–35. <https://doi.org/10.1111/ddi.12873>

987 Mayer, C. (2004). Pollination Services under Different Grazing Intensities.
988 *International Journal of Tropical Insect Science*, **24**(1), 95–103.
989 <https://doi.org/10.1079/IJT20047>

990 McDowell, N., Pockman, W. T., Allen, C. D., Breshears, D. D., Cobb, N., Kolb, T.,
991 Plaut, J., Sperry, J., West, A., Williams, D. G., & Yezpez, E. A. (2008).
992 Mechanisms of Plant Survival and Mortality during Drought: Why Do Some
993 Plants Survive While Others Succumb to Drought? *New Phytologist*, **178**(4),
994 719–39. <https://doi.org/10.1111/j.1469-8137.2008.02436.x>

995 Montràs-Janer, T., Suggitt, A. J., Fox, R., Jönsson, M., Martay, B., Roy, D. B.,
996 Walker, K. J., & Auffret, A. G. (2024). Anthropogenic Climate and Land-Use
997 Change Drive Short- and Long-Term Biodiversity Shifts across Taxa. *Nature*
998 *Ecology & Evolution*, **8**(4), 739–51. [https://doi.org/10.1038/s41559-024-](https://doi.org/10.1038/s41559-024-02326-7)
999 [02326-7](https://doi.org/10.1038/s41559-024-02326-7)

1000 Murali, G., de Oliveira Caetano, G. H., Barki, G., Meiri, S., & Roll, U. (2022).
1001 Emphasizing Declining Populations in the Living Planet Report. *Nature*,
1002 **601**(7894), E20–24. <https://doi.org/10.1038/s41586-021-04165-z>

1003 Newbold, T., Oppenheimer, P., Etard, A., & Williams, J. J. (2020). Tropical and
1004 Mediterranean Biodiversity Is Disproportionately Sensitive to Land-Use and
1005 Climate Change. *Nature Ecology & Evolution*, **4**(12), 1630–38.

1006 <https://doi.org/10.1038/s41559-020-01303-0>

1007 Nolan, R. H., Collins, L., Leigh, A., Ooi, M. K. J., Curran, T. J. Fairman, T. A., Resco
1008 de Dios, V., & Bradstock, R. (2021). Limits to Post-Fire Vegetation Recovery
1009 under Climate Change. *Plant, Cell & Environment*, **44**(11), 3471–89.
1010 <https://doi.org/10.1111/pce.14176>

1011 Ojeda, F., Carrera, C., Paniw, M., García-Moreno, L., Barbero, G. F., & Palma, M.
1012 (2021). Volatile and Semi-Volatile Organic Compounds May Help Reduce
1013 Pollinator-Prey Overlap in the Carnivorous Plant *Drosophyllum Lusitanicum*
1014 (*Drosophyllaceae*). *Journal of Chemical Ecology*, **47**(1), 73–86.
1015 <https://doi.org/10.1007/s10886-020-01235-w>

1016 Ojeda, F., Pausas, J. G., & Verdú, M. (2010). Soil Shapes Community Structure
1017 through Fire. *Oecologia*, **163**(3), 729–35. [https://doi.org/10.1007/s00442-009-](https://doi.org/10.1007/s00442-009-1550-3)
1018 [1550-3](https://doi.org/10.1007/s00442-009-1550-3)

1019 Oliver, T. H., & Morecroft, M. D. (2014). Interactions between Climate Change and
1020 Land Use Change on Biodiversity: Attribution Problems, Risks, and
1021 Opportunities. *WIREs Climate Change*, **5**(3), 317–35.
1022 <https://doi.org/10.1002/wcc.271>

1023 Olsen, S. L., Töpper, J. P., Skarpaas, O., Vandvik, V., & Klanderud, K. (2016). From
1024 Facilitation to Competition: Temperature-Driven Shift in Dominant Plant
1025 Interactions Affects Population Dynamics in Seminatural Grasslands. *Global*
1026 *Change Biology*, **22**(5), 1915–26. <https://doi.org/10.1111/gcb.13241>

1027 Paniw, M., Duncan, C., Groenewoud, F., Drewe, J. A., Manser, M., Ozgul, A., &
1028 Clutton-Brock, T. (2022). Higher Temperature Extremes Exacerbate Negative
1029 Disease Effects in a Social Mammal. *Nature Climate Change*, **12**(3), 284–90.
1030 <https://doi.org/10.1038/s41558-022-01284-x>

- 1031 Paniw, M., García-Callejas, D., Lloret, F., Bassar, R. D., Travis, J., & Godoy, O.
1032 (2023). Pathways to Global-Change Effects on Biodiversity: New
1033 Opportunities for Dynamically Forecasting Demography and Species
1034 Interactions. *Proceedings of the Royal Society B: Biological Sciences*,
1035 **290**(1993), 20221494. <https://doi.org/10.1098/rspb.2022.1494>
- 1036 Paniw, M., Gil-Cabeza, E., & Ojeda, F. (2017). Plant Carnivory beyond Bogs:
1037 Reliance on Prey Feeding in *Drosophyllum Lusitanicum* (Drosophyllaceae) in
1038 Dry Mediterranean Heathland Habitats. *Annals of Botany*, **119**(6), 1035–41.
1039 <https://doi.org/10.1093/aob/mcw247>
- 1040 Paniw, M., Maag, N., Cozzi, G., Clutton-Brock, T. H., & Ozgul, A. (2019). Life History
1041 Responses of Meerkats to Seasonal Changes in Extreme Environments.
1042 *Science*, **363**(6427), 631–35. <https://doi.org/10.1126/science.aau5905>
- 1043 Paniw, M., Quintana-Ascencio, P. F., Ojeda, F., & Salguero-Gómez, R. (2017).
1044 Interacting Livestock and Fire May Both Threaten and Increase Viability of a
1045 Fire-Adapted Mediterranean Carnivorous Plant. *Journal of Applied Ecology*,
1046 **54**(6), 1884–94. <https://doi.org/10.1111/1365-2664.12872>
- 1047 Paniw, M., de la Riva, E. G., & Lloret, F. (2021). Demographic Traits Improve
1048 Predictions of Spatiotemporal Changes in Community Resilience to Drought.
1049 *Journal of Ecology*, **109**(9), 3233–45. <https://doi.org/10.1111/1365-2745.13597>
- 1051 Paniw, M., Salguero-Gómez, R., & Ojeda, F. (2015). Local-Scale Disturbances Can
1052 Benefit an Endangered, Fire-Adapted Plant Species in Western
1053 Mediterranean Heathlands in the Absence of Fire. *Biological Conservation*,
1054 **187**(July), 74–81. <https://doi.org/10.1016/j.biocon.2015.04.010>
- 1055 Paniw, M., Salguero-Gómez, R., & Ojeda, F. (2018). Transient Facilitation of

1056 Resprouting Shrubs in Fire-Prone Habitats. *Journal of Plant Ecology*, **11**(3),
1057 475–83. <https://doi.org/10.1093/jpe/rtx019>

1058 Pascoe, C., Lawrence, B. N., Guilyardi, E., Juckes, M., & Taylor, K. E. (2020).
1059 Documenting Numerical Experiments in Support of the Coupled Model
1060 Intercomparison Project Phase 6 (CMIP6). *Geoscientific Model Development*,
1061 **13**(5), 2149–67. <https://doi.org/10.5194/gmd-13-2149-2020>

1062 Pausas, J. G., & Keeley, J. E. (2014). Abrupt Climate-Independent Fire Regime
1063 Changes. *Ecosystems*, **17**(6), 1109–20. [https://doi.org/10.1007/s10021-014-](https://doi.org/10.1007/s10021-014-9773-5)
1064 [9773-5](https://doi.org/10.1007/s10021-014-9773-5)

1065 Petrie, R., Denvil, S., Ames, S., Levavasseur, G., Fiore, S., Allen, C., Antonio, F.,
1066 Berger, K., Bretonnière P.-A., Cinquini, L., Dart, E., Dwarakanath, P., Drukem,
1067 K., Evans, B., Franchistéguy, L., Gardoll, S., Gerbier, E., Greenslade, M.,
1068 Hassell, D., ... Wagner, R. (2021). Coordinating an Operational Data
1069 Distribution Network for CMIP6 Data. *Geoscientific Model Development*,
1070 **14**(1), 629–44. <https://doi.org/10.5194/gmd-14-629-2021>

1071 Posit team. (2023). RStudio: Integrated Development Environment for R. Posit
1072 Software, PBC, Boston, MA. <http://www.posit.co/>

1073 R Core Team. (2022). R: A Language and Environment for Statistical Computing.
1074 Vienna, Austria: R Foundation for Statistical Computing. [https://www.R-](https://www.R-project.org/)
1075 [project.org/](https://www.R-project.org/)

1076 Riahi, K., Rao, S., Krey, V., Cho, C., Chirkov, V., Fischer, G., Kindermann, G.,
1077 Nakicenovic, N., & Rafaj, P. (2011). RCP 8.5—A Scenario of Comparatively
1078 High Greenhouse Gas Emissions. *Climatic Change*, **109**(1), 33.
1079 <https://doi.org/10.1007/s10584-011-0149-y>

1080 Sala, O. E., Chapin III, F. S., Armesto, J. J., Berlow, E., Bloomfield, J., Dirzo, R.,

1081 Huber-Sanwald, E., Huenneke, L. F., Jackson, R. B., Kinzig, A., Leemans, R.,
1082 Lodge, D. M., Mooney, H. A., Oesterheld, M., Poff, N. L., Sykes, M. T.,
1083 Walker, B. H., Walker, M. Wall, D. H. (2000). Global Biodiversity Scenarios for
1084 the Year 2100. *Science*, **287**(5459), 1770–74.
1085 <https://doi.org/10.1126/science.287.5459.1770>

1086 Sanderson, B. M., Knutti, R., & Caldwell, P. (2015). A Representative Democracy to
1087 Reduce Interdependency in a Multimodel Ensemble. *Journal of Climate*,
1088 **28**(13), 5171–94. <https://doi.org/10.1175/JCLI-D-14-00362.1>

1089 Selwood, K. E., McGeoch, M. A., & Mac Nally, R. (2015). The Effects of Climate
1090 Change and Land-Use Change on Demographic Rates and Population
1091 Viability. *Biological Reviews*, **90**(3), 837–53. <https://doi.org/10.1111/brv.12136>

1092 Sirami, C., Caplat, P., Popy, S., Clamens, A., Arlettaz, R., Jiguet, F., Brotons, L., &
1093 Martin, J.-L. (2017). Impacts of Global Change on Species Distributions:
1094 Obstacles and Solutions to Integrate Climate and Land Use. *Global Ecology*
1095 *and Biogeography*, **26**(4), 385–94. <https://doi.org/10.1111/geb.12555>

1096 Skates, L. M., Paniw, M., Cross, A. T., Ojeda, F., Dixon, K. W., Stevens, J. C., &
1097 Gebauer, G. (2019). An Ecological Perspective on ‘Plant Carnivory beyond
1098 Bogs’: Nutritional Benefits of Prey Capture for the Mediterranean Carnivorous
1099 Plant *Drosophyllum Lusitanicum*. *Annals of Botany*, **124**(1), 65–76.
1100 <https://doi.org/10.1093/aob/mcz045>

1101 Stearns, S. C. (1989). Trade-Offs in Life-History Evolution. *Functional Ecology*, **3**(3),
1102 259–68. <https://doi.org/10.2307/2389364>

1103 Titeux, N., Henle, K., Mihoub, J.-B., Regos, A., Geijzendorffer, I. R., Cramer, W.,
1104 Verburg, P. H., & Brotons, L. (2016). Biodiversity Scenarios Neglect Future
1105 Land-Use Changes. *Global Change Biology*, **22**(7), 2505–15.

1106 <https://doi.org/10.1111/gcb.13272>

1107 Tredennick, A. T., Hooten, M. B., Aldridge, C. L., Homer, C. G., Kleinhesselink, A.
1108 R., & Adler, P. B. (2016). Forecasting Climate Change Impacts on Plant
1109 Populations over Large Spatial Extents. *Ecosphere*, **7**(10), e01525.
1110 <https://doi.org/10.1002/ecs2.1525>

1111 Turco, M., Jerez, S., Augusto, S., Tarín-Carrasco, P., Ratola, N., Jiménez-Guerrero,
1112 P., & Trigo, R. M. (2019). Climate Drivers of the 2017 Devastating Fires in
1113 Portugal. *Scientific Reports*, **9**(1), 13886. [https://doi.org/10.1038/s41598-019-](https://doi.org/10.1038/s41598-019-50281-2)
1114 [50281-2](https://doi.org/10.1038/s41598-019-50281-2)

1115 Vilà, M., & Sardans, J. (1999). Plant Competition in Mediterranean-Type Vegetation.
1116 *Journal of Vegetation Science*, **10**(2), 281–94.
1117 <https://doi.org/10.2307/3237150>

1118 Villalobos, F. J., Sadras, V. O., & Fereres, E. (2016). Plant Density and Competition.
1119 In F. J. Villalobos & E. Fereres (Eds.), *Principles of Agronomy for Sustainable*
1120 *Agriculture* (pp. 159–168). Springer International Publishing.
1121 https://doi.org/10.1007/978-3-319-46116-8_12

1122 Villarreal-Barajas, T., & Martorell, C. (2009). Species-Specific Disturbance
1123 Tolerance, Competition and Positive Interactions along an Anthropogenic
1124 Disturbance Gradient. *Journal of Vegetation Science*, **20**(6), 1027–40.
1125 <https://doi.org/10.1111/j.1654-1103.2009.01101.x>

1126 Villellas, J., & García, M. B. (2018). Life-History Trade-Offs Vary with Resource
1127 Availability across the Geographic Range of a Widespread Plant. *Plant*
1128 *Biology*, **20**(3), 483–89. <https://doi.org/10.1111/plb.12682>

1129 Völler, E., Bossdorf, O., Prati, D., & Auge, H. (2017). Evolutionary Responses to
1130 Land Use in Eight Common Grassland Plants. *Journal of Ecology*, **105**(5),

1131 1290–97. <https://doi.org/10.1111/1365-2745.12746>

1132 Waliser, D., Gleckler, P. J., Ferraro, R., Taylor, K. E., Ames, S., Biard, J., Bosilovich,
1133 M. G., Brown, O., Chepfer, H., Cinquini, L., Durack, P.J., Eyring, V., Mathieu,
1134 P.-P., Lee, T., Pinnock, S., Potter, G. L., Rixen, M., Saunders, R., Schulz, J.,
1135 Thépaut, J.-N., Tuma, M. (2020). Observations for Model Intercomparison
1136 Project (Obs4MIPs): Status for CMIP6. *Geoscientific Model Development*,
1137 **13**(7), 2945–58. <https://doi.org/10.5194/gmd-13-2945-2020>

1138 Watson, J. E. M., Dudley, N., Segan, D. B., & Hockings, Marc. (2014). The
1139 Performance and Potential of Protected Areas. *Nature*, **515**(7525), 67–73.
1140 <https://doi.org/10.1038/nature13947>

1141 Wood, S. N. (2011). Fast Stable Restricted Maximum Likelihood and Marginal
1142 Likelihood Estimation of Semiparametric Generalized Linear Models. *Journal*
1143 *of the Royal Statistical Society Series B: Statistical Methodology*, **73**(1), 3–36.
1144 <https://doi.org/10.1111/j.1467-9868.2010.00749.x>

1145 Wood, S. N. (2017). *Generalized Additive Models: An Introduction with R, Second*
1146 *Edition*. CRC Press.

1147 Wood, S. N., Pya, N., & Säfken, B. (2016). Smoothing Parameter and Model
1148 Selection for General Smooth Models. *Journal of the American Statistical*
1149 *Association*, **111**(516), 1548–63.
1150 <https://doi.org/10.1080/01621459.2016.1180986>

1151 Zscheischler, J., Westra, S., van den Hurk, B. J. J. M., Seneviratne, S. I., Ward, P.
1152 J., Pitman, A., AghaKouchak, A., Bresh, D. N., Leonard, M., Wahl, T., &
1153 Zhang, X. (2018). Future Climate Risk from Compound Events. *Nature*
1154 *Climate Change*, **8**(6), 469–77. <https://doi.org/10.1038/s41558-018-0156-3>

1 **Appendix S1 – Methodological details and additional results**

2

3 1. Seedbank parameters

4

5 We used previously published data obtained from seed-burial and
6 greenhouse-germination experiments to parameterise the transitions of dewy-pine
7 seeds from and to the soil seedbank and to continuous germination (Table S1). More
8 specifically, following Paniw et al. (2017), we used data on seeds buried in habitat
9 conditions characteristic of early (i.e., recently burned) or late post-fire stages (i.e.,
10 long unburned) to estimate seed survival in the soil (i.e., seedbank stasis; staySB)
11 and the probability of germinating from the seedbank at least two years after burial
12 (outSB). We used estimates from recently burned habitats for anthropogenic
13 populations, which experience constant anthropogenic disturbances mimicking the
14 effects of fire (Paniw et al., 2017). For natural populations, we used estimates from
15 burned habitats in early post-fire stages (i.e., TSF₂ for staySB and TSF₁ for outSB),
16 and from unburned habitats in later post-fire stages (i.e., from TSF₃ for staySB and
17 from TSF₂ to TSF₄ for outSB). To more accurately describe the observed seedbank
18 dynamics in the first TSFs (i.e., TSF₀ and TSF₁ for staySB and TSF₀ for outSB), we
19 used previously published parameters representing the characteristically high
20 germination rates from the seedbank (outSB) in a fire year (TSF₀), and low
21 germination rates in late TSFs (TSF₅), as well as the very low seedbank stasis
22 (staySB) following a fire (TSF₀ and TSF₁) (Paniw et al., 2017; Conquet et al., 2023).
23
24 To estimate the probability of seeds germinating continuously without contributing to
25 the seedbank (goCont) and its opposite parameter determining the probability of

26 seeds contributing to the seedbank (goSB), we used data from a growth-chamber
27 germination experiment (see details in Gómez-González et al., 2018). Seeds from 15
28 individual dewy pines growing in natural or anthropogenic habitats were monitored to
29 obtain the proportion of surviving seeds germinating (goCont) and remaining
30 dormant (goSB = 1 - goCont). We used estimates from the corresponding habitat to
31 parameterise seedbank transitions of our natural and anthropogenic populations. In
32 natural populations, however, continuous germination and contribution to the
33 seedbank only starts in TSF₂ and is extremely low from TSF₅. We therefore fixed the
34 values for goCont and goSB using previously published data (Paniw et al., 2017;
35 Conquet et al., 2023) for these TSFs to represent these observed processes (Table
36 S1). Because natural populations still experience fires, we defined time-since-fire-
37 specific parameter values for these populations. Additionally, to take advantage of
38 the population-specific data available from the germination experiment for several
39 anthropogenic sites, we defined population-specific goCont and goSB values for
40 anthropogenic populations.

41

42 **Table S1 – Seedbank parameters obtained from seed-burial and germination**

43 **experiments.** We used previously published data from a seed-burial experiment in
44 recently burned and long unburned dewy-pine habitats to estimate the proportion of
45 seeds remaining in (staySB) or germinating from the seedbank (outSB). Additionally,
46 we used data from a germination experiment on seeds from natural and
47 anthropogenic habitats to estimate the proportion of seeds contributing to the
48 seedbank (goSB) or germinating continuously (goCont). The table contains
49 parameter means and, wherever available, 95% confidence intervals (with binomial

50 standard deviations calculated as $\sqrt{\frac{\mu \times (1-\mu)}{N}}$ where μ is the parameter mean and N the

51 sample size). Asterisks indicate parameter values adapted from previously published
 52 values (Paniw et al., 2017; Conquet et al., 2023), and for which the confidence
 53 interval could not be calculated.

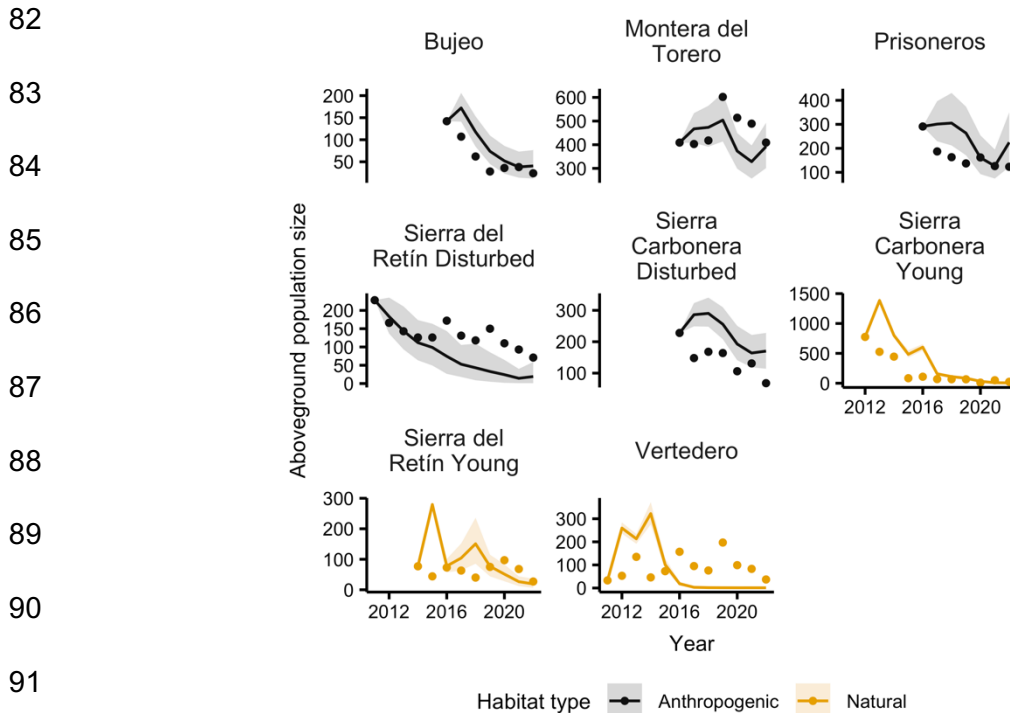
| Natural populations | | | | |
|----------------------------------|----------------------|-------------------------|-------------------------|----------------------|
| Seedbank parameters | | | | |
| Time since fire (TSF) | staySB | outSB | goCont | goSB |
| TSF ₀ | 0.1* | 0.81* | 0* | 0* |
| TSF ₁ | 0.05* | 0.061 [0.044, 0.077] | 0* | 0* |
| TSF ₂ | 0.60 [0.57, 0.63] | 0.035 [0.023, 0.046] | 0.026 [0.016, 0.037] | 0.97 [0.96, 0.98] |
| TSF ₃ | 0.85 [0.83, 0.86] | 0.035 [0.023, 0.046] | 0.026 [0.016, 0.037] | 0.97 [0.96, 0.98] |
| TSF ₄ | 0.85 [0.83, 0.86] | 0.035 [0.023, 0.046] | 0.026 [0.016, 0.037] | 0.97 [0.96, 0.98] |
| TSF ₅ | 0.85 [0.83, 0.86] | 0* | 0.01* | 0.99* |
| Anthropogenic populations | | | | |
| Seedbank parameters | | | | |
| Site | staySB | outSB | goCont | goSB |
| Sierra del Retín Disturbed | 0.60 [0.57, 0.63] | 0.061 [0.044, 0.077] | 0.11 [0, 0.28] | 0.89 [0.72, 1.0] |
| Prisioneros | 0.60 [0.57, 0.63] | 0.061 [0.044, 0.077] | 0.29 [0.0071, 0.57] | 0.71 [0.99, 0.43] |
| Bujeo | 0.60 [0.57, 0.63] | 0.061 [0.044, 0.077] | 0.16 [0.060, 0.26] | 0.84 [0.74, 0.94] |
| Montera del Torero | 0.60 [0.57, 0.63] | 0.061 [0.044, 0.077] | 0.18 [0, 0.37] | 0.82 [0.63, 1.0] |
| Sierra Carbonera Disturbed | 0.60 [0.57, 0.63] | 0.061 [0.044, 0.077] | 0.16 [0.060, 0.26] | 0.84 [0.74, 0.94] |

54 2. Seedbank parameters correction factors

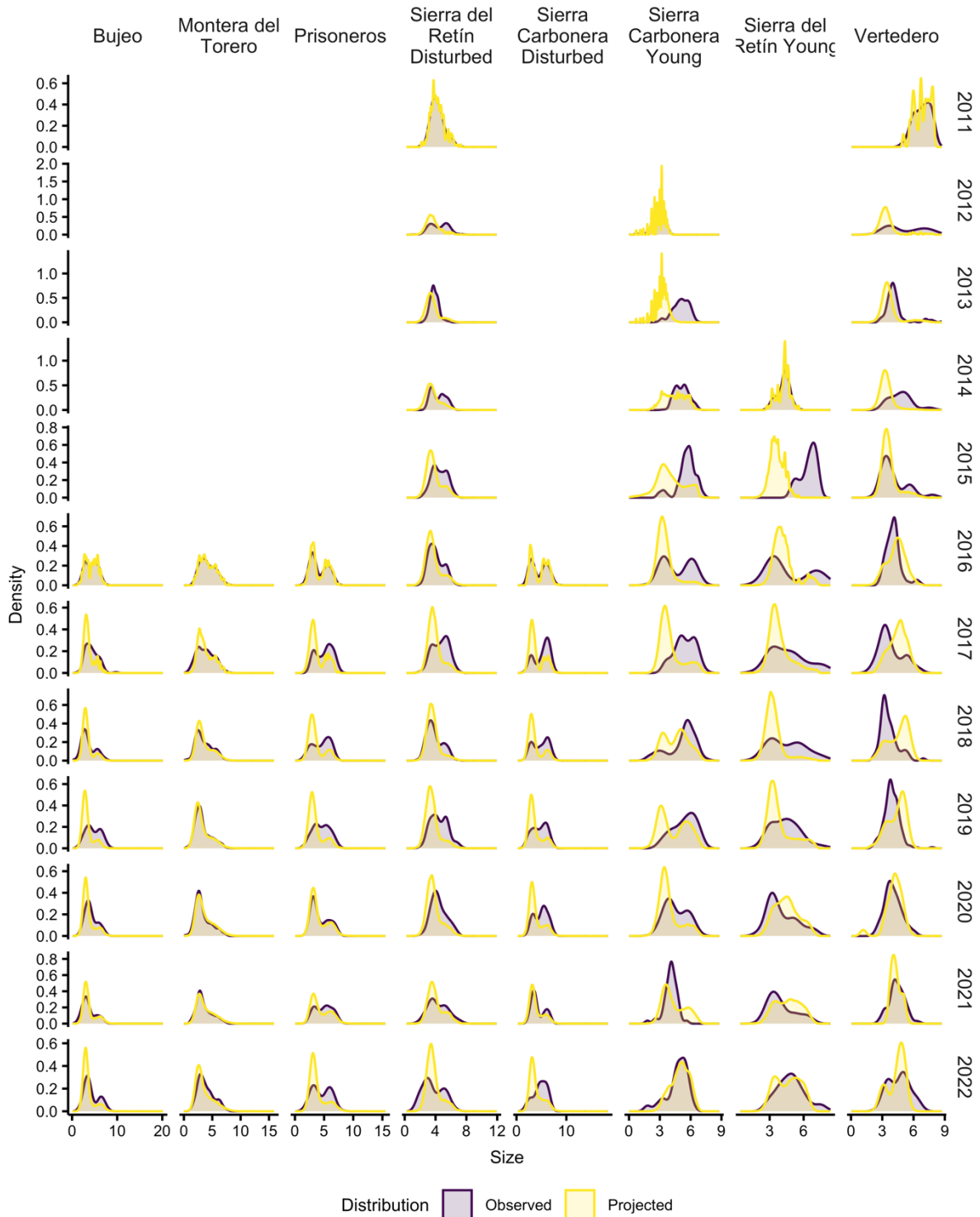
55

56 Accurately estimating seedbank parameters is complex due to the many factors
57 influencing germination and dormancy. Seed mortality is a hidden process that cannot
58 be easily determined in the field without perturbing the populations and is therefore
59 often underestimated. Therefore, to better represent the dewy-pine population
60 dynamics in anthropogenic sites, we computed a correction factor corresponding to
61 the seed aboveground survival (σ_{seed}). σ_{seed} corresponded to the proportion of seeds
62 surviving aboveground and was obtained from data on flower damage ($\sigma_{\text{seed}} = 1 -$
63 flower damage) (Paniw et al., 2017). As anthropogenic populations never returned to
64 TSF₀, we only used σ_{seed} for TSF₄ (0.33). We corrected the seedbank parameter
65 values in anthropogenic habitats by multiplying all four seedbank parameters (i.e.,
66 goCont, outSB, goSB, and staySB) by σ_{seed} . Additionally, previous model calibrations
67 showed the need to further correct several seedbank parameters to mirror the
68 observed dynamics of dewy-pine populations. To do so, we multiplied both goCont
69 and outSB by 0.4 for Sierra Carbonera Disturbed. Moreover, as we estimated plant
70 density within 1-m² quadrats, we avoided unrealistically high recruit numbers by
71 capping the number of recruits to the maximum observed number of seedlings per
72 quadrat during the study period in all natural populations and in two anthropogenic
73 populations: Bujeo and Sierra Carbonera Disturbed. In natural populations, this
74 number was TSF specific; however, data was unavailable for some TSFs in some
75 populations. When unavailable for TSF₀, we set the maximum number of recruits to
76 1.5 times the maximum observed number of seedlings in the populations; in TSF₁, we
77 set it to the maximum observed number of seedlings in the population; and in TSF₂ to
78 the average maximum observed number of seedlings in the population in TSF_{>0}. The

79 correction factors resulted in predicted abundances (out-of-sample predictions)
 80 reflecting well observed abundances, size distributions, and aboveground population
 81 growth rates (Fig. S1; Fig. S2; Fig. 4 in main text).



91
 92 **Figure S1 – Observed and projected aboveground population abundance.** We
 93 projected each natural and anthropogenic population for 500 times across the range
 94 of observed years available for each population (maximum range from 2011 to 2022)
 95 to perform an out-of-sample validation of our individual-based model parameterization.
 96 For each projection, we obtained the average (line) and 25th and 95th (shaded ribbon)
 97 percentile of the aboveground population size. We compared these projected values
 98 to the observed ones (dots).



99 **Figure S2 – Observed and projected distributions of individual size across**
 100 **time.** We projected each population from the first year it was sampled to 2022 and
 101 obtained the site- and year-specific distributions of aboveground individual size, which
 102 we compared to the observed distributions.

103

104 3. Covariate standardisation and correlation

105

106 We standardised all continuous covariates using the approach described by

107 Gelman (2008):

108

109
$$\text{covariate}_{\text{scaled}(H)} = \frac{(\text{covariate}_{\text{unscaled}(H)} - \mu_{\text{covariate}_{\text{unscaled}(H)}})}{2 \cdot \sigma_{\text{covariate}_{\text{unscaled}(H)}}}$$
 (Equation 1)

110

111 where μ and σ are respectively the mean and standard deviation of a given

112 unscaled covariate in a subset of data from a given habitat H (natural or

113 anthropogenic). In comparison with the common standardisation by one standard

114 deviation, this standardisation approach enables the comparison of the effect sizes

115 of both categorical (i.e. habitat) and continuous covariates (i.e. density-dependent

116 variables).

117

118 We checked for correlations between covariates using the Pearson correlation

119 coefficient (using the `cor` function from the stats R package; R Core Team, 2022).

120 We considered a pair of variables to be correlated when the absolute value of the

121 correlation coefficient was above 0.5. We included only one of the two correlated

122 variables in a model, choosing the first to be retained in the model selection.

123

124 4. Vital-rate model selection

125

126 We assessed the nonlinear response of dewy-pine survival, growth, flowering

127 probability, number of flowers, and seedling size to rainfall, maximum daily

128 temperature, time since fire (TSF), aboveground density of large individuals (size >

129 4.5), and individual size using Generalised Additive Models (GAMs) fitted to
130 demographic data from individual dewy pines growing in natural or anthropogenic
131 habitats. We first assessed whether rainfall and temperature influenced vital rates
132 and in which period. We did this by comparing a null model (i.e., with only year and
133 population random effects, using a random effect basis (bs = "re") in the mgcv
134 package; (Wood, 2017)) with models including cumulative rainfall or average
135 maximum daily temperature across different periods. As each census was done
136 during the flowering period, we assessed rainfall and temperature effect prior to the
137 annual population census for flowering probability, number of flowers, and seedling
138 size; or in the period between two annual censuses for survival and growth (see
139 Table S2 and Table S3). We considered further lagged climatic effects to be
140 captured by changes in plant size and density.

141 **Table S2 – Periods of average maximum daily temperature and**
 142 **cumulative rainfall considered to assess the effect of temperature and rainfall**
 143 **on dewy-pine vital rates.** We investigated the nonlinear response of dewy-pine vital
 144 rates to average maximum daily temperature ($\mu_{\max T}$) and cumulative rainfall (\sum_{rain}) in
 145 various periods of the years prior (for flowering probability, number of flowers, and
 146 seedling size; in regular text) or post the annual population census (for survival and
 147 growth; in italic).

| Period full name | Period short name | Period start | Period end |
|---------------------------------------------------------|--------------------------------------|--------------|------------------|
| Previous winter average maximum daily temperature | $\mu_{\max T_prevWinter}$ | January | April |
| Previous fall cumulative rainfall | $\sum_{\text{rain_prevFall}}$ | September | November |
| Previous winter cumulative rainfall | $\sum_{\text{rain_prevWinter}}$ | January | April |
| Next summer average maximum daily temperature | $\mu_{\max T_nextSummer}$ | <i>May</i> | <i>September</i> |
| Next fall cumulative rainfall | $\sum_{\text{rain_nextFall}}$ | September | November |
| Next winter cumulative rainfall | $\sum_{\text{rain_nextWinter}}$ | January | April |
| Next fall and winter cumulative rainfall | $\sum_{\text{rain_nextFallWinter}}$ | September | April |

148 We selected the best model among the possible rainfall and temperature periods
149 using the Akaike Information Criterion (AIC), through the *model.sel* and *AICtab*
150 functions of the MuMIn (Bartoń, 2022) and *bbmle* R packages (Bolker, 2022); we
151 used a threshold of $\Delta AIC < 2$ to identify models with no strong difference, and
152 selected the model with the lowest number of degrees of freedom if more than one
153 model were within that threshold. If both models with effects of rainfall and
154 temperature performed better than the null model, we calculated Pearson's
155 correlation coefficient using the *cor.test* function of the stats R package (R Core
156 Team, 2022) to check whether the two variables were correlated. If they were (i.e.,
157 correlation coefficient $> |0.5|$), we used the AIC and the number of degrees of
158 freedom to select the best model between the one with rainfall and the one with
159 temperature. Conversely, if the two variables were not correlated (i.e., correlation
160 coefficient $\leq |0.5|$) We compared the models including one of rainfall and
161 temperature to a model with both climatic variables, including their interaction (Table
162 S3). Finally, we performed a forward selection—using the AIC and the degrees of
163 freedom—, progressively adding aboveground density, size (except for seedling
164 size), and time since fire (TSF; for natural populations only) in the model. While
165 Table S3 only shows splines, we included the linear effects of all covariates in the
166 model selection. We then included interactions between covariates in the model
167 selection if at least one of them was retained in the single effect selection.
168 Additionally, we included terms for site-specific random slopes (e.g., random size
169 effect depending on the site).

170 **Table S3 – Example of the model selection process.** We selected the best model
 171 to predict a given vital rate (vr) using the Akaike Information Criterion (AIC). We first
 172 assessed whether rainfall and temperature affected the vital rate by comparing a null
 173 model (with only year and population random effects (**M1**) to models including rainfall
 174 or temperature values in various periods of the year (Step 1 for temperature and 2
 175 for rainfall). If both models with temperature and rainfall performed better than the
 176 null model, we compared them with a model containing both climatic variables (Step
 177 3), and also included their interaction (Step 4). We then progressively added size,
 178 time since fire (TSF), and aboveground density of large individuals (density) to see if
 179 their introgression improved the model (Steps 5–7). Finally, we included interactions
 180 between covariates when at least one of the two members of the interaction had
 181 been previously retained in the model selection (Steps 8–9). For each step, the *Best*
 182 *model according to the AIC* column shows the best model (**M**) according to the AIC.
 183 This model is then used as a comparison to the newer models in the next step.
 184 Newly added covariates at each time step are shown in green.

| Model selection step | Models compared | Best model according to the AIC |
|----------------------|---------------------------------------------------------------------------------------------------------------------------------------------------------------------------------------------------------------------------------------------------------------------------------------------------|---------------------------------|
| 1 | M1 = vr ~ s(time, bs = "re") + s(site, bs = "re") M2 = vr ~ s($\mu_{\max T_prevWinter}$, k = 3, bs = "cr") + s(time, bs = "re") + s(site, bs = "re") | M2 |
| 2 | M3 = vr ~ s(time, bs = "re") + s(site, bs = "re") M4 = vr ~ s($\sum_{rain_prevFall}$, k = 3, bs = "cr") + s(time, bs = "re") + s(site, bs = "re") M5 = vr ~ s($\sum_{rain_prevFall}$, k = 3, bs = "cr") + s(time, bs = "re") + s(site, bs = "re") | M5 |

| | | |
|---|----------------------------------------------------------------------------------------------------------------------------------------------------------------------------------------------------------------------------------------------------------------------------------------------------------------------------------------------------------------------------------------------------------------------------------------------------------------------------------------------------------------------------------------------------------------------------------------------------------------------------------------------------------------------------------------------------------------------------------------------------------------------------------------------------------------------------------------------------------------------------------------------------------------------------------------------------------------------------------------------------------------------|-----------|
| 3 | <p>M2 = $vr \sim s(\mu_{\max T_prevWinter}, k = 3, bs = "cr") + s(\text{time}, bs = "re") + s(\text{site}, bs = "re")$</p> <p>M5 = $vr \sim s(\sum_{\text{rain_prevFall}}, k = 3, bs = "cr") + s(\text{time}, bs = "re") + s(\text{site}, bs = "re")$</p> <p>M6 = $vr \sim s(\mu_{\max T_prevWinter}, k = 3, bs = "cr") + s(\sum_{\text{rain_prevFall}}, k = 3, bs = "cr") + s(\text{time}, bs = "re") + s(\text{site}, bs = "re")$</p> | M6 |
| 4 | <p>M6 = $vr \sim s(\mu_{\max T_prevWinter}, k = 3, bs = "cr") + s(\sum_{\text{rain_prevFall}}, k = 3, bs = "cr") + s(\text{time}, bs = "re") + s(\text{site}, bs = "re")$</p> <p>M7 = $vr \sim s(\mu_{\max T_prevWinter}, k = 3, bs = "cr") + s(\sum_{\text{rain_prevFall}}, k = 3, bs = "cr") + ti(\mu_{\max T_prevWinter}, \sum_{\text{rain_prevFall}}, k = 3, bs = "cr") + s(\text{time}, bs = "re") + s(\text{site}, bs = "re")$</p> | M7 |
| 5 | <p>M7 = $vr \sim s(\mu_{\max T_prevWinter}, k = 3, bs = "cr") + s(\sum_{\text{rain_prevFall}}, k = 3, bs = "cr") + ti(\mu_{\max T_prevWinter}, \sum_{\text{rain_prevFall}}, k = 3, bs = "cr") + s(\text{time}, bs = "re") + s(\text{site}, bs = "re")$</p> <p>M8 = $vr \sim s(\mu_{\max T_prevWinter}, k = 3, bs = "cr") + s(\sum_{\text{rain_prevFall}}, k = 3, bs = "cr") + ti(\mu_{\max T_prevWinter}, \sum_{\text{rain_prevFall}}, k = 3, bs = "cr") + s(\text{size}, k = 3, bs = "cr") + s(\text{time}, bs = "re") + s(\text{site}, bs = "re")$</p> <p>M9 = $vr \sim s(\mu_{\max T_prevWinter}, k = 3, bs = "cr") + s(\sum_{\text{rain_prevFall}}, k = 3, bs = "cr") + ti(\mu_{\max T_prevWinter}, \sum_{\text{rain_prevFall}}, k = 3, bs = "cr") + s(\text{density}, k = 3, bs = "cr") + s(\text{time}, bs = "re") + s(\text{site}, bs = "re")$</p> <p>M10 = $vr \sim s(\mu_{\max T_prevWinter}, k = 3, bs = "cr") +$</p> | M9 |

| | | |
|---|--------------------------------------------------------------------------------------------------------------------------------------------------------------------------------------------------------------------------------------------------------------------------------------------------------------------------------------------------------------------------------------------------------------------------------------------------------------------------------------------------------------------------------------------------------------------------------------------------------------------------------------------------------------------------------------------------------------------------------------------------------------------------------------------------------------------------------------------------------------------------------------------------------------------------------------------------------------------------------------------------------------------------------------------------------------------------------------------------------------------------------------------------------------------------------------------------------------------------------------------------------------------------------------------------------------------------------------------------------------------------------------------------------------------------------------------------------------------------------------------------------------------------------------------------------------------------------------------------------------------------------------------------------------------------------------|------------|
| | <p> $s(\sum \text{rain_prevFall}, k = 3, \text{bs} = \text{"cr"}) +$ $ti(\mu_{\text{maxT_prevWinter}}, \sum \text{rain_prevFall}, k = 3, \text{bs} = \text{"cr"})$ + $s(\text{TSF}, k = 3, \text{bs} = \text{"cr"}) +$ $s(\text{time}, \text{bs} = \text{"re"}) +$ $s(\text{site}, \text{bs} = \text{"re"})$ </p> | |
| 6 | <p> M9 = $vr \sim s(\mu_{\text{maxT_prevWinter}}, k = 3, \text{bs} = \text{"cr"}) +$ $s(\sum \text{rain_prevFall}, k = 3, \text{bs} = \text{"cr"}) +$ $ti(\mu_{\text{maxT_prevWinter}}, \sum \text{rain_prevFall}, k = 3, \text{bs} = \text{"cr"})$ + $s(\text{density}, k = 3, \text{bs} = \text{"cr"}) +$ $s(\text{time}, \text{bs} = \text{"re"}) +$ $s(\text{site}, \text{bs} = \text{"re"})$ M11 = $vr \sim s(\mu_{\text{maxT_prevWinter}}, k = 3, \text{bs} = \text{"cr"}) +$ $s(\sum \text{rain_prevFall}, k = 3, \text{bs} = \text{"cr"}) +$ $ti(\mu_{\text{maxT_prevWinter}}, \sum \text{rain_prevFall}, k = 3, \text{bs} = \text{"cr"})$ + $s(\text{density}, k = 3, \text{bs} = \text{"cr"}) +$ $s(\text{size}, k = 3, \text{bs} = \text{"cr"}) +$ $s(\text{time}, \text{bs} = \text{"re"}) +$ $s(\text{site}, \text{bs} = \text{"re"})$ M12 = $vr \sim s(\mu_{\text{maxT_prevWinter}}, k = 3, \text{bs} = \text{"cr"}) +$ $s(\sum \text{rain_prevFall}, k = 3, \text{bs} = \text{"cr"}) +$ $ti(\mu_{\text{maxT_prevWinter}}, \sum \text{rain_prevFall}, k = 3, \text{bs} = \text{"cr"})$ + $s(\text{density}, k = 3, \text{bs} = \text{"cr"}) +$ $s(\text{TSF}, k = 3, \text{bs} = \text{"cr"}) +$ $s(\text{time}, \text{bs} = \text{"re"}) +$ $s(\text{site}, \text{bs} = \text{"re"})$ </p> | M12 |

| | | |
|---|--------------------------------------------------------------------------------------------------------------------------------------------------------------------------------------------------------------------------------------------------------------------------------------------------------------------------------------------------------------------------------------------------------------------------------------------------------------------------------------------------------------------------------------------------------------------------------------------------------------------------------------------------------------------------------------------------------------------------------------------------------------------------------------------------------------------------------------------------------------------------------------------------------------------------------------------------------------------------------------------------------------------------------------------------------------------------------------------------------------------------------------------------------------------------------------------------------------------------------------------------------------------------------------------------------------------------------------------------------------------------------------------------------------------------------------------------------|------------|
| 7 | <p>M12 = $vr \sim s(\mu_{\max T_prevWinter}, k = 3, bs = "cr") +$ $s(\sum rain_prevFall, k = 3, bs = "cr") +$ $ti(\mu_{\max T_prevWinter}, \sum rain_prevFall, k = 3, bs = "cr")$</p> <p>+</p> <p>$s(density, k = 3, bs = "cr") +$ $s(TSF, k = 3, bs = "cr") +$ $s(time, bs = "re") +$ $s(site, bs = "re")$</p> <p>M13 = $vr \sim s(\mu_{\max T_prevWinter}, k = 3, bs = "cr") +$ $s(\sum rain_prevFall, k = 3, bs = "cr") +$ $ti(\mu_{\max T_prevWinter}, \sum rain_prevFall, k = 3, bs = "cr")$</p> <p>+</p> <p>$s(density, k = 3, bs = "cr") +$ $s(TSF, k = 3, bs = "cr") +$ $s(size, k = 3, bs = "cr") +$ $s(time, bs = "re") +$ $s(site, bs = "re")$</p> | M12 |
| 8 | <p>M12 = $vr \sim s(\mu_{\max T_prevWinter}, k = 3, bs = "cr") +$ $s(\sum rain_prevFall, k = 3, bs = "cr") +$ $ti(\mu_{\max T_prevWinter}, \sum rain_prevFall, k = 3, bs = "cr")$</p> <p>+</p> <p>$s(density, k = 3, bs = "cr") +$ $s(TSF, k = 3, bs = "cr") +$ $s(time, bs = "re") +$ $s(site, bs = "re")$</p> <p>M14 = $vr \sim s(\mu_{\max T_prevWinter}, k = 3, bs = "cr") +$ $s(\sum rain_prevFall, k = 3, bs = "cr") +$ $ti(\mu_{\max T_prevWinter}, \sum rain_prevFall, k = 3, bs = "cr")$</p> <p>+</p> <p>$s(density, k = 3, bs = "cr") +$ $s(TSF, k = 3, bs = "cr") +$ $ti(\mu_{\max T_prevWinter}, density, k = 3, bs = "cr") +$ $s(time, bs = "re") +$ $s(site, bs = "re")$</p> <p>M15 = $vr \sim s(\mu_{\max T_prevWinter}, k = 3, bs = "cr") +$ $s(\sum rain_prevFall, k = 3, bs = "cr") +$ $ti(\mu_{\max T_prevWinter}, \sum rain_prevFall, k = 3, bs = "cr")$</p> <p>+</p> <p>$s(density, k = 3, bs = "cr") +$ $s(TSF, k = 3, bs = "cr") +$ $ti(\mu_{\max T_prevWinter}, TSF, k = 3, bs = "cr") +$ $s(time, bs = "re") +$ $s(site, bs = "re")$</p> | M15 |

| | |
|---------------------------------------------------------------------------------------------------------------------------------------------------------------------------------------------------------------------------------------------------------------------------------------------------------------------------------------------------------------------------------------------------------------------------------------------------------------------------------------------------------------------------------------------------------------------------------------------------------------------------------------------------------------------------------------------------------------------------------------------------------------------------------------------------------------------------------------------------------------------------------------------------------------------------------------------------------------------------------------------------------------------------------------------------------------------------------------------------------------------------------------------------------------------------------------------------------------------------------------------------------------------------------------------------------------------------------------------------------------------------------------------------------------------------------------------------------------------------------------------------------------------------------------------------------------------------------------------------------------------------------------------------------------------------------------------------------------------------------------------------------------------------------------------------------------------------------------------------------------------------------------------------------------------------------------------------------------------------------------------------------------------------------------------------------------------------------------------------------------------------------------------------------------------------------------------------------------------------------------------------------------------------------------------------------------------------------------------------------------------------------|--|
| <p>M16 = $vr \sim s(\mu_{\max T_prevWinter}, k = 3, bs = "cr") +$ $s(\sum rain_prevFall, k = 3, bs = "cr") +$ $ti(\mu_{\max T_prevWinter}, \sum rain_prevFall, k = 3, bs = "cr")$</p> <p>+</p> <p>$s(density, k = 3, bs = "cr") +$ $s(TSF, k = 3, bs = "cr") +$ $ti(\mu_{\max T_prevWinter}, size, k = 3, bs = "cr") +$ $s(time, bs = "re") +$ $s(site, bs = "re")$</p> <p>M17 = $vr \sim s(\mu_{\max T_prevWinter}, k = 3, bs = "cr") +$ $s(\sum rain_prevFall, k = 3, bs = "cr") +$ $ti(\mu_{\max T_prevWinter}, \sum rain_prevFall, k = 3, bs = "cr")$</p> <p>+</p> <p>$s(density, k = 3, bs = "cr") +$ $s(TSF, k = 3, bs = "cr") +$ $ti(\sum rain_prevFall, density, k = 3, bs = "cr") +$ $s(time, bs = "re") +$ $s(site, bs = "re")$</p> <p>M18 = $vr \sim s(\mu_{\max T_prevWinter}, k = 3, bs = "cr") +$ $s(\sum rain_prevFall, k = 3, bs = "cr") +$ $ti(\mu_{\max T_prevWinter}, \sum rain_prevFall, k = 3, bs = "cr")$</p> <p>+</p> <p>$s(density, k = 3, bs = "cr") +$ $s(TSF, k = 3, bs = "cr") +$ $ti(\sum rain_prevFall, TSF, k = 3, bs = "cr") +$ $s(time, bs = "re") +$ $s(site, bs = "re")$</p> <p>M19 = $vr \sim s(\mu_{\max T_prevWinter}, k = 3, bs = "cr") +$ $s(\sum rain_prevFall, k = 3, bs = "cr") +$ $ti(\mu_{\max T_prevWinter}, \sum rain_prevFall, k = 3, bs = "cr")$</p> <p>+</p> <p>$s(density, k = 3, bs = "cr") +$ $s(TSF, k = 3, bs = "cr") +$ $ti(\sum rain_prevFall, size, k = 3, bs = "cr") +$ $s(time, bs = "re") +$ $s(site, bs = "re")$</p> <p>M20 = $vr \sim s(\mu_{\max T_prevWinter}, k = 3, bs = "cr") +$ $s(\sum rain_prevFall, k = 3, bs = "cr") +$ $ti(\mu_{\max T_prevWinter}, \sum rain_prevFall, k = 3, bs = "cr")$</p> <p>+</p> <p>$s(density, k = 3, bs = "cr") +$ $s(TSF, k = 3, bs = "cr") +$</p> | |
|---------------------------------------------------------------------------------------------------------------------------------------------------------------------------------------------------------------------------------------------------------------------------------------------------------------------------------------------------------------------------------------------------------------------------------------------------------------------------------------------------------------------------------------------------------------------------------------------------------------------------------------------------------------------------------------------------------------------------------------------------------------------------------------------------------------------------------------------------------------------------------------------------------------------------------------------------------------------------------------------------------------------------------------------------------------------------------------------------------------------------------------------------------------------------------------------------------------------------------------------------------------------------------------------------------------------------------------------------------------------------------------------------------------------------------------------------------------------------------------------------------------------------------------------------------------------------------------------------------------------------------------------------------------------------------------------------------------------------------------------------------------------------------------------------------------------------------------------------------------------------------------------------------------------------------------------------------------------------------------------------------------------------------------------------------------------------------------------------------------------------------------------------------------------------------------------------------------------------------------------------------------------------------------------------------------------------------------------------------------------------------|--|

| | | |
|---|-----------------------------------------------------------------------------------------------------------------------------------------------------------------------------------------------------------------------------------------------------------------------------------------------------------------------------------------------------------------------------------------------------------------------------------------------------------------------------------------------------------------------------------------------------------------------------------------------------------------------------------------------------------------------------------------------------------------------------------------------------------------------------------------------------------------------------------------------------------------------------------------------------------------------------------------------------------------------------------------------------------------------------------------------------------------------------------------------------------------------------------------------------------------------------------------------------------------------------------------------------------------------------------------------------------------------------------------------------------------------------------------------------------------------------------------------------------------------------------------------------------------------------------------------------------------------------------------------------------------------------------------------------------------------------------------------------------|-----|
| | <p> $ti(\text{density}, \text{TSF}, k = 3, \text{bs} = \text{"cr"}) +$ $s(\text{time}, \text{bs} = \text{"re"}) +$ $s(\text{site}, \text{bs} = \text{"re"})$ </p> <p> M21 = $vr \sim s(\mu_{\text{maxT_prevWinter}}, k = 3, \text{bs} = \text{"cr"}) +$ $s(\sum_{\text{rain_prevFall}}, k = 3, \text{bs} = \text{"cr"}) +$ $ti(\mu_{\text{maxT_prevWinter}}, \sum_{\text{rain_prevFall}}, k = 3, \text{bs} = \text{"cr"})$ </p> <p>+</p> <p> $s(\text{density}, k = 3, \text{bs} = \text{"cr"}) +$ $s(\text{TSF}, k = 3, \text{bs} = \text{"cr"}) +$ $ti(\text{density}, \text{size}, k = 3, \text{bs} = \text{"cr"}) +$ $s(\text{time}, \text{bs} = \text{"re"}) +$ $s(\text{site}, \text{bs} = \text{"re"})$ </p> <p> M22 = $vr \sim s(\mu_{\text{maxT_prevWinter}}, k = 3, \text{bs} = \text{"cr"}) +$ $s(\sum_{\text{rain_prevFall}}, k = 3, \text{bs} = \text{"cr"}) +$ $ti(\mu_{\text{maxT_prevWinter}}, \sum_{\text{rain_prevFall}}, k = 3, \text{bs} = \text{"cr"})$ </p> <p>+</p> <p> $s(\text{density}, k = 3, \text{bs} = \text{"cr"}) +$ $s(\text{TSF}, k = 3, \text{bs} = \text{"cr"}) +$ $ti(\text{TSF}, \text{size}, k = 3, \text{bs} = \text{"cr"}) +$ $s(\text{time}, \text{bs} = \text{"re"}) +$ $s(\text{site}, \text{bs} = \text{"re"})$ </p> | |
| 9 | <p> M15 = $vr \sim s(\mu_{\text{maxT_prevWinter}}, k = 3, \text{bs} = \text{"cr"}) +$ $s(\sum_{\text{rain_prevFall}}, k = 3, \text{bs} = \text{"cr"}) +$ $ti(\mu_{\text{maxT_prevWinter}}, \sum_{\text{rain_prevFall}}, k = 3, \text{bs} = \text{"cr"})$ </p> <p>+</p> <p> $s(\text{density}, k = 3, \text{bs} = \text{"cr"}) +$ $s(\text{TSF}, k = 3, \text{bs} = \text{"cr"}) +$ $ti(\mu_{\text{maxT_prevWinter}}, \text{TSF}, k = 3, \text{bs} = \text{"cr"}) +$ $s(\text{time}, \text{bs} = \text{"re"}) +$ $s(\text{site}, \text{bs} = \text{"re"})$ </p> <p> M23 = $vr \sim s(\mu_{\text{maxT_prevWinter}}, k = 3, \text{bs} = \text{"cr"}) +$ $s(\sum_{\text{rain_prevFall}}, k = 3, \text{bs} = \text{"cr"}) +$ $ti(\mu_{\text{maxT_prevWinter}}, \sum_{\text{rain_prevFall}}, k = 3, \text{bs} = \text{"cr"})$ </p> <p>+</p> <p> $s(\text{density}, k = 3, \text{bs} = \text{"cr"}) +$ $s(\text{TSF}, k = 3, \text{bs} = \text{"cr"}) +$ $ti(\mu_{\text{maxT_prevWinter}}, \text{TSF}, k = 3, \text{bs} = \text{"cr"}) +$ $ti(\mu_{\text{maxT_prevWinter}}, \text{density}, k = 3, \text{bs} = \text{"cr"}) +$ $s(\text{time}, \text{bs} = \text{"re"}) +$ $s(\text{site}, \text{bs} = \text{"re"})$ </p> <p> M24 = $vr \sim s(\mu_{\text{maxT_prevWinter}}, k = 3, \text{bs} = \text{"cr"}) +$ $s(\sum_{\text{rain_prevFall}}, k = 3, \text{bs} = \text{"cr"}) +$ </p> | M15 |

| | | |
|--|---------------------------------------------------------------------------------------------------------------------------------------------------------------------------------------------------------------------------------------------------------------------------------|--|
| | $ti(\mu_{\max T_prevWinter}, \sum_{\text{rain_prevFall}}, k = 3, bs = "cr")$ | |
| | $+$ $s(\text{density}, k = 3, bs = "cr") +$ $s(\text{TSF}, k = 3, bs = "cr") +$ $ti(\mu_{\max T_prevWinter}, \text{TSF}, k = 3, bs = "cr") +$ $ti(\mu_{\max T_prevWinter}, \text{size}, k = 3, bs = "cr") +$ $s(\text{time}, bs = "re") +$ $s(\text{site}, bs = "re")$ | |
| | $\mathbf{M25} = vr \sim s(\mu_{\max T_prevWinter}, k = 3, bs = "cr") +$ $s(\sum_{\text{rain_prevFall}}, k = 3, bs = "cr") +$ $ti(\mu_{\max T_prevWinter}, \sum_{\text{rain_prevFall}}, k = 3, bs = "cr")$ | |
| | $+$ $s(\text{density}, k = 3, bs = "cr") +$ $s(\text{TSF}, k = 3, bs = "cr") +$ $ti(\mu_{\max T_prevWinter}, \text{TSF}, k = 3, bs = "cr") +$ $ti(\sum_{\text{rain_prevFall}}, \text{density}, k = 3, bs = "cr") +$ $s(\text{time}, bs = "re") +$ $s(\text{site}, bs = "re")$ | |
| | $\mathbf{M26} = vr \sim s(\mu_{\max T_prevWinter}, k = 3, bs = "cr") +$ $s(\sum_{\text{rain_prevFall}}, k = 3, bs = "cr") +$ $ti(\mu_{\max T_prevWinter}, \sum_{\text{rain_prevFall}}, k = 3, bs = "cr")$ | |
| | $+$ $s(\text{density}, k = 3, bs = "cr") +$ $s(\text{TSF}, k = 3, bs = "cr") +$ $ti(\mu_{\max T_prevWinter}, \text{TSF}, k = 3, bs = "cr") +$ $ti(\sum_{\text{rain_prevFall}}, \text{TSF}, k = 3, bs = "cr") +$ $s(\text{time}, bs = "re") +$ $s(\text{site}, bs = "re")$ | |
| | $\mathbf{M27} = vr \sim s(\mu_{\max T_prevWinter}, k = 3, bs = "cr") +$ $s(\sum_{\text{rain_prevFall}}, k = 3, bs = "cr") +$ $ti(\mu_{\max T_prevWinter}, \sum_{\text{rain_prevFall}}, k = 3, bs = "cr")$ | |
| | $+$ $s(\text{density}, k = 3, bs = "cr") +$ $s(\text{TSF}, k = 3, bs = "cr") +$ $ti(\mu_{\max T_prevWinter}, \text{TSF}, k = 3, bs = "cr") +$ $ti(\sum_{\text{rain_prevFall}}, \text{size}, k = 3, bs = "cr") +$ $s(\text{time}, bs = "re") +$ $s(\text{site}, bs = "re")$ | |
| | $\mathbf{M28} = vr \sim s(\mu_{\max T_prevWinter}, k = 3, bs = "cr") +$ $s(\sum_{\text{rain_prevFall}}, k = 3, bs = "cr") +$ | |

| | | |
|--|-----------------------------------------------------------------------------------------------------------------------------------------------------------------------------------------------------------------------------------------------------------------------------------------------------------------------------------------------------------------------------------------------------------------------------------------------------------------------------------------------------------------------------------------------------------------------------------------------------------------------------------------------------------------------------------------------------------------------------------------------------------------------------------------------------------------------------------------------------------------------------------------------------------------------------------------------------------------------------------------------------------------------------------------------------------------------------------------------------------------------------------------------------------------------------------------------------------------------------------------------------------------------------------------------------------------------------------------------------------------------------------------------------------------------------------------------------------------------------------------------------------------------------------------------|--|
| | <p> $ti(\mu_{\max T_prevWinter}, \sum_{rain_prevFall}, k = 3, bs = "cr")$ + $s(density, k = 3, bs = "cr") +$ $s(TSF, k = 3, bs = "cr") +$ $ti(\mu_{\max T_prevWinter}, TSF, k = 3, bs = "cr") +$ $ti(density, TSF, k = 3, bs = "cr") +$ $s(time, bs = "re") +$ $s(site, bs = "re")$ </p> <p> M29 = $vr \sim s(\mu_{\max T_prevWinter}, k = 3, bs = "cr") +$ $s(\sum_{rain_prevFall}, k = 3, bs = "cr") +$ $ti(\mu_{\max T_prevWinter}, \sum_{rain_prevFall}, k = 3, bs =$ "cr") + $s(density, k = 3, bs = "cr") +$ $s(TSF, k = 3, bs = "cr") +$ $ti(\mu_{\max T_prevWinter}, TSF, k = 3, bs = "cr") +$ $ti(density, size, k = 3, bs = "cr") +$ $s(time, bs = "re") +$ $s(site, bs = "re")$ </p> <p> M30 = $vr \sim s(\mu_{\max T_prevWinter}, k = 3, bs = "cr") +$ $s(\sum_{rain_prevFall}, k = 3, bs = "cr") +$ $ti(\mu_{\max T_prevWinter}, \sum_{rain_prevFall}, k = 3, bs = "cr")$ + $s(density, k = 3, bs = "cr") +$ $s(TSF, k = 3, bs = "cr") +$ $ti(\mu_{\max T_prevWinter}, TSF, k = 3, bs = "cr") +$ $ti(TSF, size, k = 3, bs = "cr") +$ $s(time, bs = "re") +$ $s(site, bs = "re")$ </p> | |
|--|-----------------------------------------------------------------------------------------------------------------------------------------------------------------------------------------------------------------------------------------------------------------------------------------------------------------------------------------------------------------------------------------------------------------------------------------------------------------------------------------------------------------------------------------------------------------------------------------------------------------------------------------------------------------------------------------------------------------------------------------------------------------------------------------------------------------------------------------------------------------------------------------------------------------------------------------------------------------------------------------------------------------------------------------------------------------------------------------------------------------------------------------------------------------------------------------------------------------------------------------------------------------------------------------------------------------------------------------------------------------------------------------------------------------------------------------------------------------------------------------------------------------------------------------------|--|

186 5. Vital-rate estimation results

187

188 **Table S4 – Most parsimonious generalised additive models for dewy-**

189 **pine vital rates.** For natural and anthropogenic populations, we estimated survival

190 (σ), growth of aboveground plants (φ), flowering probability (p_{fi}), number of flowers

191 ($n_{flowers}$), and seedling size (Φ) as a function of monthly average daily maximum

192 temperature in a given period (μ_{maxT_period}), monthly cumulative rainfall in a given

193 period (\sum_{rain_period}), aboveground density of large individuals (density), individual

194 size, and—for natural populations—time since fire (TSF). We selected the best

195 model to predict a given vital rate using the Akaike Information Criterion (AIC). The

196 function $s(x_{edf})$ is the spline smoothing function (i.e. simple effect) of x , and $ti(x, y_{edf})$

197 is the tensor product smoothing function of x and y . We used a cubic regression

198 spline (bs = “cr” in the mgcv package; Wood, 2011; Wood et al., 2016; Wood, 2017)

199 for all smoothing parameters, with a dimension $k = 3$ (except for the size effect on

200 the number of flowers, where we used $k = 4$ to force a decline in the number of

201 flowers of large individuals and avoid an ever-increasing number of flowers).

202 Additionally, all models include a year and site random effect. edf is the

203 corresponding effective degrees of freedom (Wood, 2017), which represents the

204 amount of nonlinearity in the model component ($edf = 1$ corresponds to a linear fit),

205 and n in the sample size. For the intercept and linear predictors (i.e., outside of s and

206 ti smoothing functions), we report the estimated β -coefficients and the standard

207 error.

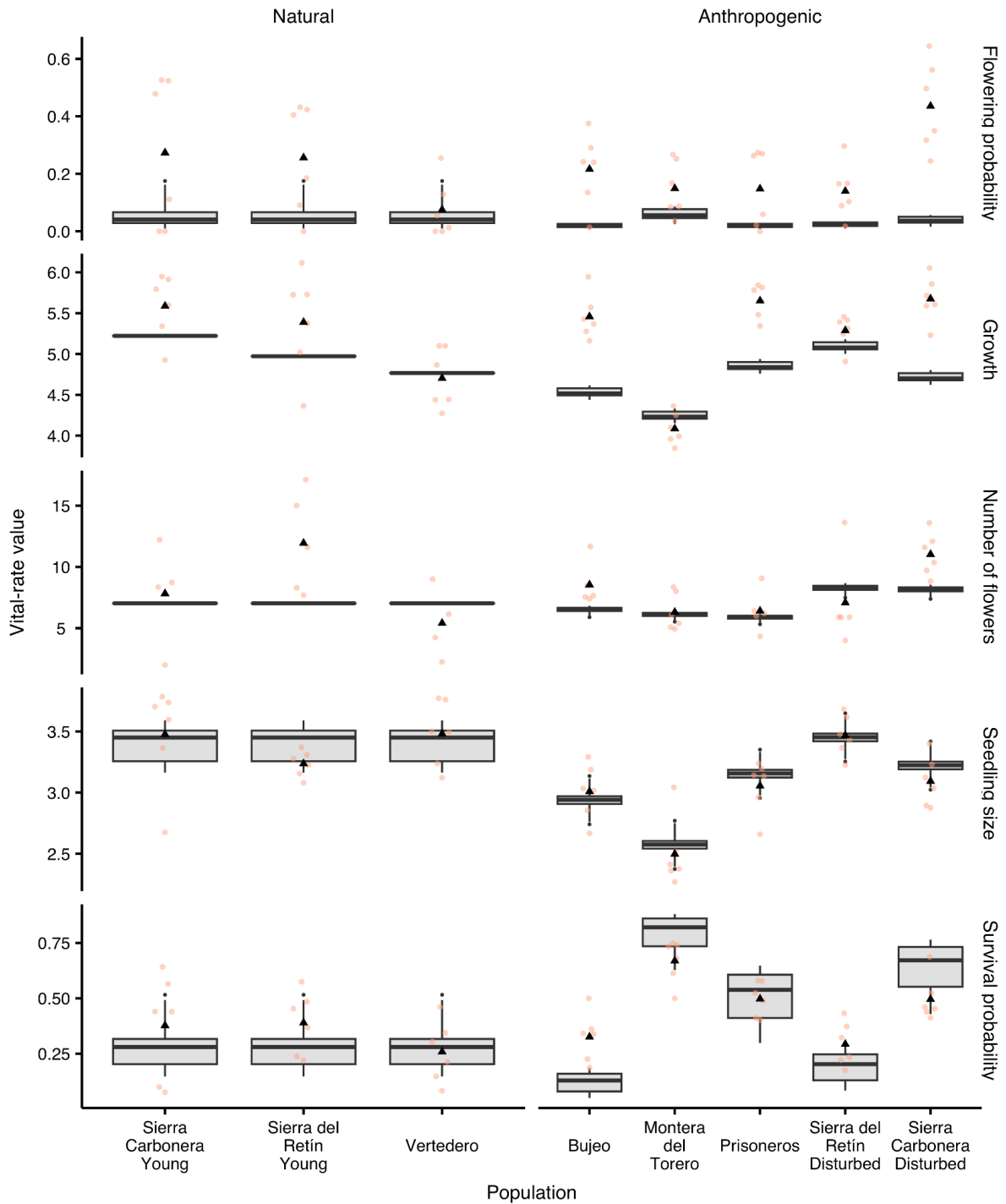
208

| Vital rate | Family (link function) | Most parsimonious model | <i>n</i> |
|----------------------------------|----------------------------|---------------------------------------------------------------------------------------------------------------------------------------------------------------------------------------------------------------------------------------------------------------------------------------------------------------------------------------------------------------------------------------------------------------------------------------------------------------------------------------------------------------------------------------------------------------------------------------------------------------------------------------------------------------------------------------------------------------|----------|
| Natural populations | | | |
| σ | Binomial (logit) | -1.1 _(0.28) + 0.27 _(0.47) $\mu_{\max T_nextSummer}$ + 0.11 _(0.48) $\sum_{rain_nextFall}$ + ti($\sum_{rain_nextFall}$, $\mu_{\max T_nextSummer}$ edf=0.88) + s(size edf=1.7) + s(TSF edf=0.00018) + s($\mu_{\max T_nextSummer}$, site edf=1.5, bs = "re") + ti(size, TSF edf=2.1) + ti($\sum_{rain_nextFall}$, density edf=2.7) - 1.4 _(0.46) $\sum_{rain_nextFall}$ *TSF + ti($\mu_{\max T_nextSummer}$, size edf=0.74) - 0.26 _(0.096) $\mu_{\max T_nextSummer}$ *density + ti($\mu_{\max T_nextSummer}$, TSF edf=0.93) + ti($\sum_{rain_nextFall}$, size edf=1.7) + s(time edf=3.8, bs = "re") + s(site edf=0.00010, bs = "re") | 1493 |
| γ | Scaled <i>t</i> (identity) | 5.1 _(0.12) + s($\sum_{rain_nextFall}$ edf=0.000063) + 1.5 _(0.14) size + s(TSF edf=1.7) - 0.074 _(0.018) density + s(size, site edf=1.6, bs = "re") + ti($\sum_{rain_nextFall}$, TSF edf=0.81) + ti($\sum_{rain_nextFall}$, density edf=2.1) + ti(size, density edf=0.83) + s(time edf=0.000019, bs = "re") + s(site edf=1.8, bs = "re") | 482 |
| ρ_{fi} | Binomial (logit) | -4.0 _(0.57) + 0.93 _(0.95) $\sum_{rain_prevFall}$ + ti($\sum_{rain_prevFall}$, $\mu_{\max T_prevWinter}$ edf=1.5) + 5.5 _(0.44) size + s(TSF edf=0.0000079) + ti(TSF, $\mu_{\max T_prevWinter}$ edf=0.91) + ti(TSF, density edf=0.58) + ti($\sum_{rain_prevFall}$, TSF edf=0.61) + ti($\sum_{rain_prevFall}$, density edf=1.3) + ti(size, density edf=1.2) + s(time edf=3.8, bs = "re") + s(site edf=0.000041, bs = "re") | 1487 |
| $n_{flowers}$ | Negative binomial (log) | 2.0 _(0.052) + s($\mu_{\max T_prevWinter}$ edf=0.00041) + s(size edf=2.8) - 0.40 _(1.4) TSF + s(time edf=0.0013, bs = "re") + s(site edf=0.000056, bs = "re") | 185 |
| Φ | Scaled <i>t</i> (identity) | 3.4 _(0.073) + s($\mu_{\max T_prevWinter}$ edf=0.66) + s(density edf=0.49) + 0.16 _(0.079) TSF + s(density, site edf=0.000064, bs = "re") + s(TSF, site edf=0.69, bs = "re") + ti($\mu_{\max T_prevWinter}$, density edf=1.3) + ti($\mu_{\max T_prevWinter}$, TSF edf=0.76) + ti(density, TSF edf=0.69) + s(time edf=4.8, bs = "re") + s(site edf=0.000071, bs = "re") | 745 |
| Anthropogenic populations | | | |
| σ | Binomial (logit) | -0.55 _(0.60) + s($\sum_{rain_nextFall}$ edf=0.015) - 1.8 _(0.41) $\mu_{\max T_nextSummer}$ + ti($\sum_{rain_nextFall}$, $\mu_{\max T_nextSummer}$ edf=0.00017) + s(size edf=1.9) + s(size, site edf=3.6, bs = "re") + s($\sum_{rain_nextFall}$, site edf=3.2, bs = "re") + ti($\sum_{rain_nextFall}$, size edf=0.92) + 0.11 _(0.037) size*density + s(time edf=4.5, bs = "re") + s(site edf=3.9, bs = "re") | 6008 |
| γ | Scaled <i>t</i> (identity) | 5.0 _(0.13) + s($\mu_{\max T_nextSummer}$ edf=0.37) + s(size edf=1.6) - 0.028 _(0.0053) density + s(size, site edf=3.9, bs = "re") + s($\mu_{\max T_nextSummer}$, site edf=3.9, bs = "re") + s(time edf=3.9, bs = "re") + s(site edf=3.8, bs = "re") | 3202 |
| ρ_{fi} | Binomial (logit) | -4.7 _(0.36) + s($\sum_{rain_prevWinter}$ edf=0.50) + s(size edf=2.0) + s(density, edf=1.6) + s(size, site edf=3.6, bs = "re") + s($\sum_{rain_prevWinter}$, site edf=2.4, bs = "re") + s(density, site edf=2.7, bs = "re") + s(time edf=5.0, bs = "re") + s(site edf=3.0, bs = "re") | 6254 |
| $n_{flowers}$ | Negative binomial (log) | 1.9 _(0.072) + s($\sum_{rain_prevFall}$ edf=0.0012) + s(size edf=2.8) + s($\sum_{rain_prevFall}$, site edf=4.0, bs = "re") + s(size, site edf=3.7, bs = "re") + s(time edf=3.0, bs = "re") + s(site edf=0.015, bs = "re") | 899 |
| Φ | Scaled <i>t</i> (identity) | 3.0 _(0.14) + s($\mu_{\max T_prevWinter}$ edf=0.50) - 0.057 _(0.012) density + s($\mu_{\max T_prevWinter}$, site edf=2.9, bs = "re") + s(density, site edf=1.9, bs = "re") + ti($\mu_{\max T_prevWinter}$, density edf=0.64) + s(time edf=5.5, bs = "re") + s(site edf=3.9, bs = "re") | 2608 |

210 *Among-site variation in average vital rates and climate effects*

211

212 Dewy-pine vital rates varied between natural and anthropogenic habitat as
213 well as between sites. Among-site variation was larger in anthropogenic than in
214 natural conditions, possibly because of the among-population differences in the level
215 of anthropogenic disturbance. This variation was especially large for survival rates,
216 which ranged from 0.11 [0.058, 0.20] in Bujeo to 0.80 [0.72, 0.86] in Montera del
217 Torero, while it remained stable at 0.27 [0.17, 0.40] on average in natural
218 populations (Fig. S3).



219

220

Figure S3 – Among-site variation in average vital-rate values in natural

221

and anthropogenic populations. The boxplots represent the distribution of the

222

average values of site-specific survival, growth, and flowering rates, as well as the

223

number of flowers and seedling size estimated for each year. The whiskers

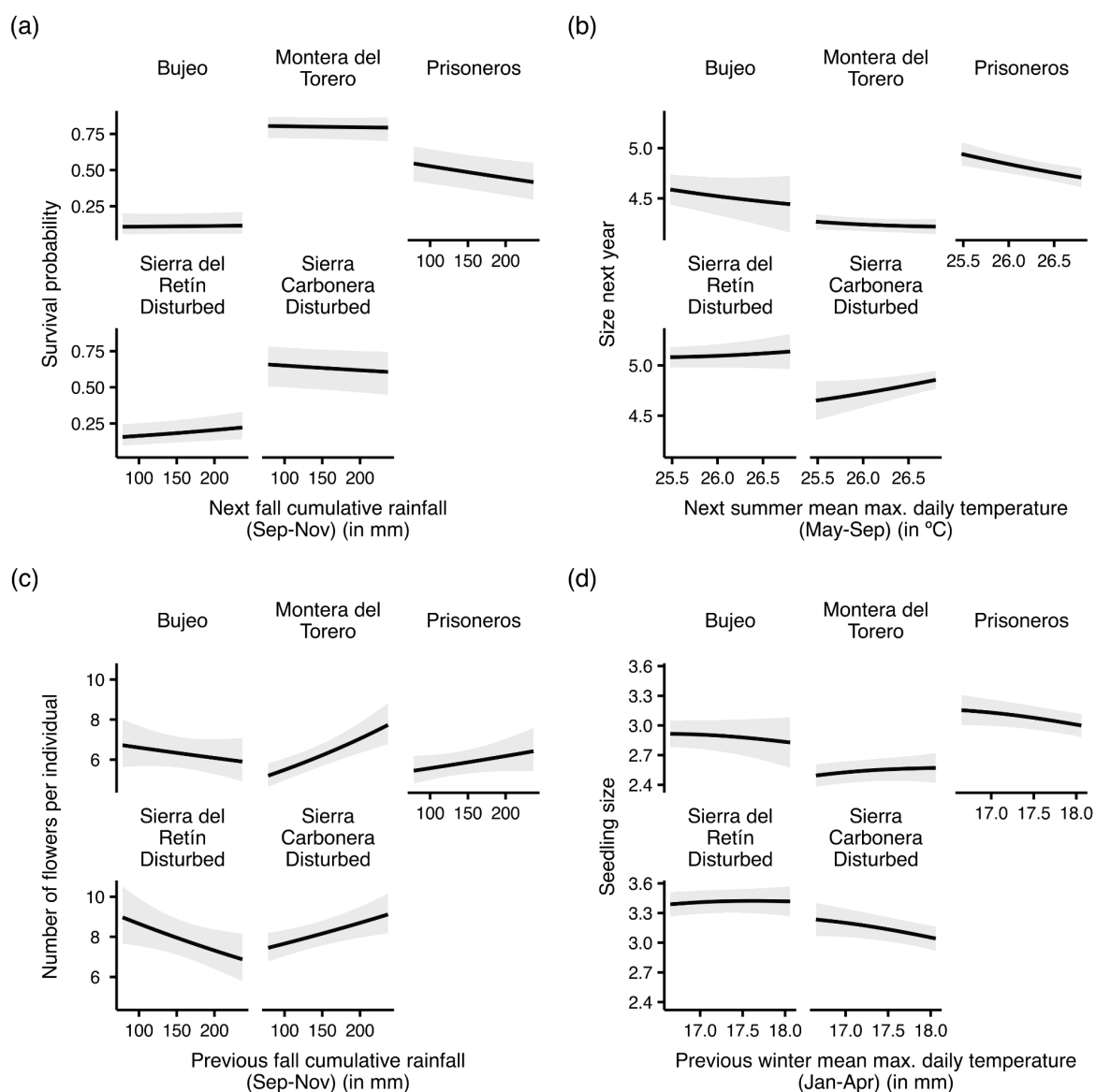
224

represent the 2.5th and 97.5th percentiles and the black triangle the mean estimate.

225 We kept covariates at their mean values (scaled value = 0) except for the number of
226 flowers, where we used the mean size of reproducing individuals. The coloured dots
227 represent the observed average vital rates in each population and year.

228

229 In anthropogenic habitats, we found among-site disparities in the direction of
230 association between climatic variables and survival, growth, number of flowers per
231 individual, and seedling size (Fig. S4). For instance, the number of flowers was
232 positively associated with increasing rainfall in Montera del Torero population (e.g.
233 from 5.5 [5.0, 6.1] under 100 mm of rain to 7.0 [6.3, 7.8] under 200 mm), but
234 negatively in Sierra del Retín Disturbed (e.g. from 8.7 [7.5, 9.9] to 7.3 [6.4, 8.4]). In
235 contrast, there was no such among-site variation in natural habitats. For example,
236 seedlings were bigger with higher winter temperatures (January–April); seedling size
237 increased from 3.0 [2.8, 3.3] under 16 °C to 3.4 [3.3, 3.6] under 18 °C (Fig. S5).



238

239

Figure S4 – Among-site variation in the association between climatic

240

variables and vital rates in anthropogenic populations. We predicted the values

241

of (a) survival probability, (b) size in the next year, (c) number of flowers per

242

individual, and (d) seedling size for a range of rainfall and temperature values in

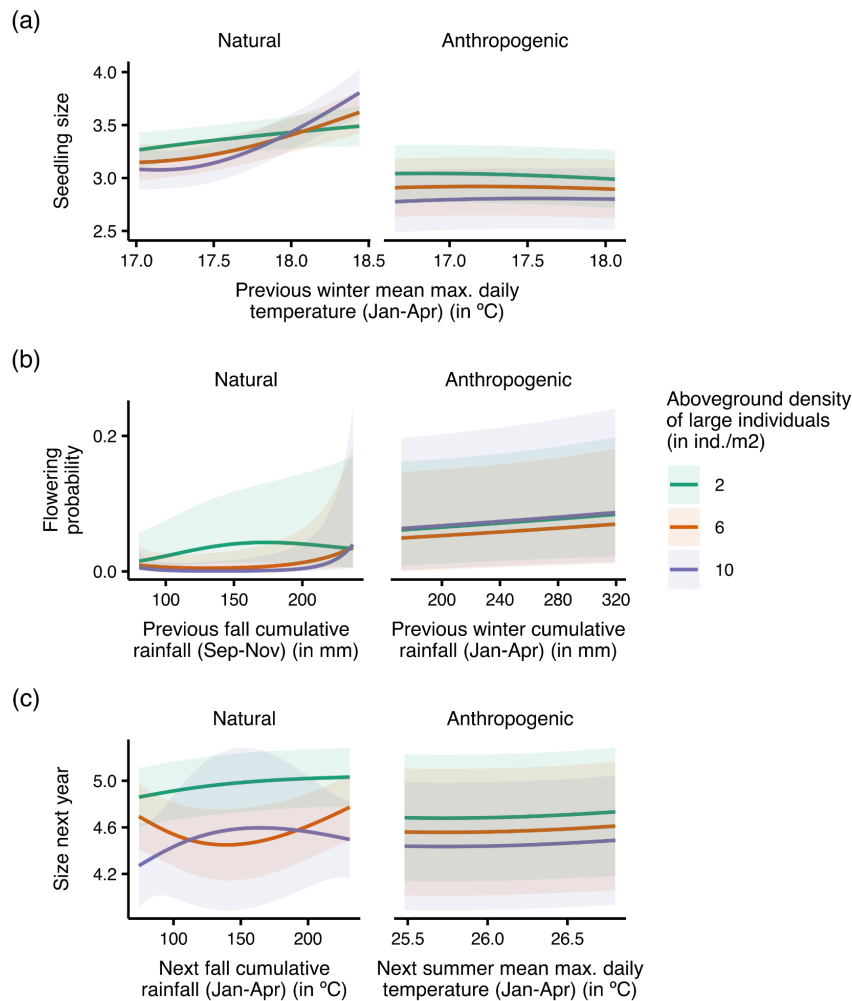
243

each anthropogenic population of dewy pines. The lines represent the average vital-

244

rate value and the shaded ribbon the 95% confidence interval. We kept all other

245 covariates at their mean values (scaled value = 0) except for the number of flowers,
 246 where we used the mean size of reproducing individuals.



247

248 **Figure S5 – Density-dependent variation in vital-rate responses to**

249 **climate.** We predicted the values of (a) seedling size, (b) flowering probability, and

250 (c) size in the next year for a range of rainfall and temperature values and three

251 levels of aboveground densities in natural and anthropogenic habitats. The lines

252 represent the average vital-rate value and the shaded ribbon the 95% confidence

253 interval. We kept all other covariates at their mean values (scaled value = 0) except

254 for the number of flowers, where we used the mean size of reproducing individuals.

255

256 *Vital-rate responses to large aboveground individual density and climate-*
257 *density interactions*

258

259 Seedling size decreased with higher numbers of large individuals aboveground (from
260 3.0 [2.8, 3.3] at 2 ind./m² to 2.8 [2.5, 3.1] at 10 ind./m² in anthropogenic populations
261 and from 3.4 [3.2, 3.5] to 3.1 [3.0, 3.3] in natural ones; Fig. S5a; Table S5). Density
262 also mediated the association between seedling size and winter temperature in
263 natural populations, with a stronger positive correlation between the two variables
264 with 6 ind./m² (3.2 [3.1, 3.4] at 17.5 °C and 3.7 [3.4, 3.9] at 18.5 °C) than with 2
265 ind./m² (3.4 [3.2, 3.5] and 3.5 [3.3, 3.7]) (Fig. S5a; Table S5). Additionally, with high
266 densities in natural populations, flowering probability was low except for high
267 amounts of rainfall (e.g. with 6 ind./m², 0.19 [0.035, 0.60] for 150 mm of rainfall and
268 0.37 [0.096, 0.76] for 200 mm; but with 2 ind./m², 0.71 [0.43, 0.88] and 0.71 [0.38,
269 0.90]) (Fig. S5b; Table S5), and the pattern was similar for growth (e.g. with 6
270 ind./m², 4.5 [4.1, 4.8] for 150 mm of rainfall and 4.6 [4.3, 4.9] for 200 mm; but with 2
271 ind./m², 5.0 [4.7, 5.2] and 5.0 [4.8, 5.3]) (Fig. S5c; Table S5).

272

273 *Vital-rate responses to time since fire and size*

274

275 As expected from previous work and observations, individuals in natural populations
276 had a short lifespan, as indicated by the decrease in survival with time since fire
277 (TSF) (0.42 [0.28, 0.57] and 0.29 [0.18, 0.42] respectively 3 and 7 years after a fire)
278 and size (0.26 [0.16, 0.40] with a size of 5.0 and 0.22 [0.12, 0.37] with 6.2) (Fig.
279 S6a,b; Table S5). This early decline in survival was accompanied by investment into
280 reproduction from early post-fire stages, with flowering probability decreasing from

281 0.16 [0.038, 0.48] to 0.051 [0.016, 0.15] respectively 3 and 7 years after a fire and
282 the number of flowers per individual from 10 [8.2, 13] to 7.6 [6.8, 8.4] (Fig. 5c,d;
283 Table S5). Dewy pines growing in natural conditions also appeared to reproduce
284 throughout most of their lifetime, as both flowering probabilities and number of
285 flowers continuously increased with size (individuals had a probability of flowering of
286 0.17 [0.061, 0.38] and 2.9 [2.4, 3.5] flowers with a size of 5.0, which respectively
287 increased to 0.74 [0.47, 0.90] and 7.8 [6.9, 8.7] with 6.2) (Fig. S6e,f; Table S5). In
288 contrast, the largest individuals had the highest survival in anthropogenic habitats
289 (0.61 [0.32, 0.84] and 0.75 [0.46, 0.91] with sizes of 5.0 and 6.2; Fig. S6b; Table S5),
290 but did not invest as much in reproduction with both flowering probability and number
291 of flowers declining after reaching a peak for a size of 7.3 (probability of flowering of
292 0.69 [0.34, 0.91]) and 8.2 (19 [13, 28] flowers) (Fig. S6e,f; Table S5).

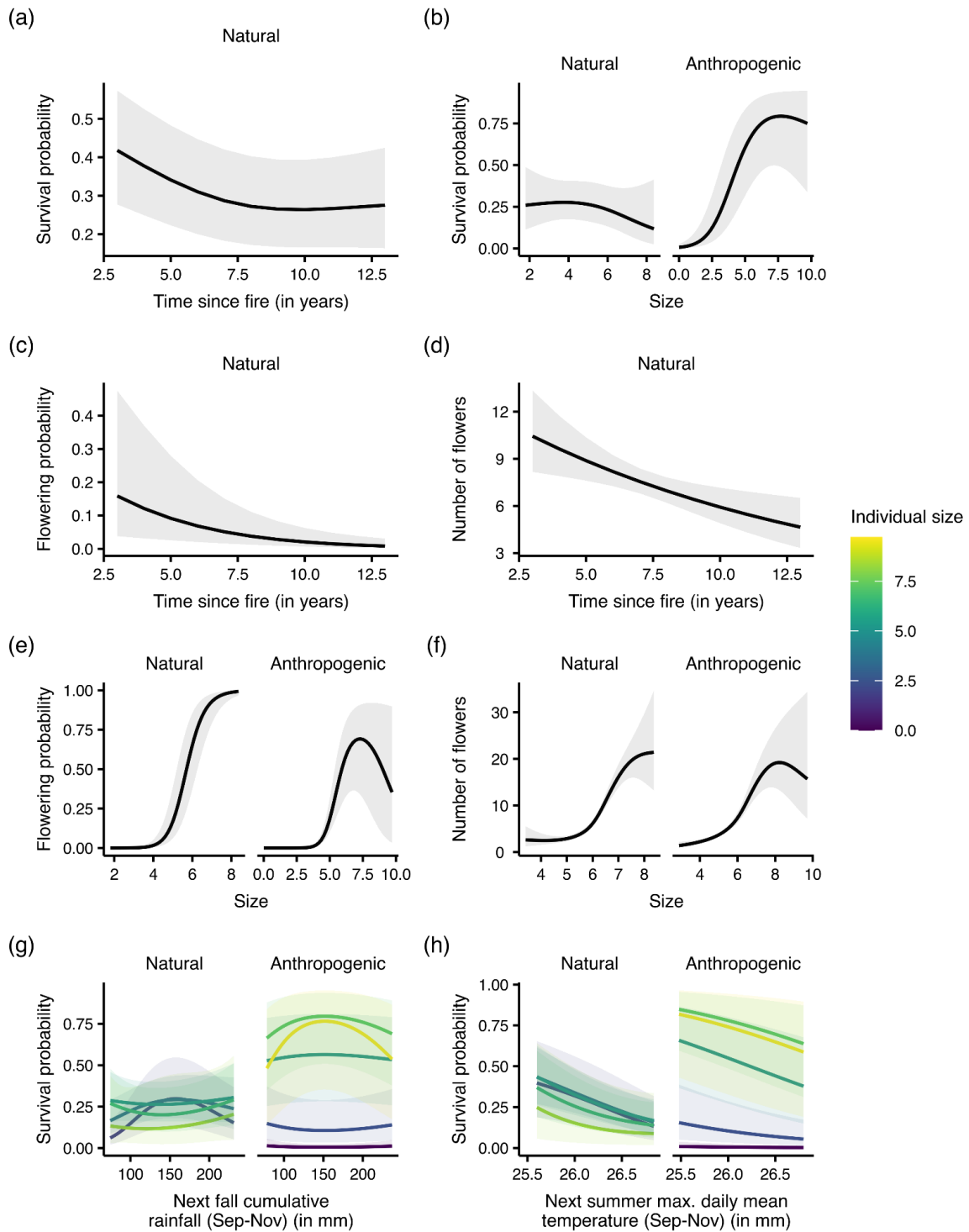
293

294 *Vital-rate responses to size-climate interactions*

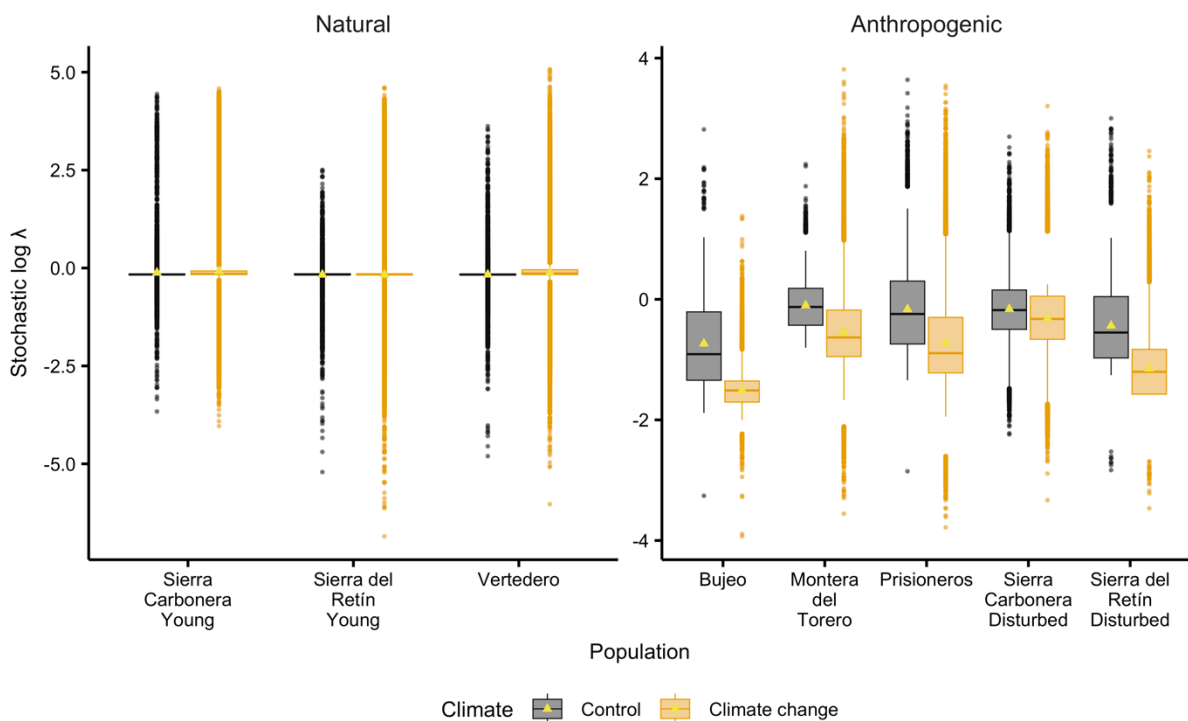
295

296 In natural populations, small individuals survived best at intermediate rainfall (e.g.
297 0.29 [0.18, 0.43] with 150 mm of rain for an individual of size 3.4) than for high or low
298 amounts of rainfall (0.18 [0.098, 0.30] with 80 mm and 0.26 [0.14, 0.43] with 210
299 mm), while large individuals survived best at low or high rainfall (e.g., for an
300 individual of size 6.6, 0.26 [0.13, 0.45] with 80 mm, 0.20 [0.10, 0.37] with 150 mm,
301 and 0.26 [0.13, 0.45] with 210 mm; Fig. S6g; Table S5). Additionally, survival rates
302 decreased faster with summer temperature for large than for small individuals (from
303 0.60 [0.32, 0.83] at 25 °C to 0.26 [0.13, 0.44] at 26 °C with a size of 6.6, and from
304 0.57 [0.32, 0.79] to 0.34 [0.22, 0.49] with a size of 3.4; Fig. S6h; Table S5). We also
305 found size dependence in the association between survival and rainfall in

306 anthropogenic populations, where large individuals survived best at intermediate
 307 amounts of rain in fall (e.g., for an individual with a size of 6.6, 0.67 [0.37, 0.88] at 80
 308 mm of rain, 0.78 [0.49, 0.93] at 150 mm, and 0.73 [0.44, 0.91] at 210 mm), while
 309 small individuals were not affected by changes in rainfall (Fig. S6g; Table S5).



310 **Figure S6 – Vital-rate responses to time since fire, size, and size-climate**
 311 **interactions.** We predicted the values of survival and flowering probability as well as
 312 the number of flowers per individual for a range of number of years since the last fire
 313 (time since fire) in natural habitats (a, c, d) and for a range of individual sizes in both
 314 natural and anthropogenic habitats (b, e, f). Finally, we predicted the values of
 315 survival probability for a range of individual sizes as well as (h) rainfall and (g)
 316 temperature values. The lines represent the average vital-rate value and the shaded
 317 ribbon the 95% confidence interval. In each case, we kept all other covariates at their
 318 mean values (scaled value = 0) except for the number of flowers, where we used the
 319 mean size of reproducing individuals.



320 **Figure S7 – Site-specific population growth rate.** For each population, we
 321 calculated the stochastic growth rate $\log \lambda_s$ as the average of all annual $\log \lambda$ in each
 322 of 500 projections.

323 **References – Appendix S1**

324

325 Bartoń, K. (2022). MuMIn: Multi-Model Inference. R. [https://CRAN.R-](https://CRAN.R-project.org/package=MuMIn)

326 [project.org/package=MuMIn](https://CRAN.R-project.org/package=MuMIn)

327 Bolker, B. (2022). Bbmle: Tools for General Maximum Likelihood Estimation. R.

328 <https://CRAN.R-project.org/package=bbmle>

329 Conquet, E., Ozgul, A., Blumstein, D. T., Armitage, K. B., Oli, M. K., Martin, J. G. A.,

330 Clutton-Brock, T. H., & Paniw, M. (2023). Demographic Consequences of

331 Changes in Environmental Periodicity. *Ecology*, **104**(3), e3894.

332 <https://doi.org/10.1002/ecy.3894>

333 Gelman, A. (2008). Scaling Regression Inputs by Dividing by Two Standard

334 Deviations. *Statistics in Medicine*, **27**(15), 2865–73.

335 <https://doi.org/10.1002/sim.3107>

336 Gómez-González, S., Paniw, M., Antunes, K., & Ojeda, F. (2018). Heat Shock and

337 Plant Leachates Regulate Seed Germination of the Endangered Carnivorous

338 Plant *Drosophyllum Lusitanicum*. *Web Ecology*, **18**(1), 7–13.

339 <https://doi.org/10.5194/we-18-7-2018>

340 Paniw, M., Quintana-Ascencio, P. F., Ojeda, F., & Salguero-Gómez, R. (2017).

341 Interacting Livestock and Fire May Both Threaten and Increase Viability of a

342 Fire-Adapted Mediterranean Carnivorous Plant. *Journal of Applied Ecology*,

343 **54**(6), 1884–94. <https://doi.org/10.1111/1365-2664.12872>

344 R Core Team. (2022). R: A Language and Environment for Statistical Computing.

345 Vienna, Austria: R Foundation for Statistical Computing. [https://www.R-](https://www.R-project.org/)

346 [project.org/](https://www.R-project.org/)

347 Wood, S. N. (2011). Fast Stable Restricted Maximum Likelihood and Marginal

348 Likelihood Estimation of Semiparametric Generalized Linear Models. *Journal*
349 *of the Royal Statistical Society Series B: Statistical Methodology*, **73**(1), 3–36.
350 <https://doi.org/10.1111/j.1467-9868.2010.00749.x>

351 Wood, S. N. (2017). *Generalized Additive Models: An Introduction with R, Second*
352 *Edition*. CRC Press.

353 Wood, S. N., Pya, N., & Säfken, B. (2016). Smoothing Parameter and Model
354 Selection for General Smooth Models. *Journal of the American Statistical*
355 *Association*, **111**(516), 1548–63.
356 <https://doi.org/10.1080/01621459.2016.1180986>

1 **Appendix S2 – Current and future rainfall and temperature data in dewy-pine**
2 **populations**

3

4 1. Current rainfall and temperature data

5

6 We modelled the response of dewy-pine vital rates to rainfall and maximum
7 daily temperature using observed daily climatic data at dewy-pine population
8 locations (Table 1) from the E-OBS dataset from the EU-FP6 project UERRA and the
9 Copernicus Climate Change Service (Cornes et al., 2018; accessible at
10 https://surfobs.climate.copernicus.eu/dataaccess/access_eobs.php). We used the
11 ncdf4 R package to process the raw netCDF weather data (Pierce, 2021), and
12 transformed the daily rainfall and maximum daily temperature into monthly
13 cumulative rainfall and average maximum daily temperature. For each population,
14 we then obtained monthly cumulative rainfall and average maximum temperature
15 data from the year prior the first census (i.e., 2010 for Sierra del Retín Disturbed and
16 Vertedero, 2011 for Sierra Carbonera Young, 2014 for Sierra del Retín Young, and
17 2015 for all other populations). To do so, we averaged the recorded climate values
18 within a buffer of 0.1×1.5 degrees around the GPS location of each population.

19 **Table S1 – GPS locations of dewy-pine populations.** Longitude and latitude of
 20 population locations are given in decimal degrees.

| Population | Habitat type | Latitude | Longitude | First sampled | Last fire |
|----------------------------|---------------|----------------------------|----------------------------|---------------|-----------|
| Sierra Carbonera Young | Natural | 36.209722 or 36°13' N | -5.36 or 5°22' W | 2012 | 2011 |
| Sierra del Retín Young | Natural | 36.17694444 or 36°11' N | -5.833055556 or 5°50' W | 2015 | 2013 |
| Vertedero | Natural | 36.121667 or 36°7' N | -5.49 or 5°29' W | 2011 | 2009 |
| Sierra del Retín Disturbed | Anthropogenic | 36.198056 or 36°12' N | -5.823611 or 5°49' W | 2011 | 1996 |
| Prisioneros | Anthropogenic | 36.105 or 36°6' N | -5.486388889 or 5°29' W | 2016 | 1950 |
| Bujeo | Anthropogenic | 36.072461 or 36°4' N | -5.52654 or 5°32' W | 2016 | 1950 |
| Montera del Torero | Anthropogenic | 36.226389 or 36°14' N | -5.585278 or 5°35' W | 2016 | 1950 |
| Sierra Carbonera Disturbed | Anthropogenic | 36.10638889 or 36°12' N | -5.360555556 or 5°22' W | 2016 | 1950 |

21

22 **2. Projected rainfall and temperature data**

23

24 To project dewy-pine populations under climate change, we used projected
 25 rainfall and temperature values at dewy-pine population locations from 11 global
 26 circulation models (GCM; see Table 2) from the Coupled Model Intercomparison
 27 Project 6 (CMIP6; Eyring et al., 2016; Pascoe et al., 2020; Waliser et al., 2020)
 28 available from the Earth System Grid Federation (ESFG; Petrie et al., 2021;
 29 available at <https://aims2.llnl.gov/search>). For each model, we selected the best
 30 variant using the GCMeval tool (Parding et al., 2020; accessible at

31 <https://gcmeval.met.no/>). For each GCM, we downloaded data for the worst scenario
32 of atmospheric greenhouse gas Representative Concentration Pathway (RCP),
33 corresponding to a level of radiative forcing reaching 8.5 Watts per square metre
34 (Wm^{-2}) by 2100 (RCP 8.5). We processed the raw data from each climate projection
35 model using the ncd4 R package (Pierce, 2021) to obtain monthly cumulative rainfall
36 and average maximum temperature in each population by averaging the values
37 recorded within a buffer of 0.1×1.5 degrees around the population coordinates (i.e.,
38 1.5 times the grid resolution).

39

40 Most GCMs comprised projected rainfall and temperature values beyond the values
41 observed in our populations. To avoid predicting vital rates using values of climate
42 variables outside the observed range, we capped these values to the maximum and
43 minimum observed. For example, while the observed maximum cumulative rainfall in
44 fall was 245 mm, six of the considered GCM predicted greater values in some years,
45 ranging from 250 to 463 mm; we transformed these values to the maximum
46 observed (245 mm). This allowed us to investigate the response of dewy-pine
47 populations to increases in the frequency of extreme climatic conditions, rather than
48 changes in absolute rainfall and temperature values.

49 **Table S2 – List of global circulation models used to project dewy-pine**
 50 **populations under climate change.**

| Source ID | Experiment | Variant | Version | Institution | Modelling centre | Citation |
|-----------|------------|----------|----------|----------------------------------------------------------------------------------------------------------------------------------------------------------------------------------------------------------------------------------------------------------------------------------------------------------------------------------------------------------------------------------------------------------------------------------------------------------------------------------------------------------------------------------------------------------------------------------------------------------------------------------------------------------------------------------------------------------------------------------------------------|---------------------|----------------------------------------|
| CanESM5 | ssp585 | r1i1p1f1 | 20190429 | Canadian Centre for Climate Modelling and Analysis, Environment and Climate Change Canada, Victoria, BC V8P 5C2, Canada | CCCma | (Swart et al., 2019) |
| EC_Earth3 | ssp585 | r4i1p1f1 | 20200425 | AEMET, Spain; BSC, Spain; CNR-ISAC, Italy; DMI, Denmark; ENEA, Italy; FMI, Finland; Geomar, Germany; ICHEC, Ireland; ICTP, Italy; IDL, Portugal; IMAU, The Netherlands; IPMA, Portugal; KIT, Karlsruhe, Germany; KNMI, The Netherlands; Lund University, Sweden; Met Eireann, Ireland; NLeSC, The Netherlands; NTNU, Norway; Oxford University, UK; surfSARA, The Netherlands; SMHI, Sweden; Stockholm University, Sweden; Unite ASTR, Belgium; University College Dublin, Ireland; University of Bergen, Norway; University of Copenhagen, Denmark; University of Helsinki, Finland; University of Santiago de Compostela, Spain; Uppsala University, Sweden; Utrecht University, The Netherlands; Vrije Universiteit Amsterdam, the Netherlands; | EC-Earth-Consortium | (EC-Earth Consortium (EC-Earth), 2019) |

| | | | | | | |
|--------------|--------|----------|----------|--------------------------------------------------------------------------------------------------------------------------------------------------------------------------------------------------------------------------------------------------------------------------------|-----------|--------------------------------------------------------------|
| | | | | Wageningen University, The Netherlands. Mailing address: EC-Earth consortium, Rossby Center, Swedish Meteorological and Hydrological Institute/SMHI, SE-601 76 Norrkoping, Sweden | | |
| FGOALS_G3 | ssp585 | r1i1p1f1 | 20190818 | Chinese Academy of Sciences, Beijing 100029, China | CAS | (Li, 2019) |
| GFDL_ESM4 | ssp585 | r1i1p1f1 | 20180701 | National Oceanic and Atmospheric Administration, Geophysical Fluid Dynamics Laboratory, Princeton, NJ 08540, USA | NOAA-GFDL | (John et al., 2018) |
| GISS_E2_1_G | ssp585 | r1i1p1f2 | 20200115 | Goddard Institute for Space Studies, New York, NY 10025, USA | NASA-GISS | (NASA Goddard Institute for Space Studies (NASA/GISS), 2020) |
| INM_CM4_8 | ssp585 | r1i1p1f1 | 20190603 | Institute for Numerical Mathematics, Russian Academy of Science, Moscow 119991, Russia | INM | (Volodin et al., 2019) |
| IPSL_CM6A_LR | ssp585 | r1i1p1f1 | 20190903 | Institut Pierre Simon Laplace, Paris 75252, France | IPSL | (Boucher et al., 2019) |
| MIROC6 | ssp585 | r1i1p1f1 | 20191016 | JAMSTEC (Japan Agency for Marine-Earth Science and Technology, Kanagawa 236-0001, Japan), AORI (Atmosphere and Ocean Research Institute, The University of Tokyo, Chiba 277-8564, Japan), NIES (National Institute for Environmental Studies, Ibaraki 305-8506, Japan), and R- | MIROC | (Shiogama et al., 2019) |

| | | | | | | |
|---------------|--------|-----------|----------|---------------------------------------------------------------------------------------------------------------------------------------------------------------------------------------------------------------------------------------------------------------------------------------------------------------------------------------------------------------------------------------------------------------------------------------------------------------------------------------------------------------------------------------|-------|-------------------------|
| | | | | CCS (RIKEN Center for Computational Science, Hyogo 650-0047, Japan) | | |
| MPI_ESM1_2_LR | ssp585 | r10i1p1f1 | 20190710 | Max Planck Institute for Meteorology, Hamburg 20146, Germany | MPI-M | (Wieners et al., 2019) |
| MRI_ESM2_0 | ssp585 | r1i1p1f1 | 20191108 | Meteorological Research Institute, Tsukuba, Ibaraki 305-0052, Japan | MRI | (Yukimoto et al., 2019) |
| NorESM2_MM | ssp585 | r1i1p1f1 | 20191108 | NorESM Climate modeling Consortium consisting of CICERO (Center for International Climate and Environmental Research, Oslo 0349), MET-Norway (Norwegian Meteorological Institute, Oslo 0313), NERSC (Nansen Environmental and Remote Sensing Center, Bergen 5006), NILU (Norwegian Institute for Air Research, Kjeller 2027), UiB (University of Bergen, Bergen 5007), UiO (University of Oslo, Oslo 0313) and UNI (Uni Research, Bergen 5008), Norway. Mailing address: NCC, c/o MET-Norway, Henrik Mohns plass 1, Oslo 0313, Norway | NCC | (Bentsen et al. 2019) |

51

52 **3. Current and future climatic trends**

53

54 Temperatures have increased in the past decades, with an average trend

55 (mean and 95% confidence interval) of 0.033 °C [0.021; 0.044] per year between

1980 and 2022. This trend will continue and intensify in the future, as climate-change models predict an increase of 0.055 °C [0.053; 0.057] per year on average between 2015 and 2100 under the RCP 8.5 global change scenario (Moss et al., 2010; van Vuuren et al., 2011; Riahi et al., 2011). Average monthly cumulative rainfall and its variability show opposite trends between the current and projected conditions. Both the yearly mean and variability increased on average between 1980 and 2022 (0.18 [-0.23, 0.59] and 0.083 mm [-0.47, 0.63] per year, respectively) but are predicted to decrease until 2100 according to future projections under the RCP 8.5 scenario (-0.16 [-0.19, -0.13] and -0.11 mm [-0.14, -0.077]). Notably, while the RCP 4.5 global change scenario predicts a more moderate increase in temperature, both scenarios show the same trend for the 30 years of our projections (Fig. S1; Fig. S2a).

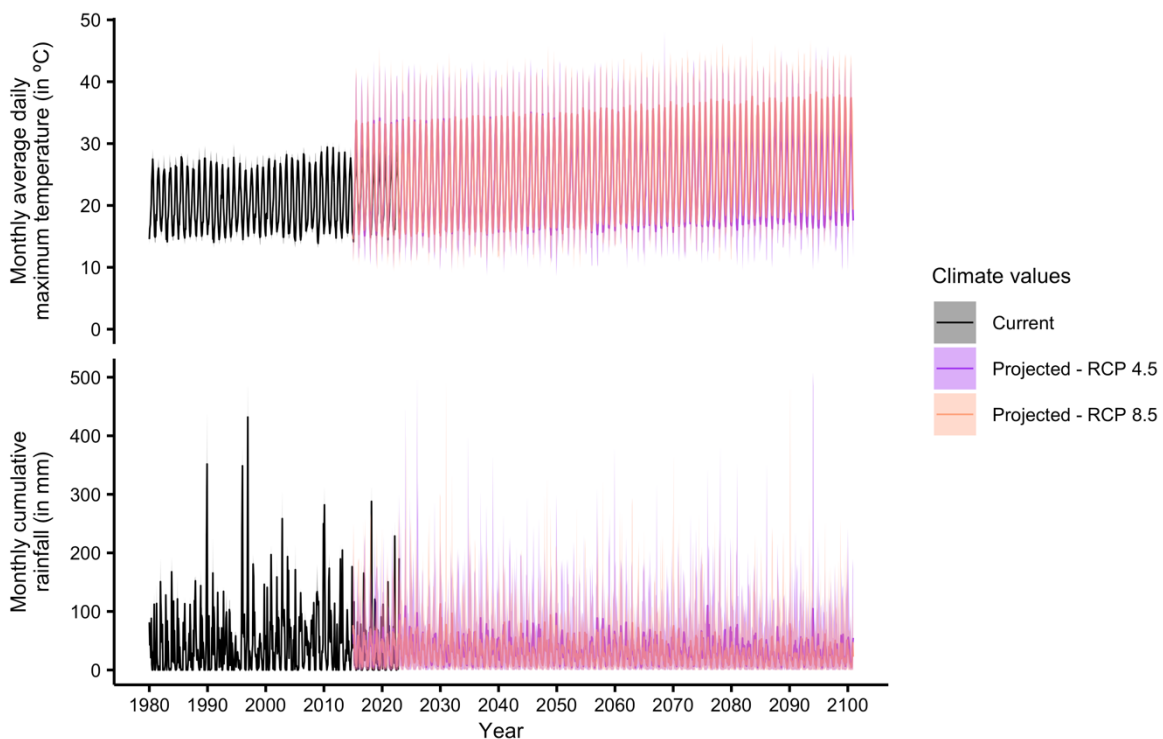
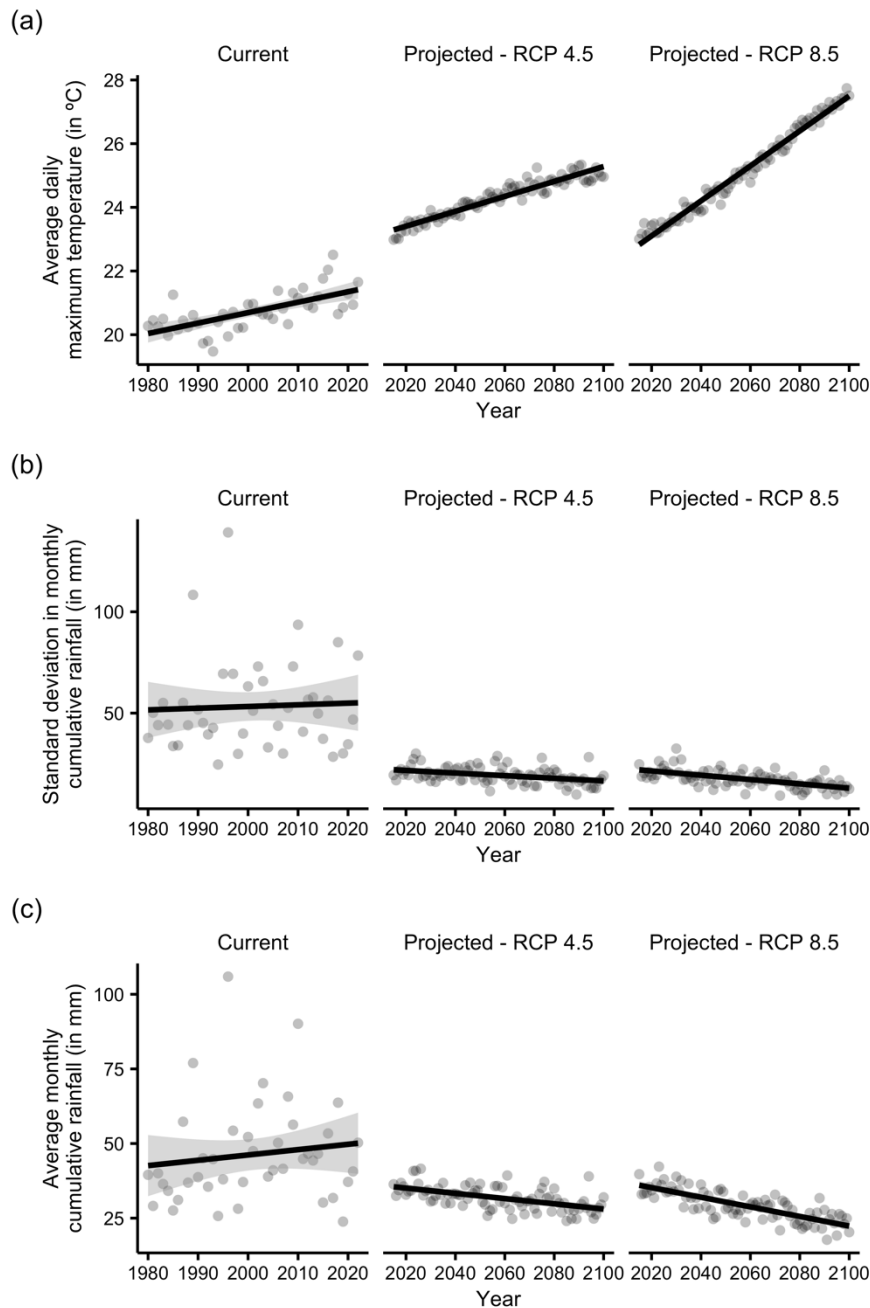


Figure S1 – Current and projected monthly temperature and rainfall data.

We obtained current data on daily maximum temperature and daily rainfall amounts from the E-OBS dataset from the EU-FP6 project UERRA and the Copernicus Climate Change Service. We extracted the projected rainfall and temperature values

71 under the RCP 4.5 and 8.5 global change scenarios from 11 global change models
72 from the Coupled Model Intercomparison Project 6 (CMIP6; available from the Earth
73 System Grid Federation).



74 **Figure S2 – Current and projected trends in temperature and rainfall.** We
75 investigated yearly changes in (a) average daily maximum temperature, (b) standard
76 deviation in monthly cumulative rainfall, and (c) average monthly cumulative rainfall,
77 for the current (1980–2022) and projected conditions (2015–2100) under the RCP

78 4.5 and 8.5 global change scenarios. Dots represent the observed values and lines
79 and shaded ribbons represent the mean and 95% confidence interval of linear
80 models fitted to each data subset.

81 **References – Appendix S2**

82

83 Bentsen, M., Olivière, D. J. L., Seland, Ø., Toniazzi, T., Gjermundsen, A., Graff, L. S.,
84 Debernard, J. B., Gupta, A. K., He, Y., Kirkevåg, A., Schwinger, J., Tjiputra,
85 J., Aas, K. S., Bethke, I., Fan, Y., Griesfeller, J., Grini, A., Guo, C., Ilicak, M.,
86 ... Schulz, M. (2019). *NCC NorESM2-MM Model Output Prepared for CMIP6*
87 *ScenarioMIP ssp585*. Version 20191108. Earth System Grid Federation.
88 <https://doi.org/10.22033/ESGF/CMIP6.8321>

89 Boucher, O., Denvil, S., Levavasseur, G., Cozic, A., Caubel, A., Foujols, M.-A.,
90 Meurdesoif, Y., Cadule, P., Devilliers, M., Dupont, E., & Lurton, T. (2019).
91 IPSL IPSL-CM6A-LR Model Output Prepared for CMIP6 ScenarioMIP ssp585.
92 Version 20190903. Earth System Grid Federation.
93 <https://doi.org/10.22033/ESGF/CMIP6.5271>

94 Cornes, R. C., van der Schrier, G., van den Besselaar, E. J. M., & Jones, P. D.
95 (2018). An Ensemble Version of the E-OBS Temperature and Precipitation
96 Data Sets. *Journal of Geophysical Research: Atmospheres*, **123**(17), 9391–
97 409. <https://doi.org/10.1029/2017JD028200>

98 EC-Earth Consortium (EC-Earth). (2019). *EC-Earth-Consortium EC-Earth3 Model*
99 *Output Prepared for CMIP6 ScenarioMIP ssp585*. Version 20200425. Earth
100 System Grid Federation. <https://doi.org/10.22033/ESGF/CMIP6.4912>

101 Eyring, V., Bony, S., Meehl, G. A., Senior, C. A., Stevens, B., Stouffer, R. J., &
102 Taylor, K. E. (2016). Overview of the Coupled Model Intercomparison Project
103 Phase 6 (CMIP6) Experimental Design and Organization. *Geoscientific Model*
104 *Development*, **9**(5), 1937–58. <https://doi.org/10.5194/gmd-9-1937-2016>

105 John, J. G., Blanton, C., McHugh, C., Radhakrishnan, A., Rand, K., Vahlenkamp, H.,

106 Wilson, C., Zadeh, N. T., Dunne, J. P., Dussin, R., Horowitz, L. W., Krasting,
107 J. P., Lin, P., Malyshev, S., Naik, V., Ploshay, J., Shevliakova, E., Silvers, L.
108 Stock, C., Winton, M., & Zeng, Y. (2018). *NOAA-GFDL GFDL-ESM4 Model*
109 *Output Prepared for CMIP6 ScenarioMIP ssp585*. Version 20180701. Earth
110 System Grid Federation. <https://doi.org/10.22033/ESGF/CMIP6.8706>

111 Li, L. (2019). *CAS FGOALS-G3 Model Output Prepared for CMIP6 ScenarioMIP*
112 *ssp585*. Version 20190818. Earth System Grid Federation.
113 <https://doi.org/10.22033/ESGF/CMIP6.3503>

114 Moss, R. H., Edmonds, J. A., Hibbard, K. A., Manning, M. R., Rose, S. K., van
115 Vuuren, D. P., Carter, T. R., Emori, S., Kainuma, M., Kram, T., Meehl, G. A.,
116 Mitchell, J. F. B., Nakicenovic, N., Riahi, K., Smith, S. J., Stouffer, R. J.,
117 Thomson, A. M., Weyant, J. P., & Wilbanks, T. J. (2010). The next generation
118 of scenarios for climate change research and assessment. *Nature*, 463, 747–
119 756. <https://doi.org/10.1038/nature08823>

120 NASA Goddard Institute for Space Studies (NASA/GISS). (2020). *NASA-GISS*
121 *GISS-E2.1G Model Output Prepared for CMIP6 ScenarioMIP ssp585*. Version
122 20200115. Earth System Grid Federation.
123 <https://doi.org/10.22033/ESGF/CMIP6.7460>

124 Parding, K. M., Dobler, A., McSweeney, C. F., Landgren, O. A., Benestad, R.,
125 Erlandsen, H. B., Mezghani, A., Gregow, H., Rätty, O., Viktor, E., El Zohbi, J.,
126 Christensen, O. B., & Loukos, H. (2020). GCMeval – An Interactive Tool for
127 Evaluation and Selection of Climate Model Ensembles. *Climate Services*,
128 **18**(April), 100167. <https://doi.org/10.1016/j.cliser.2020.100167>

129 Pascoe, C., Lawrence, B. N., Guilyardi, E., Juckes, M., & Taylor, K. E. (2020).
130 Documenting Numerical Experiments in Support of the Coupled Model

131 Intercomparison Project Phase 6 (CMIP6). *Geoscientific Model Development*,
132 **13**(5), 2149–67. <https://doi.org/10.5194/gmd-13-2149-2020>

133 Petrie, R., Denvil, S., Ames, S., Levavasseur, G., Fiore, S., Allen, C., Antonio, F.,
134 Berger, K., Bretonnière P.-A., Cinquini, L., Dart, E., Dwarakanath, P., Drukem,
135 K., Evans, B., Franchistéguy, L., Gardoll, S., Gerbier, E., Greenslade, M.,
136 Hassell, D., ... Wagner, R. (2021). Coordinating an Operational Data
137 Distribution Network for CMIP6 Data. *Geoscientific Model Development*,
138 **14**(1), 629–44. <https://doi.org/10.5194/gmd-14-629-2021>

139 Pierce, D. (2021). Ncdf4: Interface to Unidata netCDF (Version 4 or Earlier) Format
140 Data Files. R. <https://CRAN.R-project.org/package=ncdf4>

141 Riahi, K., Rao, S., Krey, V., Cho, C., Chirkov, V., Fischer, G., Kindermann, G.,
142 Nakicenovic, N., & Rafaj, P. (2011). RCP 8.5—A Scenario of Comparatively
143 High Greenhouse Gas Emissions. *Climatic Change*, **109**(1), 33.
144 <https://doi.org/10.1007/s10584-011-0149-y>

145 Shiogama, H., Abe, M., & Tatebe, H. (2019). *MIROC MIROC6 Model Output*
146 *Prepared for CMIP6 ScenarioMIP ssp585. Version 20191016*. Earth System
147 Grid Federation. <https://doi.org/10.22033/ESGF/CMIP6.5771>

148 Swart, N. C., Cole, J. N. S., Kharin, V. V., Lazare, M., Scinocca, J. F., Gillett, N. P.,
149 Anstey, J., Arora, V., Christian, J. R., Jiao, Y., Lee, W. G., Majaess, F.,
150 Saenko, O. A., Seiler, C., Seinen, C., Shao, A., Solheim, L., von Salzen, K.,
151 Yango, D., Winter, B., & Sigmond, M. (2019). *CCCma CanESM5 Model*
152 *Output Prepared for CMIP6 ScenarioMIP ssp585. Version 20190429*. Earth
153 System Grid Federation. <https://doi.org/10.22033/ESGF/CMIP6.3696>

154 van Vuuren, D. P., Edmonds, J., Kainuma, M., Riahi, K., Thomson, A., Hibbard, K.,
155 Hurtt, G. C., Kram, T., Krey, V., Lamarque, J.-L., Masui, T., Meinshausen, M.,

156 Nakicenovic, N., Smith, S. J. & Rose, S. K. (2011). The representative
157 concentration pathways: an overview. *Climatic Change*, **109**, 5.
158 <https://doi.org/10.1007/s10584-011-0148-z>

159 Volodin, E., Mortikov, E., Gritsun, A., Lykossov, V., Galin, V., Diansky, N., Gusev, A.,
160 Kostykin, S., Iakovlev, N., Shestakova, A., & Emelina, S. (2019). *INM INM-*
161 *CM4-8 Model Output Prepared for CMIP6 ScenarioMIP ssp585*. Version
162 20190603. Earth System Grid Federation.
163 <https://doi.org/10.22033/ESGF/CMIP6.12337>

164 Waliser, D., Gleckler, P. J., Ferraro, R., Taylor, K. E., Ames, S., Biard, J., Bosilovich,
165 M. G., Brown, O., Chepfer, H., Cinquini, L., Durack, P.J., Eyring, V., Mathieu,
166 P.-P., Lee, T., Pinnock, S., Potter, G. L., Rixen, M., Saunders, R., Schulz, J.,
167 Thépaut, J.-N., Tuma, M. (2020). Observations for Model Intercomparison
168 Project (Obs4MIPs): Status for CMIP6. *Geoscientific Model Development*,
169 **13**(7), 2945–58. <https://doi.org/10.5194/gmd-13-2945-2020>

170 Wieners, K.-H., Giorgetta, M., Jungclaus, J., Reick, C., Esch, M., Bittner, M., Gayler,
171 V., Haak, H., de Vrese, P., Raddatz, T., Mauritsen, T., von Storch, J.-S.,
172 Behrens, J., Brovkin, V., Claussen, M., Crueger, T., Fast, I., Fiedler, S.,
173 Hagemann, S., ... Roeckner, E. (2019). *MPI-M MPI-ESM1.2-LR Model Output*
174 *Prepared for CMIP6 ScenarioMIP ssp585*. Version 20190710. Earth System
175 Grid Federation. <https://doi.org/10.22033/ESGF/CMIP6.6705>

176 Yukimoto, S., Koshiro, T., Kawai, H., Oshima, N., Yoshida, K., Urakawa, S., Tsujino,
177 H., Deushi, M., Tanaka, T., Hosaka, M., Yoshimura, H., Shindo, E., Mizuta,
178 R., Ishii, M., Obata, A., & Adachi, Y. (2019). *MRI MRI-ESM2.0 Model Output*
179 *Prepared for CMIP6 ScenarioMIP ssp585*. Version 20191108. Earth System
180 Grid Federation. <https://doi.org/10.22033/ESGF/CMIP6.6929>

1 **Appendix S3 – Individual-based model description**

2

3 The model description follows the ODD (Overview, Design concepts, Details)
4 protocol for describing individual- and agent-based models (Grimm et al., 2006), as
5 updated by (Grimm et al., 2020).

6

7 1. Purpose and patterns

8

9 The purpose of the model is to predict population growth rates and extinction
10 probabilities of dewy-pine (*Drosophyllum lusitanicum*) populations in natural and
11 anthropogenic habitats in response to projected changes in rainfall and temperature
12 values. We evaluate our model by its ability to reproduce the observed dynamics in
13 the mean changes in aboveground abundance in each population, or at least follow
14 a similar trend.

15

16 2. Entities, state variables, and scales

17

18 *Entities and state variables*

19

20 The **environment** is a single entity representing the population. Its role is to
21 describe the environment (e.g. climate variables) and keep track of simulated time.
22 Environment state variables correspond to dynamic global variables and are
23 presented in Table 1.

24 **Table 1 – Environment state variables**

| Variable name | Variable type and units | Range | Meaning |
|-----------------------|------------------------------|-----------------|------------------------------------------------------------------------------------------------|
| <i>time_sim</i> | Integer; dynamic | ≥1 | Number of years that passed since the start of the projection |
| <i>year_obs</i> | Integer; dynamic (e.g. 2020) | ≥2016 | Current year in the projection |
| <i>year</i> | Integer; dynamic (e.g. 2020) | ≥2016 | Year randomly sampled from the available observed years |
| <i>TSF</i> | Integer; dynamic | ≥0 | Number of years since the last fire |
| <i>TSFcat</i> | Categorical; dynamic (0–4) | {0, 1, 2, 3, 4} | Post-fire habitat stage, with any number of years after a fire ≥ 4 corresponding to 4 |
| <i>corr_seed_surv</i> | Probability; dynamic | [0, 1] | Correction factor representing the survival probability of seeds above the ground |
| <i>summerT</i> | Real number; °C; dynamic | ≥0 | Average minimum daily temperature in summer (May–September) following the annual survey in May |
| <i>prevwinterT</i> | Real number; °C; dynamic | ≥0 | Average minimum daily temperature in winter (January–April) prior to the annual survey in May |
| <i>fallR</i> | Integer; mm; dynamic | ≥0 | Cumulative rainfall in fall (September–November) following the annual survey in May |
| <i>prevfallR</i> | Integer; mm; dynamic | ≥0 | Cumulative rainfall in fall (September–November) prior to the annual survey in May |
| <i>prevwinterR</i> | Integer; mm; dynamic | ≥0 | Cumulative rainfall in winter (January–April) prior to the annual survey in May |
| <i>extinction</i> | Binary; dynamic | {0, 1} | Current state of the population: extinct (1) or not (0) |

25

26 **Plants** are entities representing the aboveground—as opposed to seeds—individual

27 dewy pines in the population. They correspond to individuals from the seedling stage

28 in the species life cycle. The state variables unique to each plant are presented in
 29 Table 2.

30

31 **Table 2 – Plant state variables**

| Variable name | Variable type and units | Range | Meaning |
|------------------|--------------------------|----------|--------------------------------------------------------------------------------------------------------------------------------------|
| <i>ID</i> | Character string; static | NA | Unique identifier of the plant |
| <i>quadratID</i> | Character string; static | NA | Unique identifier of the quadrat corresponding to the location of the plant |
| <i>size</i> | Real number; dynamic | ≥ 0 | Plant size in the current time step, corresponding to $\log(\text{number of leaves} \times \text{length of the longest leaf in cm})$ |
| <i>survival</i> | Binary; dynamic | {0, 1} | State of the plant at the next time step: alive (1) or dead (0) |
| <i>sizeNext</i> | Real number; dynamic | ≥ 0 | Plant size in the next time step, corresponding to $\log(\text{number of leaves} \times \text{length of the longest leaf in cm})$ |
| <i>flowering</i> | Binary; dynamic | {0, 1} | Reproductive state of the plant in the current time step: flowering (1) or not (0) |
| <i>nbFlowers</i> | Integer; dynamic | ≥ 0 | Number of flowers on the plant |
| <i>nb_seeds</i> | Integer; dynamic | ≥ 0 | Number of seeds per flower produced by the plant |

32

33 Seeds are entities representing individuals before they germinate and become
 34 seedlings. Because they are concerned by different processes, we divided seeds
 35 between two types of entities: **Seedbank seeds** are entities representing the seeds
 36 in the soil seedbank and **produced seeds** are entities representing the individuals
 37 that have been produced by aboveground reproducing dewy pines in the current
 38 time step. Their state variables are presented in Table 3 and Table 4.

39 **Table 3 – Seedbank seed state variables**

| Variable name | Variable type and units | Range | Meaning |
|------------------|--------------------------|----------|-------------------------------------------------------------------------------------------------------------------------------------------------------------------------------|
| <i>ID</i> | Character string; static | NA | Unique identifier of the seed |
| <i>quadratID</i> | Character string; static | NA | ID of the quadrat corresponding to the location of the seed |
| <i>size</i> | Real number; dynamic | ≥ 0 | Size of the seedling growing from the germinating seed in the next time step, corresponding to $\log(\text{number of leaves} \times \text{length of the longest leaf in cm})$ |
| <i>outSB</i> | Binary; dynamic | {0, 1} | Seed germination (1) or not (0) |
| <i>staySB</i> | Binary; dynamic | {0, 1} | Seed dormancy (1) or not (0) |

40

41 **Table 4 – Produced seed state variables**

| Variable name | Variable type and units | Range | Meaning |
|------------------|--------------------------|----------|-------------------------------------------------------------------------------------------------------------------------------------------------------------------------------|
| <i>ID</i> | Character string; static | NA | Unique identifier of the seed |
| <i>quadratID</i> | Character string; static | NA | ID of the quadrat corresponding to the location of the seed |
| <i>size</i> | Real number; dynamic | ≥ 0 | Size of the seedling growing from the germinating seed in the next time step, corresponding to $\log(\text{number of leaves} \times \text{length of the longest leaf in cm})$ |
| <i>goCont</i> | Binary; dynamic | {0, 1} | Seed germination (1) or not (0) |
| <i>goSB</i> | Binary; dynamic | {0, 1} | Seed entering the seedbank (1) or not (0) |

42

43 **Quadrats** are two-dimensional squares representing the monitoring units in which
44 plants are censused in a population. Quadrats are only associated with one dynamic
45 state variable, *abLarge*, an integer (≥ 0) corresponding to the number of plants with a
46 size > 4.5 present in a quadrat.

47

48 *Scales*

49

50 The model is spatially explicit and represents a population in a two-dimensional
51 space extending over 40 m² divided in 1-m² quadrats. These quadrats are discrete
52 units in which individual plants and seeds are distributed, and correspond to the units
53 in which dewy pines are monitored every year—more specifically in four separated
54 transects of ten quadrats each.

55

56 The model represents time via discrete time steps, each corresponding to one year,
57 to replicate the annual surveys that take place in May in the various populations.

58

59 3. Process overview and scheduling

60

61 *Process overview*

62

63 The model covers the life cycle of dewy pines. At each time step, the
64 **environment** updates the environmental variables and simulation time; the **plants**
65 reproduce, survive, and grow; the **seedbank seeds** germinate or stay dormant; and
66 the **produced seeds** germinate or go to the seedbank. The **quadrats** get new
67 aboveground density values.

68 *Schedule summary*

69

70 Throughout the model, the update of each state variable through a given process for
71 **plants** and **produced** or **seedbank seeds** is done simultaneously for all entities, as
72 each process in a given entity is assumed to be independent from the processes in
73 another entity.

74

75 At each timestep, the model resets the ensemble of **seeds produced** to zero. The
76 population of **plants** is also reset if a fire occurred, as all aboveground individuals
77 are burned. The **environment** then updates the environmental variables (rainfall and
78 temperature) as well as the simulation year and the number of years after the last
79 fire. The latter two are used to update the correction factor representing seed
80 survival (*corr_seed_surv*).

81

82 Aboveground **plants** then reproduce (see *Reproduction* submodel); that is, they
83 flower and produce a certain number of flowers, which in turn produce seeds. The
84 number of flowers is capped to the user-selected value if needed. The fate of the
85 **seeds produced** is updated; they can either germinate, contribute to the seedbank,
86 or die (i.e., none of the two former processes). **Produced seeds** that do not die are
87 then assigned an ID, and those that germinate a size, and the maximum ID number
88 is updated.

89

90 After reproducing, **plants** survive and grow (*Survival and growth* submodel). The
91 size is capped or adjusted if needed. Seedbank processes take place next
92 (*Seedbank* submodel), with **seedbank seeds** germinating, staying dormant, or dying

93 (i.e., none of the two former processes). Seeds that germinate are attributed a size.
94 **Produced seeds** that were assigned to go dormant are added to the seedbank, and
95 those that germinate are added to the aboveground population after capping their
96 number in each **quadrat**.

97

98 After each timestep, the population growth rate and mean change in aboveground
99 population abundance are calculated and the yearly individual data is merged to the
100 full data. The **environment** updates the simulation time and the extinction status to 1
101 if the quasi-extinction threshold is reached, and the size of each surviving **plant** is
102 updated to its size at the next time step. Finally, the aboveground density in each
103 **quadrat** is updated.

104

105 *Schedule details*

106

107 The schedule follows the processes of the dewy-pine life cycle during a year from
108 the annual census occurring in May. This census occurs during the flowering period
109 and the model replicates this by starting with the *Reproduction* submodel. The
110 *Survival and growth* and *Seedbank* submodels could come in any order after
111 reproduction took place, as they are independent from each other.

112

113 In natural populations, the schedule depends on the fire regime. Reproduction does
114 not happen until the second year after a fire occurs, and only survival and growth, as
115 well as germination or dormancy in the seedbank, are represented in the year of a
116 fire and the following year.

117 4. Design concepts

118

119 1. Basic principles

120

121 This model relies on previous knowledge on the life cycle of dewy pines
122 (Paniw et al., 2017; Conquet et al., 2023) to perform a population viability analysis
123 (PVA), a modelling approach commonly used in population ecology. By projecting
124 population dynamics into the future, a PVA aims at assessing the probability of
125 persistence of populations and allows for the introduction of stochasticity in
126 environmental conditions (e.g. fire return, or sampling from a distribution of
127 temperature and rainfall values). While this model is designed for plant populations
128 and does not include any representation of social organisation or individual's
129 decision processes, it allows to take into account demographic stochasticity (by
130 sampling demographic processes from distributions), which is often unaccounted for
131 in PVAs due to the use of simplified population models such as matrix population
132 models (MPM) or integral projection models (IPM).

133

134 2. Emergence

135

136 Changes in aboveground population size emerge from individual fate, which in turn
137 emerges from the relationship between demographic processes (e.g. survival or
138 reproduction) and individual traits (plant size), density, and environmental variables.
139 Individual traits and density vary with changes in demographic processes affecting
140 individual fate. How the various demographic processes interact to shape individual
141 life histories is imposed by previous empirical observations on the species' life cycle.

142 Seedbank processes emerge from the simulated sequence of post-fire habitat
143 stages (in natural populations) or from site-specific parameters that do not vary
144 through time parameters (in anthropogenic populations).

145

146 3. Adaptation

147

148 Individuals do not make any decisions based on objectives in this model.

149

150 4. Objectives

151

152 Individuals do not use any fitness measure to make decisions.

153

154 5. Learning

155

156 Learning is not implemented in this model.

157

158 6. Prediction

159

160 Prediction is not implemented in this model.

161

162 7. Sensing

163

164 Sensing is not implemented in this model.

165 8. Interaction

166

167 Interactions between individuals in this model are mediated by competition for
168 resources (e.g. light or prey) and facilitation (e.g. provision of shade). These
169 interactions are represented by the effect of density at the beginning of year t on
170 demographic processes, and in turn individual fate, from time t to $t+1$. Here, density
171 corresponds more specifically to the number of aboveground individuals of size > 4.5
172 in a given 1-m² quadrat, as we expect from observations that individuals further than
173 the quadrat are too far to affect focal plants, and that smaller individuals only have a
174 small effect on other individuals.

175

176 9. Stochasticity

177

178 Stochasticity occurs at several levels of the model. First, if the user chooses to
179 project the population under current climatic conditions, the sequence of years of the
180 desired length will be created by randomly sampling from the list of observed years.
181 If the user chooses to project the population under future climate-change conditions,
182 this random sampling of observed years is used to obtain the sequence of years to
183 be used as random effects in the submodels, that is, the years representing the
184 variation in demographic processes that is not explained by environmental
185 conditions, individual traits, or density.

186

187 Additionally, all demographic processes governing the fate of both aboveground
188 **plants** and **produced and seedbank seeds** are stochastic. For each **plant**, the
189 survival, size (at the next time step or after germinating), flowering status, and

190 number of flowers are sampled from binomial, scaled Student t , and Poisson
191 distributions with parameters obtained from predictions of generalised additive
192 models and depending on the environmental conditions, individual traits, and
193 density. For each **seed**, whether it germinates, stays dormant, or contributes to the
194 seedbank is sampled from a binomial distribution with parameters depending on the
195 site in which the simulation is performed or the time since last fire. The number of
196 seeds per flower for each **plant** is sampled from a Poisson distribution with a fixed
197 mean previously used in population projections for this system (Paniw et al., 2017;
198 Conquet et al., 2023).

199

200 Moreover, the location of each seed in the seedbank at the start of the simulation is
201 attributed randomly, with each quadrat having the same probability

202 $\frac{1}{\text{total number of quadrats}}$ to be designated as a seed's location. In subsequent years, all

203 **produced seeds** are assigned to the quadrat of the parent **plant**. This approach
204 allows us to reproduce the lack of active dispersal mechanisms in dewy pines,
205 leading most seeds to fall and establish next to the mother plant.

206

207 Finally, when the number of **plants** to add to the population is higher than the
208 capping threshold set by the user, the new individuals to be removed from the
209 recruits are sampled at random.

210

211 10. Collectives

212

213 There are no collectives in this model.

214

215 11. Observation

216

217 The two main outputs of this model are (1), for each simulation the yearly population
218 growth rates ($\log \lambda = \frac{N_t}{N_{t-1}}$, where N_t is the total population size—above ground and in
219 the seedbank—in year t and N_{t-1} in year $t-1$) that can be used to calculate the
220 stochastic growth rate over the whole simulation ($\log \lambda_S = \frac{\sum_{t=2}^T \log \lambda_t}{T}$ where T is the
221 number of simulated years), and (2) whether the population went extinct within the
222 number of simulated years, which can be used to obtain the probability of quasi-
223 extinction (proportion of simulations where the population went under the quasi-
224 extinction threshold, i.e., $10 >$ aboveground individuals and $50 >$ seeds in the
225 seedbank) across a number of simulations defined by the user.

226 In addition, the output of the model contains the full individual data across the whole
227 simulation, the mean change in aboveground population abundance (i.e. the
228 population growth rate without taking the seedbank into account), as well as
229 population size and population density (i.e. number of individuals of size > 4.5 per 1-
230 m² quadrat).

231

232 5. Initialization

233

234 For both habitats (natural and anthropogenic) and all scenarios (control and
235 climate change) the initial number of aboveground **plants**, as well as their size and
236 location (**quadrat**) corresponds to that observed in the population and first year
237 chosen by the user for the simulation, as does the density in each **quadrat**. The
238 number of **seeds** present in the seedbank when starting the simulation is defined by
239 the user (by default 10,000 for natural populations and 3,000 for anthropogenic

240 populations), and the **seeds** are initially assigned randomly to their **quadrat**. The
241 number of **produced seeds** and the extinction status are initialised at 0. The
242 sequence of yearly population growth rates, mean change in aboveground
243 population abundance, and population density are initialised with NAs.

244

245 In both scenarios, the required number of years (set by the user) is sampled among
246 the years observed in the full individual data (e.g. 30 samples of years 2016–2021).
247 This sequence of years is used to represent random year variation (i.e., random
248 effects in vital-rate models). However, the sequence of yearly temperature and
249 rainfall values depends on the scenario. Under the control scenario, these values
250 correspond to the observed climate in each year of the sampled sequence. When
251 the population is projected under climate change, the temperature and rainfall values
252 reflect the projected climate values obtained from the global circulation models
253 (GCM) from the first year defined by the user and following a chronological order
254 until the end of the simulation.

255

256 Finally, projecting natural populations requires to initialise a sequence of post-fire
257 habitat stages (0–4). In the first year, this corresponds to the stage observed in the
258 first year of the simulation (defined by the user). The following stages are determined
259 by a Markov chain (Fig. S1; see also Paniw et al., 2017; Conquet et al., 2023), where
260 the transition from the last to the first stage (fire year) depends on the probability of
261 fire return (p), which is set by the user (1/30 by default). The sequence of number of
262 years since the last fire (TSF) is initialised using the observed number in the first

263 year of the simulation, with the subsequent TSFs being inferred from the sequence
 264 of post-fire habitat stages.

265 Environment at t

266

267

268

269

270

| | | | | | | |
|----------------------|---|---|---|---|---|-------|
| | | 1 | 2 | 3 | 4 | 5 |
| Environment at $t+1$ | 1 | 0 | 0 | 0 | 0 | p |
| | 2 | 1 | 0 | 0 | 0 | 0 |
| | 3 | 0 | 1 | 0 | 0 | 0 |
| | 4 | 0 | 0 | 1 | 0 | 0 |
| | 5 | 0 | 0 | 0 | 1 | $1-p$ |

271 **Figure S1 - Markov chain determining the succession of post-fire**
 272 **habitats for the dewy pine population.** The first four states (from the fire year to
 273 the third year after a fire) constitute the deterministic part of the Markov chain and
 274 thus always follow each other in a sequence of 1 to 4 (probability of transition = 1).
 275 The fifth state (from the fourth year after a fire) is stochastic, and the transition from
 276 this state depends on the fire frequency p (i.e., the population will remain in state 5
 277 until a fire occurs).

278

279 6. Input data

280

281 The model uses as input data individual-based data on dewy pines
 282 (aboveground **plants**) in the population chosen by the user. These data have been
 283 collected during annual population surveys occurring in May since at least 2016
 284 (earlier for some populations, see Appendix S2). These surveys enabled us to obtain
 285 data on individuals' survival, size (log[length of the longest leaf x number of leaves]),
 286 reproductive status, and number of flowers (Paniw et al., 2017). Additionally, the
 287 model uses input data containing values from 2016 to 2050 of (1) average daily

288 minimum temperature (in °C) in summer and fall following a census and fall and
289 winter prior to a census, and (2) cumulative rainfall (in mm) in fall and winter
290 following a prior to a census. Details on data sources and preparation can be found
291 in Appendix S2.

292

293 7. Submodels

294

295 *Reproduction*

296

297 Flowering: Individuals can reproduce from two years after a fire occurred in natural
298 populations (Paniw et al., 2017). The reproductive status of individuals (0 or 1) is
299 drawn from a binomial distribution which probability is predicted from a generalised
300 additive model (GAM) describing the observed relationship between flowering
301 probability and winter mean daily maximum temperature, fall cumulative rainfall,
302 individual size, aboveground density of individuals with size > 4.5, and time since last
303 fire in natural populations (see Appendix S1: Table S5 for the full equation linking the
304 various covariates to flowering probability).

305

306 Number of flowers per individual: Reproductive individuals (i.e., flowering = 1) can
307 produce flowers, their number being drawn from a negative binomial distribution
308 which probability is predicted from a generalised additive model (GAM) describing
309 the observed relationship between the number of flowers and winter mean daily
310 maximum temperature, individual size, and time since last fire in natural populations
311 (see Appendix S1: Table S5 for the full equation linking the various covariates to the
312 number of flowers per individual).

313

314 Number of seeds per flower: The number of seeds for each flower is drawn from a
315 Poisson distribution with a mean fixed at 9.8, which corresponds to the value used in
316 previous population projections of the dewy-pine system (Paniw et al., 2017;
317 Conquet et al., 2023).

318

319 *Survival and growth*

320

321 Survival: Individual survival (0 or 1) is sampled from a binomial distribution which
322 probability is predicted from a generalised additive model (GAM) describing the
323 observed relationship between survival and summer mean daily maximum
324 temperature, fall cumulative rainfall, individual size, aboveground density of
325 individuals with size > 4.5, and time since last fire in natural populations (see
326 Appendix S1: Table S5 for the full equation linking the various covariates to survival).

327

328 Growth: The size of surviving individuals in the following year is sampled from a
329 truncated scaled Student t distribution with location (i.e. mean), scale (i.e. standard
330 deviation) and degrees of freedom obtained from a generalised additive model
331 describing the observed relationship between individuals' size in the next year and
332 fall cumulative rainfall, individual size, aboveground density of individuals with size >
333 4.5, and time since last fire in natural populations (see Appendix S1: Table S5 for the
334 full equation linking the various covariates to growth). The minimum or maximum
335 observed sizes were assigned to individuals with infinite size values.

336 *Seedbank*

337

338 Continuous germination and contribution to the seedbank: For each **produced seed**,
339 whether it germinated directly without going to the seedbank (0 or 1) was sampled
340 from a binomial distribution with a mean determined by the probability to germinate
341 when produced (goCont) which depended on time since last fire (in natural
342 populations) or site (in anthropogenic populations) (see Appendix S1: Table S1 for
343 details on the mean values). Among the seeds that will not germinate, seeds that will
344 contribute to the seedbank in the next year (0 or 1) were then sampled from a
345 binomial distribution with a mean determined by 1-goCont. The rest of the seeds
346 were considered dead and removed from the population. In anthropogenic
347 populations, the probabilities of continuous germination and contribution to the
348 seedbank were corrected for seed survival (i.e., multiplied by 0.33) and, in one
349 population (Sierra Carbonera Disturbed), further multiplied by 0.4 to replicate more
350 accurately the observed population dynamics.

351

352 Germination from the seedbank: For each **seedbank seed**, whether it germinated
353 from the seedbank (0 or 1) was sampled from a binomial distribution with a mean
354 depending on time since last fire (in natural populations) or site (in anthropogenic
355 populations) (see Appendix S1: Table S1 for details on the mean values). In
356 anthropogenic populations, the probability of germination from the seedbank was
357 corrected for seed survival (i.e., multiplied by 0.33) and, in one population (Sierra
358 Carbonera Disturbed), further multiplied by 0.4 to replicate more accurately the
359 observed population dynamics.

360

361 Dormancy: For each **seedbank seed**, whether it remained dormant in the seedbank
362 (0 or 1) was sampled from a binomial distribution with a mean depending on time
363 since last fire (in natural populations) or site (in anthropogenic populations) (see
364 Appendix S1: Table S1 for details on the mean values). In anthropogenic
365 populations, the probability of dormancy was corrected for seed survival (i.e.,
366 multiplied by 0.33) to replicate more accurately the observed population dynamics.

367

368 Seedling size: The size of a germinating seed is sampled from a truncated scaled
369 Student *t* distribution with location (i.e. mean), scale (i.e. standard deviation) and
370 degrees of freedom obtained from a generalised additive model describing the
371 observed relationship between seedling size and winter mean daily maximum
372 temperature, aboveground density of individuals with size > 4.5, and time since last
373 fire in natural populations (see Appendix S1: Table S5 for the full equation linking the
374 various covariates to seedling size). The minimum or maximum observed sizes were
375 assigned to individuals with infinite size values.

376 **References – Appendix S3**

377

378 Conquet, E., Ozgul, A., Blumstein, D. T., Armitage, K. B., Oli, M. K., Martin, J. G. A.,
379 Clutton-Brock, T. H., & Paniw, M. (2023). Demographic Consequences of
380 Changes in Environmental Periodicity. *Ecology*, **104**(3), e3894.
381 <https://doi.org/10.1002/ecy.3894>

382 Grimm, V., Berger, U., Bastiansen, F., Eliassen, S., Ginot, V., Giske, J., Goss-
383 Custard, J., Grand, T., Heinz, S. K., Huse, G., Huth, A., Jepsen, J. U.,
384 Jørgensen, C., Mooij, W. M., Müller, B., Pe'er, G., Piou, C., Railsback, S. F.,
385 Robbins, A. M., ... DeAngelis, D. L. (2006). A Standard Protocol for
386 Describing Individual-Based and Agent-Based Models. *Ecological Modelling*,
387 **198**(1), 115–26. <https://doi.org/10.1016/j.ecolmodel.2006.04.023>

388 Grimm, V., Railsback, S. F., Vincenot, C. E., Berger, U., Gallagher, C., DeAngelis, D.
389 L., Edmonds, B., Ge, J., Giske, J., Groeneveld, J., Johnston, A. S. A., Milles,
390 A., Nabe-Nielsen, J., Polhill, J. G., Radchuk, V., Rohwäder, M.-S., Stillman, R.
391 A., Thiele, J. C., & Ayllón, D. (2020). The ODD Protocol for Describing Agent-
392 Based and Other Simulation Models: A Second Update to Improve Clarity,
393 Replication, and Structural Realism. *Journal of Artificial Societies and Social*
394 *Simulation*, **23**(2), 7. <https://doi.org/10.18564/jasss.4259>

395 Paniw, M., Quintana-Ascencio, P. F., Ojeda, F., & Salguero-Gómez, R. (2017).
396 Interacting Livestock and Fire May Both Threaten and Increase Viability of a
397 Fire-Adapted Mediterranean Carnivorous Plant. *Journal of Applied Ecology*,
398 **54**(6), 1884–94. <https://doi.org/10.1111/1365-2664.12872>